(2)

ARL-TR-91-26

Copy No. 37

CHARACTERIZATION OF DISCRETE-TIME LINEAR PERIODICALLY TIME-VARYING SYSTEMS

Technical Report under ARL:UT Independent Research and Development Program

Kevin W. Baugh

APPLIED RESEARCH LABORATORIES
THE UNIVERSITY OF TEXAS AT AUSTIN
POST OFFICE BOX 8029, AUSTIN, TEXAS 78713-8029

26 July 1991

Technical Report

Approved for public release; distribution is unlimited.

Prepared for:

APPLIED RESEARCH LABORATORIES
INDEPENDENT RESEARCH AND DEVELOPMENT PROGRAM

REPORT DOCUMENTATION PAGE

Form Approved
OMB No. 0704-0188

1. AGENCY USE ONLY (Leave blank)	2. REPORT DATE	3. REPORT TYPE AND DATES COVERED
	26 Jul 91	technical

4. TITLE AND SUBTITLE
Characterization of Discrete-Time Linear Periodically Time-Varying Systems, Technical Report under ARL:UT Independent Research and Development Program

5. FUNDING NUMBERS
Applied Research Laboratories Independent Research and Development Program

6. AUTHOR(S)
Baugh, Kevin W.

7. PERFORMING ORGANIZATION NAMES(S) AND ADDRESS(ES)
Applied Research Laboratories
The University of Texas at Austin
P.O. Box 8029
Austin, Texas 78713-8029

8. PERFORMING ORGANIZATION REPORT NUMBER
ARL-TR-91-20

9. SPONSORING/MONITORING AGENCY NAME(S) AND ADDRESS(ES)
Applied Research Laboratories
The University of Texas at Austin
P.O. Box 8029
Austin, Texas 78713-8029

10. SPONSORING/MONITORING AGENCY REPORT NUMBER

11. SUPPLEMENTARY NOTES

12a. DISTRIBUTION/AVAILABILITY STATEMENT
Approved for public release; distribution is unlimited.

12b. DISTRIBUTION CODE

13. ABSTRACT (Maximum 200 words)

Techniques for empirically characterizing linear time-invariant systems are well established in the technical literature. Classic techniques rely on both the linearity of the underlying system and on the time invariance of the system parameters. Methods for analytically characterizing linear time-varying systems are also well-established in the literature. Typically, these methods rely on the time-varying impulse response or on the system response function. The focus of these methods is on the analytical evaluation of systems with known parameters, not on the empirical characterization of systems. The following paper presents techniques for empirically characterizing discrete-time linear time-varying systems whose system parameters may be only partially specified.

14. SUBJECT TERMS
system identification
time-varying systems
nonstationary processes

15. NUMBER OF PAGES
115

16. PRICE CODE

17. SECURITY CLASSIFICATION OF REPORT	18. SECURITY CLASSIFICATION OF THIS PAGE	19. SECURITY CLASSIFICATION OF ABSTRACT	20. LIMITATION OF ABSTRACT
UNCLASSIFIED	UNCLASSIFIED	UNCLASSIFIED	SAR

TABLE OF CONTENTS

Page

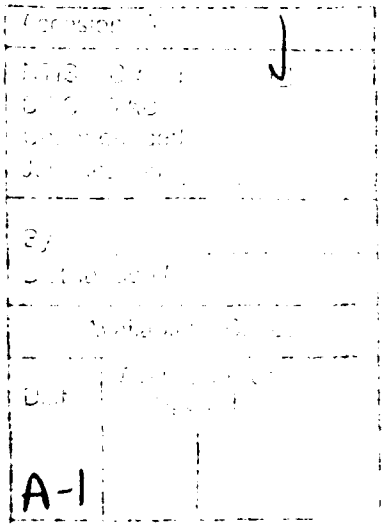

LIST OF FIGURES

PREFACE

This material was originally published in May 1991 as a dissertation, in partial fulfillment of the requirements for the degree of Ph.D. in Electrical Engineering, The University of Texas at Austin.

1. INTRODUCTION

The empirical characterization of linear time-invariant (LTI) systems is a subject that is well-established in the technical literature. The use of deterministic functions (e.g., unit impulse functions, unit step functions, and controlled sinusoids) for the characterization of LTI systems is intimately related to concepts governing the analytical characterization of these systems (e.g., the unit impulse response, the unit step response, and the system frequency response). The use of non-deterministic signals for the characterization of LTI systems is intimately related to concepts governing the analytical characterization of stationary random processes (e.g., covariance functions and the power spectrum). In either case, the empirical characterization of LTI systems proceeds amid a framework of familiar analytical concepts.

The analytical characterization of linear time-varying (LTV) systems is also well-established in the technical literature. Appropriate extensions of concepts governing the analysis of time-invariant systems provide useful insight into the behavior of systems with known time-varying parameters. The empirical characterization of continuous-time LTV systems has received some attention in the technical literature, but the subtleties of applying these techniques to discrete-time LTV systems and their practical limitations have not been discussed.

The objective of the following work is the application of techniques for empirically characterizing discrete-time linear periodically time-varying (LPTV) systems. Specifically, we wish to characterize certain LPTV structures found in multi-rate quadrature sampling and quadrature demodulation systems (see Baugh, 1988). Chapter 2 presents methods for the analysis of LTV systems in both the time domain and in the frequency domain. These analytical methods rely on the concepts of the time-varying system response function and the system transmission function (see Zadeh, 1961, Zadeh and Desoer, 1963, D'Angelo, 1970, Claasen and Mecklenbrauker, 1982, and Crochiere and Rabiner, 1983). Chapter 3 presents a discussion of the analysis of random processes generated by LTV systems. The evolutionary spectral representation of a nonstationary signal and its relation to the underlying LTV system model is presented. Techniques for the empirical characterization of discrete-time LPTV systems are presented in Chapter 4. These techniques are presented within the framework of concepts for the analytical characterization of LPTV and the signals produced by such systems discussed previously. The limitations of application of these empirical techniques in practice are also presented. The results of applying these techniques to LPTV systems of interest are presented in Chapter 5.

2. REVIEW OF THE THEORY OF DISCRETE-TIME LINEAR TIME-VARYING SYSTEMS

The theory and analysis of discrete and continuous time linear time-varying (LTV) systems has been the subject of research for some time (see Zadeh, 1961, Zadeh and Desoer, 1963, D'Angelo, 1970, Claasen and Mecklenbrauker, 1982, and Crochiere and Rabiner, 1983). Characterizations of such systems in both the time domain using the concept of the time-varying system response function and in the frequency domain using various concepts related to the system response function have been proposed. In this chapter, we will review some of these concepts for the characterization of discrete-time LTV systems. For a more thorough treatment of the subject, see D'Angelo, 1970, Crochiere and Rabiner, 1983, and Zadeh and Desoer, 1963.

2.1 TIME-DOMAIN REPRESENTATIONS OF LINEAR TIME-VARYING SYSTEMS

A discrete-time linear time-varying system may be described mathematically as a linear mapping of input signals, x(t), to output signals, y(t), so that

$$L_t[x(t)] = y(t) \quad . \tag{2.1.1}$$

The operator $L_t[\ ]$ has the property of linearity; that is, if

$$L_t[x_1(t)] = y_1(t) \tag{2.1.2}$$

and

$$L_t[x_2(t)] = y_2(t) \quad , \tag{2.1.3}$$

then

$$L_t[\alpha x_1(t)+\beta x_2(t)] = \alpha y_1(t) + \beta y_2(t) \tag{2.1.4}$$

for any scalar α and β. However, since the operator $L_t[\ ]$ evolves over time,

$$L_t[x(t+\tau)] \neq y(t+\tau) \quad . \tag{2.1.5}$$

One suitable form for the operator $L_t[\ ]$ is the discrete-time superposition sum

$$y(t) = \sum_{\tau = -\infty}^{\infty} k(t,\tau)\, x(\tau) \quad , \tag{2.1.6}$$

where the function $k(t,\tau)$ is the system response function, or Green's function (see D'Angelo, 1970, pp. 63-65). In one sense, the system response function characterizes the response of the system at some time, t, to an input applied at time τ. The system can also be described in terms of a time-varying impulse response, $h(t,\lambda)$, as

$$y(t) = \sum_{\lambda = -\infty}^{\infty} h(t,\lambda)\, x(t-\lambda) \quad . \tag{2.1.7}$$

The time-varying impulse response can be thought of as the response of the system at time t due to an input signal applied λ samples earlier. The system response and the time-varying impulse response are related by

$$k(t,\tau) = h(t,t-\tau) \quad . \tag{2.1.8}$$

In the discussions which follow, we will concern ourselves primarily with the system response function, $k(t,\tau)$. This choice will facilitate our presentation of characterization techniques for multirate discrete-time systems (e.g., decimators and interpolators). In these systems, the input and output sampling rates are not the same. Use of the time-varying impulse response function, $h(t,\lambda)$, could lead to ambiguities in the characterization of multirate systems since it is not clear what is meant by "the response of the system at time t due to an input signal applied λ samples earlier."

2.2 STABILITY CONSIDERATIONS FOR LINEAR TIME-VARYING SYSTEMS

It is relatively straightforward to show that the system is Bounded Input - Bounded Output (BIBO) stable for each t if

$$\sum_{\tau = -\infty}^{\infty} |k(t,\tau)| < \infty \tag{2.2.1}$$

for each t. First, assume that $k(t,\tau)$ is absolutely summable over τ for each t and that we apply some bounded input, $x(\tau)$, such that

$$|x(\tau)| < X < \infty \tag{2.2.2}$$

for all τ. It then follows that

$$|y(t)| = \left| \sum_{\tau = -\infty}^{\infty} k(t,\tau)\, x(\tau) \right| < \sum_{\tau = -\infty}^{\infty} |k(t,\tau)\, x(\tau)| , \tag{2.2.3}$$

or

$$|y(t)| < X \sum_{\tau = -\infty}^{\infty} |k(t,\tau)| < \infty \ . \tag{2.2.4}$$

Now assume $k(t,\tau)$ is not absolutely summable over all τ for some t, and define

$$x(\tau) = \text{sgn}\,(k(t,\tau)) \tag{2.2.5}$$

for that particular t. We have introduced the function

$$\text{sgn}(\gamma) = \begin{cases} +1 & ; \ \gamma > 0 \\ -1 & ; \ \gamma < 0 \end{cases} \ . \tag{2.2.6}$$

Notice that $x(\tau)$ is a bounded function for all τ. The system output corresponding to this input is given by

$$y(t) = \sum_{\tau = -\infty}^{\infty} k(t,\tau)\, \text{sgn}(k(t,\tau)) = \sum_{\tau = -\infty}^{\infty} |k(t,\tau)| \ , \tag{2.2.7}$$

which, by assumption, is unbounded.

Hereafter, we will assume that the systems of interest are BIBO stable for all t; in other words

$$\sum_{\tau=-\infty}^{\infty} |k(t,\tau)| < \infty \qquad (2.2.8)$$

holds for all t. We make this assumption for two reasons. First, a detailed study of criteria for the stability of LTV systems is beyond the scope of the present effort. Second, by making this reasonable assumption on the systems of interest, we obtain interesting and useful results when we consider frequency-domain techniques for characterizing LTV systems. For a more detailed discussion of stability issues for LTV systems, see D'Angelo, 1970, pp. 221-272.

Notice also that equation (2.2.8) implies

$$\lim_{\tau \to -\infty} |k(t,\tau)| = 0 \qquad (2.2.9)$$

so that the contribution to the system output at sample time t due to an input at some sample time τ in the remote past is negligible. In a sense, then, a BIBO stable system can be said to possess limited memory (see Zadeh and Desoer, 1963, pp. 45-46). This will prove useful to us when we consider the estimation of statistical parameters for random processes produced by stable LTV systems.

2.3 FREQUENCY DOMAIN CHARACTERIZATIONS OF LINEAR TIME-VARYING SYSTEMS

In order to introduce the concept of a frequency-domain characterization for LTV systems, let us first consider the characterization of a LTI system in the frequency domain. For the LTI system, the impulse response function does not vary with time, t, but is a function only of the time difference, $t-\tau$ (see Zadeh and Desoer, 1963, p. 154). The superposition sum for the LTI system is therefore given by

$$y(t) = \sum_{\tau=-\infty}^{\infty} h(t-\tau)\, x(\tau) \quad , \qquad (2.3.1)$$

where $h(\lambda)$ is the familiar LTI impulse response function (see Zadeh and Desoer, 1963, p. 156). Assume that the input to the LTI system is a complex sinusoid of frequency α; in other words

$$x(\tau) = e^{i\alpha\tau} \tag{2.3.2}$$

for $-\pi \leq \alpha \leq \pi$. The output of the LTI system due to this input signal is given by

$$y_\alpha(t) = \sum_{\tau = -\infty}^{\infty} h(t-\tau)\, e^{i\alpha\tau} \quad , \tag{2.3.3}$$

or by a change of variables

$$y_\alpha(t) = \left(\sum_{\lambda = -\infty}^{\infty} h(\lambda)\, e^{-i\alpha\lambda} \right) e^{i\alpha t} \quad . \tag{2.3.4}$$

Notice that

$$|h(\lambda)\, e^{-i\alpha\lambda}| = |h(\lambda)| \tag{2.3.5}$$

for all values of α, so for a BIBO stable LTI system the summation enclosed in brackets in equation (2.3.5) above converges uniformly to a function which is continuous in α by the Weierstrass M-test (see Kaplan, 1962, p. 169). Let

$$H(\alpha) = \sum_{\lambda = -\infty}^{\infty} h(\lambda)\, e^{-i\alpha\lambda} \quad , \tag{2.3.6}$$

so that the response of the LTI system due to a complex sinusoid of frequency α is given by

$$y_\alpha(t) = H(\alpha)\, e^{i\alpha t} \quad . \tag{2.3.7}$$

The function $H(\alpha)$ is referred to as the frequency response function of the LTI system (see Kaplan, 1962, pp. 95-96). Notice that in some sense the frequency response function indicates how frequency components of the input signal are mapped into frequency components of the output signal.

Now consider a deterministic input signal, $x(\tau)$, whose Fourier transform exists and assume that the Fourier transform of the output signal, defined by

$$Y(\omega) = \sum_{t=-\infty}^{\infty} y(t)\, e^{-i\omega t} , \tag{2.3.8}$$

exists. Substituting for $y(t)$ in (2.3.8) above yields

$$Y(\omega) = \sum_{t=-\infty}^{\infty} \sum_{\tau=-\infty}^{\infty} h(t-\tau)\, x(\tau)\, e^{-i\omega t} , \tag{2.3.9}$$

or by a change of variables, and assuming the system is BIBO stable

$$Y(\omega) = \left(\sum_{\tau=-\infty}^{\infty} x(\tau)\, e^{-i\omega\tau} \right) \left(\sum_{\lambda=-\infty}^{\infty} h(\lambda)\, e^{-i\omega\lambda} \right) , \tag{2.3.10}$$

so that, since the Fourier transform of the input, $x(\tau)$, exists

$$Y(\omega) = X(\omega)\, H(\omega) \tag{2.3.11}$$

(see Priestly, 1981, p. 210).

Equation (2.3.11) presents one of the fundamental concepts of the theory of frequency-domain characterizations for LTI systems: a Fourier transform can represent a linear convolution of series in the time domain by a simple product of functions in the frequency domain. For this reason, a Fourier transform is said to be a *compatible transform* for the class of LTI systems (see D'Angelo, 1970, pp. 275-276). One early approach to the frequency-domain characterization of LTV systems was based on the idea of defining new transforms which would be compatible transforms over some restricted class of LTV systems (see Aseltine, 1954, and Johnson and Kilmer, 1962). For example, the Mellin transform defined by

$$Y(\mu) = \int_0^\infty y(t)\, t^{\mu-1}\, dt \tag{2.3.12}$$

is a compatible transform for continuous LTV systems governed by the Euler-Cauchy differential equation (see Aseltine, 1954). One obvious shortcoming to this approach is that specific compatible transforms must be developed for each specific class of LTV system, depending on the time-varying differential equation governing that class of systems. Also, the familiar notion of "frequency" can be lost in the new compatible transform domain. For example, it is not obvious how the parameter μ in the Mellin transform of equation (2.3.12) above can be related to some familiar notion of "frequency" for the signal y(t).

An alternative approach, introduced in Zadeh, 1950, and presented for continuous-time LTV systems in Zadeh, 1961, Gersho, 1963, and Brikker, 1966, and presented for discrete-time LTV systems in Claasen and Mecklenbrauker, 1982, and Crochiere and Rabiner, 1983, pp. 100-126, is based on the idea of using an incompatible transform to obtain a characterization of the LTV system. This incompatible transform retains the concept of "frequency" of the input and output signals. In order to introduce this concept, we first consider applying a complex sinusoidal input of frequency α to a LTV system. Let the response of the LTV system due to this sinusoidal input be denoted as $k(t,\alpha)$. By equation (2.1.6), $k(t,\alpha)$ is given by

$$\kappa(t,\alpha) = \sum_{\tau=-\infty}^{\infty} k(t,\tau)\, e^{i\alpha\tau} \quad . \tag{2.3.13}$$

If the LTV system is BIBO stable for all t, then

$$\sum_{\tau=-\infty}^{\infty} |k(t,\tau)| < \infty \tag{2.3.14}$$

for all t, and since

$$|k(t,\tau)\, e^{i\alpha\tau}| = |k(t,\tau)| \tag{2.3.15}$$

for all t, by the Weierstrass M-test $\kappa(t,\alpha)$ exists and is continuous in α for all t (see Kaplan, 1962, p. 169). Note that $\kappa(t,\alpha)$ is simply the response of the LTV system to an applied complex sinusoid of frequency α. We could therefore refer to $\kappa(t,\alpha)$ as the time-varying frequency response function for the LTV system. If the system were time-invariant, we know from equation (2.3.7) that this response function would be a scaled version of the original complex sinusoid. In Zadeh, 1950, the time-varying system function, $H(t,\alpha)$, for a LTV system is defined to be

$$H(t,\alpha) = \kappa(t,\alpha)\, e^{-i\alpha t} \quad . \tag{2.3.16}$$

In a sense, the time-varying system function is the complex envelope of the response of the LTV system to an applied complex sinusoid (see Zadeh, 1950).

Now consider a signal, $x(\tau)$, whose Fourier transform exists; in other words,

$$X(\alpha) = \sum_{\tau=-\infty}^{\infty} x(\tau)\, e^{-i\alpha\tau} \tag{2.3.17}$$

exists. We could therefore describe the signal $x(\tau)$ as

$$x(\tau) = \frac{1}{2\pi} \int_{-\pi}^{\pi} X(\alpha)\, e^{i\alpha\tau}\, d\alpha \quad . \tag{2.3.18}$$

Applying this signal to the LTV system of equation (2.1.6) yields an output signal, $y(t)$, given by

$$y(t) = \frac{1}{2\pi} \sum_{\tau=-\infty}^{\infty} k(t,\tau) \int_{-\pi}^{\pi} X(\alpha)\, e^{i\alpha\tau}\, d\alpha \quad . \tag{2.3.19}$$

Interchanging the order of summation and integration yields

$$y(t) = \frac{1}{2\pi} \int_{-\pi}^{\pi} \left(\sum_{\tau=-\infty}^{\infty} k(t,\tau)\, e^{i\alpha\tau} \right) X(\alpha)\, d\alpha \quad . \tag{2.3.20}$$

Notice that the term in brackets in equation (2.3.20) above is the time-varying frequency response function, $\kappa(t,\alpha)$. Equation (2.3.20) may therefore be rewritten as

$$y(t) = \frac{1}{2\pi} \int_{-\pi}^{\pi} \kappa(t,\alpha)\, X(\alpha)\, d\alpha \quad . \tag{2.3.21}$$

Now assume that the Fourier transform of the output signal, $y(t)$, exists; in other words

$$Y(\omega) = \sum_{t=-\infty}^{\infty} y(t)\, e^{-i\omega t} \tag{2.3.22}$$

exists. Substituting equation (2.3.21) into (2.3.22) above yields

$$Y(\omega) = \frac{1}{2\pi} \sum_{t=-\infty}^{\infty} \int_{-\pi}^{\pi} \kappa(t,\alpha)\, X(\alpha)\, d\alpha\, e^{-i\omega t} \quad . \tag{2.3.23}$$

Interchanging the order of summation and integration, we obtain

$$Y(\omega) = \frac{1}{2\pi} \int_{-\pi}^{\pi} \left(\sum_{t=-\infty}^{\infty} \kappa(t,\alpha)\, e^{-i\omega t} \right) X(\alpha)\, d\alpha \quad . \tag{2.3.24}$$

For the moment, assume that the summation in brackets in equation (2.3.24) above exists, and define

$$K(\omega,\alpha) = \sum_{t=-\infty}^{\infty} \kappa(t,\alpha)\, e^{-i\omega t} \quad . \tag{2.3.25}$$

Conditions for the existence of $K(\omega,\alpha)$ and the implications of these conditions will be examined in Section 2.5. Substituting equation (2.3.25) into equation (2.3.24) we obtain

$$Y(\omega) = \frac{1}{2\pi} \int_{-\pi}^{\pi} K(\omega,\alpha)\, X(\alpha)\, d\alpha \quad . \tag{2.3.26}$$

Notice that equation (2.3.26) in some sense gives a description of how input frequency components contribute to output frequency components. It is not the simple one-to-one relationship one finds for LTI systems, and it is for this reason that this characterization of LTV systems is considered to be an incompatible transform technique (see D'Angelo, 1970, p. 294). The function $K(\omega,\alpha)$ is referred to as the time-varying system transmission function (see Claasen and Mecklenbrauker, 1982, and Crochiere and Rabiner, 1983, p. 103).

2.4 ANALYSIS OF NETWORK STRUCTURES FOR DISCRETE-TIME LINEAR TIME-VARYING SYSTEMS

We have introduced time and frequency-domain representations for discrete-time LTV systems in the previous sections. In this section, we consider the analysis of network structures obtained by connecting LTV subsystems. Two fundamental structures will be considered: the parallel connection of two LTV subsystems, and the series connection of two LTV subsystems. More complicated network structures may be analyzed by extension of the methods presented below.

Consider two LTV systems with response functions $k_1(t,\tau)$ and $k_2(t,\tau)$. Assume that the corresponding transmission functions, $K_1(\omega,\alpha)$ and $K_2(\omega,\alpha)$, exist for these two systems. A parallel connection of the systems is indicated schematically in Figure 2.4.1. The response of the overall system to some input signal, $x(\tau)$, is

$$y(t) = \left(\sum_{\tau = -\infty}^{\infty} k_1(t,\tau)x(\tau) \right) + \left(\sum_{\tau = -\infty}^{\infty} k_2(t,\tau)x(\tau) \right). \qquad (2.4.1)$$

If we were to apply a unit impulse function at some time $\tau = \tau_0$ to this composite system, the observed output would be the response function for the overall LTV system for the fixed input time $\tau = \tau_0$, $k(t,\tau_0)$. Let the unit impulse function be denoted by $\zeta(\tau)$; in other words define

$$\zeta(\tau) = \begin{cases} 1 & ; \quad \tau = 0 \\ 0 & ; \quad \tau \neq 0 \end{cases} . \qquad (2.4.2)$$

The response function for the overall system is given by

$$k(t,\tau_0) = \left(\sum_{\tau=-\infty}^{\infty} k_1(t,\tau)\zeta(\tau-\tau_0) \right) + \left(\sum_{\tau=-\infty}^{\infty} k_2(t,\tau)\zeta(\tau-\tau_0) \right) . \qquad (2.4.3)$$

Simplifying this expression we obtain

$$k(t,\tau_0) = k_1(t,\tau_0) + k_2(t,\tau_0) \ ; \qquad (2.4.4)$$

in other words, the response function of a parallel connection of LTV systems is simply the sum of the individual response functions. Also note that if $k_1(t,\tau)$ and $k_2(t,\tau)$ represent BIBO stable LTV systems, then the overall LTV system is also BIBO stable.

Next consider applying a complex sinusoid of frequency α to the composite system of Figure 2.4.1. We know that the output of the composite system for this input will be the frequency response function for the overall system at frequency α, $\kappa(t,\alpha)$. From equation (2.4.1) we may express $\kappa(t,\alpha)$ as

$$\kappa(t,\alpha) = \left(\sum_{\tau=-\infty}^{\infty} k_1(t,\tau)\, e^{i\alpha\tau} \right) + \left(\sum_{\tau=-\infty}^{\infty} k_2(t,\tau)\, e^{i\alpha\tau} \right) . \qquad (2.4.5)$$

Simplifying this expression, we obtain

$$\kappa(t,\alpha) = \kappa_1(t,\alpha) + \kappa_2(t,\alpha) \ , \qquad (2.4.6)$$

where $\kappa_1(t,\alpha)$ and $\kappa_2(t,\alpha)$ are the frequency response functions corresponding to $k_1(t,\tau)$ and $k_2(t,\tau)$. From equation (2.3.25) we can express the transmission function of the overall system, $K(\omega,\alpha)$, as

$$K(\omega,\alpha) = \sum_{t=-\infty}^{\infty} \left(\kappa_1(t,\alpha) + \kappa_2(t,\alpha) \right) e^{-i\omega t} \ . \qquad (2.4.7)$$

Simplifying this expression we obtain

$$K(\omega,\alpha) = K_1(\omega,\alpha) + K_2(\omega,\alpha) \ , \qquad (2.4.8)$$

where $K_1(\omega,\alpha)$ and $K_2(\omega,\alpha)$ are the transmission functions corresponding to $k_1(t,\tau)$ and $k_2(t,\tau)$. From equation (2.4.8) we see that the transmission function for a parallel connection of LTV systems is simply the sum of the individual transmission functions.

Finally, consider the series connection of LTV systems indicated schematically in Figure 2.4.2. The response of the overall system to some input signal, $x(\tau)$, is given by

$$y(t) = \sum_{\gamma=-\infty}^{\infty} k_2(t,\gamma)y_1(\gamma) \tag{2.4.9}$$

where

$$y_1(\gamma) = \sum_{\tau=-\infty}^{\infty} k_1(\gamma,\tau)x(\tau) \ . \tag{2.4.10}$$

Combining equations (2.4.9) and (2.4.10), we obtain

$$y(t) = \sum_{\gamma=-\infty}^{\infty} k_2(t,\gamma)\left(\sum_{\tau=-\infty}^{\infty} k_1(\gamma,\tau)x(\tau)\right) , \tag{2.4.11}$$

or simply

$$y(t) = \sum_{\tau=-\infty}^{\infty}\left(\sum_{\gamma=-\infty}^{\infty} k_2(t,\gamma)\ k_1(\gamma,\tau)\right)x(\tau) \ . \tag{2.4.12}$$

If we apply a unit impulse at time $\tau = \tau_0$ to this composite system, we obtain the overall system response function for input time $\tau = \tau_0$, $k(t,\tau_0)$. From equation (2.4.12), we may express $k(t,\tau_0)$ as

$$k(t,\tau_0) = \sum_{\tau=-\infty}^{\infty}\left(\sum_{\gamma=-\infty}^{\infty} k_2(t,\gamma)\ k_1(\gamma,\tau)\right)\zeta(\tau-\tau_0) \ , \tag{2.4.13}$$

or simply

$$k(t,\tau_o) = \sum_{\gamma = -\infty}^{\infty} k_2(t,\gamma)\, k_1(\gamma,\tau_o) \quad . \tag{2.4.14}$$

Equation (2.4.14) indicates that the overall system response function at input time $\tau = \tau_o$ for a series connection of two LTV systems is the response of the second LTV system when excited by the first LTV system's response function, $k_1(\gamma,\tau_o)$. Notice that, in general, a different response function (and therefore a different LTV system) is obtained when we commute the systems $k_1(t,\tau)$ and $k_2(t,\tau)$ (see Crochiere and Rabiner, 1983, pp. 108-112). Also note that if both $k_1(t,\tau)$ and $k_2(t,\tau)$ are BIBO stable LTV systems, then the overall system is also BIBO stable.

Now consider applying a complex exponential of frequency α to the composite LTV system of Figure 2.4.2. The output signal obtained in this case will be the frequency response function for the overall system at frequency α, $\kappa(t,\alpha)$. From equation (2.4.12) we may express $\kappa(t,\alpha)$ as

$$\kappa(t,\alpha) = \sum_{\tau = -\infty}^{\infty} \left(\sum_{\gamma = -\infty}^{\infty} k_2(t,\gamma)\, k_1(\gamma,\tau) \right) e^{i\alpha\tau} \quad . \tag{2.4.15}$$

On simplifying equation (2.4.15), we obtain

$$\kappa(t,\alpha) = \sum_{\gamma = -\infty}^{\infty} k_2(t,\gamma)\, \kappa_1(\gamma,\alpha) \quad . \tag{2.4.16}$$

Consider that we may express $k_2(t,\gamma)$ as

$$k_2(t,\gamma) = \frac{1}{2\pi} \int_{-\pi}^{\pi} \kappa_2(t,\beta)\, e^{-i\beta\gamma}\, d\beta \ , \tag{2.4.17}$$

so that equation (2.4.16) can be rewritten as

$$\kappa(t,\alpha) = \frac{1}{2\pi} \int_{-\pi}^{\pi} \kappa_2(t,\beta) \left(\sum_{\gamma=-\infty}^{\infty} \kappa_1(\gamma,\alpha)\, e^{-i\beta\gamma} \right) d\beta \ . \tag{2.4.18}$$

Notice that the expression in brackets in equation (2.4.18) above is the transmission function for the first LTV system, $K_1(\omega,\alpha)$. Our expression for $\kappa(t,\alpha)$ therefore becomes

$$\kappa(t,\alpha) = \frac{1}{2\pi} \int_{-\pi}^{\pi} \kappa_2(t,\beta)\, K_1(\beta,\alpha)\, d\beta \ . \tag{2.4.19}$$

Using equation (2.3.25) to obtain the transmission function for the overall LTV system, $K(\omega,\alpha)$, we obtain

$$K(\omega,\alpha) = \sum_{t=-\infty}^{\infty} \left(\frac{1}{2\pi} \int_{-\pi}^{\pi} \kappa_2(t,\beta)\, K_1(\beta,\alpha)\, d\beta \right) e^{-i\omega t} , \tag{2.4.20}$$

or simply

$$K(\omega,\alpha) = \frac{1}{2\pi} \int_{-\pi}^{\pi} K_2(\omega,\beta)\, K_1(\beta,\alpha)\, d\beta \ . \tag{2.4.21}$$

Recall that, in some sense, $K_1(\beta,\alpha)$ indicates the distribution of frequency components in the output of the first LTV system due to a complex exponential input signal of frequency α. Comparing equation (2.4.21) and (2.3.26), we see that the overall system's transmission function, $K(\omega,\alpha)$, is simply the response of the second LTV system due to a signal with frequency content $K_1(\beta,\alpha)$. Again, note that in general commuting the two LTV systems yields an overall LTV system with a different transmission function (see Crochiere and Rabiner, 1983, p. 111).

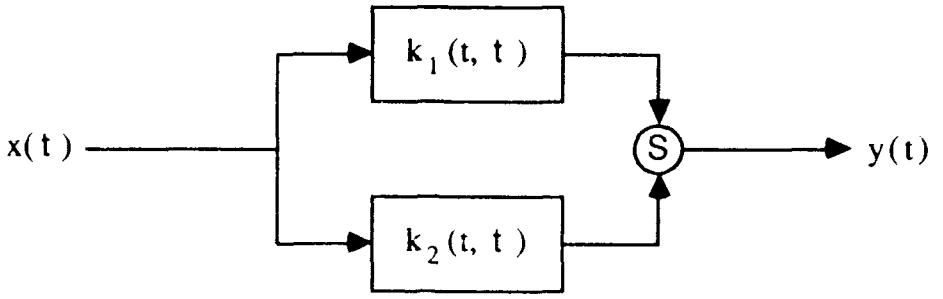

AS-91-364

FIGURE 2.4.1
PARALLEL CONNECTION OF LTV SYSTEMS

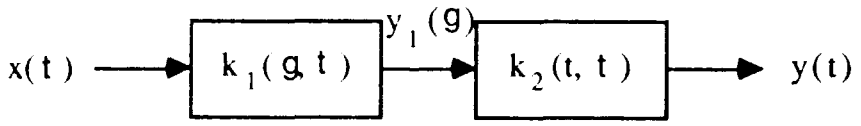

AS-91-365

FIGURE 2.4.2
SERIES CONNECTION OF LTV SYSTEMS

2.5 CLASSES OF DISCRETE-TIME LINEAR TIME-VARYING SYSTEMS

The discussions of frequency-domain characterizations of LTV systems using the system transmission function, $K(\omega,\alpha)$, presented thus far have been made by simply assuming that $K(\omega,\alpha)$ exists. We now turn our attention to the conditions under which $K(\omega,\alpha)$ exists and the implications of these conditions on the properties of the LTV system. Recall that the system transmission function was defined to be

$$K(\omega,\alpha) = \sum_{t=-\infty}^{\infty} \kappa(t,\alpha)\, e^{-i\omega t} . \tag{2.5.1}$$

Clearly, the existence of $K(\omega,\alpha)$ intimately depends on the properties of the frequency response function, $\kappa(t,\alpha)$. We will consider two classes of LTV system: the class of LTV systems whose frequency response function is a periodic function of t for all α, and the class of LTV systems whose frequency response function is an almost periodic function of t for all α.

First assume that the frequency response function is a periodic function of output time t for all α; in other words, assume

$$\kappa(t,\alpha) = \kappa(t+T(\alpha),\alpha) \tag{2.5.2}$$

for some $T(\alpha)$ for all α. Notice that equation (2.5.2) assumes that the frequency response function may be periodic with a distinct period, $T(\alpha)$, for each α. Since $\kappa(t,\alpha)$ is a periodic function in t, it has a Fourier series representation given by

$$\kappa(t,\alpha) = \sum_{n=-\infty}^{\infty} a_n(\alpha)\, e^{i2\pi nt/T(\alpha)} \tag{2.5.3}$$

where

$$a_n(\alpha) = \sum_{t=0}^{T(\alpha)} \kappa(t,\alpha)\, e^{-i2\pi nt/T(\alpha)} \tag{2.5.4}$$

(see Oppenhiem and Schafer, 1975, pp. 88-89). Substituting equation (2.5.3) into (2.5.1), we obtain

$$K(\omega,\alpha) = \sum_{t=-\infty}^{\infty} \sum_{n=-\infty}^{\infty} a_n(\alpha)\, e^{i2\pi nt/T(\alpha)}\, e^{-i\omega t} , \tag{2.5.5}$$

or simply

$$K(\omega,\alpha) = \sum_{n=-\infty}^{\infty} a_n(\alpha) \left(\sum_{t=-\infty}^{\infty} e^{-i(\omega-2\pi n/T(\alpha))t} \right) . \tag{2.5.6}$$

The term in brackets in equation (2.5.6) is given by

$$\sum_{t=-\infty}^{\infty} e^{-i(\omega-2\pi n/T(\alpha))t} = \delta(\omega-2\pi n/T(\alpha)) \tag{2.5.7}$$

where $\delta(\gamma)$ is the Dirac delta function (see Papoulis, 1962, pp. 42-46). Our expression for $K(\omega,\alpha)$ is therefore given by

$$K(\omega,\alpha) = \sum_{n=-\infty}^{\infty} a_n(\alpha)\, \delta(\omega-2\pi n/T(\alpha)) \ . \tag{2.5.8}$$

From equation (2.5.8) above we see that a LTV system whose frequency response function is a periodic function of time t will possess a system transmission function which consists of modulated impulse sheets in the (ω,α) bifrequency plane.

Finally, assume that the frequency response function is an almost periodic function of output time t for all α; in other words, for any $\varepsilon > 0$, there is some $T(\alpha)$ such that

$$|\kappa(t,\alpha) - \kappa(t+T(\alpha),\alpha)| < \varepsilon \tag{2.5.9}$$

for all α (see Wiener, 1933, p. 185). Since $\kappa(t,\alpha)$ is an almost periodic function for all α, we know that there is an increasing sequence of frequencies, $\{\ldots, \omega_{-1}(\alpha), \omega_0(\alpha), \omega_1(\alpha), \ldots\}$, such that

$$\kappa(t,\alpha) = \sum_{n=-\infty}^{\infty} a_n(\alpha)\, e^{i\omega_n(\alpha)t} \tag{2.5.10}$$

where

$$a_n(\alpha) = \lim_{t_0 \to \infty} \frac{1}{2t_0} \sum_{t=-t_0}^{t_0} \kappa(t,\alpha)\, e^{-i\omega_n(\alpha)t} \tag{2.5.11}$$

(see Wiener, 1933, p. 186 and Priestly, 1981, p. 199). Substituting equation (2.5.10) into (2.5.1), we obtain

$$K(\omega,\alpha) = \sum_{t=-\infty}^{\infty} \sum_{n=-\infty}^{\infty} a_n(\alpha)\, e^{i\omega_n(\alpha)t}\, e^{-i\omega t}, \tag{2.5.12}$$

or simply

$$K(\omega,\alpha) = \sum_{n=-\infty}^{\infty} a_n(\alpha)\, \delta(\omega-\omega_n(\alpha)) \ . \tag{2.5.13}$$

Again, we see that LTV systems which possess almost periodic frequency response functions exhibit transmission functions consisting of modulated impulse functions in the (ω,α) bifrequency plane.

In Claasen and Mecklenbrauker, 1982, the class of LTV systems with almost periodic frequency response functions is referred to as the class of "stationary" LTV systems. The authors then point out that, whereas series and parallel connections of LTV systems with periodic frequency response functions may not yield overall LTV systems with periodic frequency response functions, series and parallel connections of LTV systems with almost periodic frequency response functions always yield overall LTV

systems with almost periodic frequency response functions. In the discussions which follow, we will refer to the class of LTV systems with almost periodic frequency response functions as simply the class of linear periodically time varying (LPTV) systems.

2.6 IMPLICATIONS OF CAUSALITY ON THE TRANSMISSION FUNCTION OF LINEAR PERIODICALLY TIME-VARYING SYSTEMS

Recall from equation (2.5.13) that the system transmission function for a LPTV system is given by

$$K(\omega,\alpha) = \sum_{n=-\infty}^{\infty} a_n(\alpha)\, \delta(\omega-\omega_n(\alpha)) \quad . \tag{2.6.1}$$

The system transmission function is therefore non-zero only along the set of curves $\omega=\omega_n(\alpha)$ in the (ω,α) bifrequency plane. In Claasen and Mecklenbrauker, 1982, it is shown that for causal continuous-time LPTV systems, the system transmission function is non-zero only along a set of lines in the bifrequency plane. It is then asserted that causal discrete-time LPTV systems will similarly possess $\omega_n(\alpha)$ which are linear in α. In this section, we will show that causal LPTV systems whose input and output sampling rates are rationally related do indeed have the property that the function $\omega_n(\alpha)$ is linear in α.

First, consider a one-sided discrete-time signal, $s(\gamma)$; in other words, a sequence for $\gamma = \ldots, -1, 0, 1, \ldots$ such that

$$s(\gamma) = 0, \gamma < 0 \quad . \tag{2.6.2}$$

Assume that the Fourier transform of $s(\gamma)$ exists and is given by

$$S(\Omega) = \sum_{\gamma=0}^{\infty} s(\gamma)\, e^{-i\Omega\gamma} \quad . \tag{2.6.3}$$

Now consider the real and imaginary components of $S(\Omega)$, given by

$$S(\Omega) = S_R(\Omega) + iS_I(\Omega) \quad . \tag{2.6.4}$$

For a one-sided signal, the real and imaginary components of $S(\Omega)$ are related through a discrete Hilbert transform (see Oppenheim and Schafer, 1975, pp. 339-345). Specifically, the real and imaginary components of $S(\Omega)$ are related by

$$S_I(\Omega) = \frac{1}{2\pi} (p.v.) \int_{-\pi}^{\pi} S_R(\Theta) \cot\left(\frac{\Omega-\Theta}{2}\right) d\Theta \tag{2.6.5}$$

and

$$S_R(\Omega) = - \frac{1}{2\pi} (p.v.) \int_{-\pi}^{\pi} S_I(\Theta) \cot\left(\frac{\Omega-\Theta}{2}\right) d\Theta + s(0) \ . \tag{2.6.6}$$

In equations (2.6.5) and (2.6.6), (p.v.) indicates the Cauchy principle value of the integral. In one sense, the Hilbert transform is a circular convolution of two functions in Ω, and so is itself a linear function in Ω (see Oppenheim and Schafer, 1975, p. 345).

We must now define precisely what is meant by a causal LTV system. First, assume that the input and output sampling times, τ and t, can be related to some underlying continuous time parameter, *t*. Specifically, we will assume that output samples are taken at unit intervals in *t*, while input samples are obtained at intervals spaced ρ apart. This is indicated schematically in Figure 2.6.1. By coupling input and output sampling times to this underlying continuous parameter, we can make some sensible accounting of which output samples occur after a given input sample. A LTV system with system response function $k(t,\tau)$ is defined to be causal if

$$k(t,\tau) = 0, \ t < [\rho\tau] \ . \tag{2.6.7}$$

The notation $[x]$ for some real-valued x indicates the smallest integer which is greater than or equal to x. Notice that equation (2.6.8) indicates that observed outputs at time t depend only on inputs applied at some earlier absolute time. Systems for which $\rho = 1$ will be called constant-rate systems, since the input and output sampling rates are the same. Systems for which $\rho < 1$ or $\rho > 1$ will be called rate-reduction and rate-increase systems, respectively.

Assume that $k(t,\tau)$ is the system response function for a causal, stable, constant-rate LPTV system. From equations (2.3.13) and (2.3.25), we may express the system transmission function as

$$K(\omega,\alpha) = \sum_{t=-\infty}^{\infty} \sum_{\tau=-\infty}^{\infty} k(t,\tau)\, e^{i\alpha\tau}\, e^{-i\omega t} \quad . \tag{2.6.8}$$

Now consider that

$$K(\omega,\omega-\alpha) = \sum_{t=-\infty}^{\infty} \sum_{\tau=-\infty}^{\infty} k(t,\tau)\, e^{i(\omega-\alpha)\tau}\, e^{-i\omega t} \quad , \tag{2.6.9}$$

or

$$K(\omega,\omega-\alpha) = \sum_{\tau=-\infty}^{\infty} \left(\sum_{t=-\infty}^{\infty} k(t,\tau)\, e^{-i\omega(t-\tau)} \right) e^{-i\alpha\tau} \quad . \tag{2.6.10}$$

Substituting $\gamma = t-\tau$, we obtain

$$K(\omega,\omega-\alpha) = \sum_{\tau=-\infty}^{\infty} \left(\sum_{\gamma=-\infty}^{\infty} k(\gamma+\tau,\tau)\, e^{-i\omega\gamma} \right) e^{-i\alpha\tau} \quad . \tag{2.6.11}$$

Define the sequence $s(\gamma,\tau)$ to be

$$s(\gamma,\tau) = k(\gamma+\tau,\tau) \quad , \tag{2.6.12}$$

so that equation (2.6.11) becomes

$$K(\omega,\omega-\alpha) = \sum_{\tau=-\infty}^{\infty} \left(\sum_{\gamma=-\infty}^{\infty} s(\gamma,\tau)\, e^{-i\omega\gamma} \right) e^{-i\alpha\tau} \quad . \tag{2.6.13}$$

The summation in brackets in equation (2.6.13) above is the Fourier transform of $s(\gamma,\tau)$ with respect to γ. However, from equation (2.6.10) we know that $s(\gamma,\tau)$ is a one-sided sequence; in other words,

$$s(\gamma,\tau) = 0 \ , \ \gamma < 0 \ . \tag{2.6.14}$$

If we define

$$S(\omega,\tau) = \sum_{\gamma = -\infty}^{\infty} s(\gamma,\tau)\, e^{-i\omega\gamma} = S_R(\omega,\tau) + iS_I(\omega,\tau) \ , \tag{2.6.15}$$

then we know that the real and imaginary components of $S(\omega,\tau)$ are related by

$$S_I(\omega,\tau) = \frac{1}{2\pi} \text{ (p.v.)} \int_{-\pi}^{\pi} S_R(\Theta,\tau) \cot\left(\frac{\omega-\Theta}{2}\right) d\Theta \tag{2.6.16}$$

and

$$S_R(\omega,\tau) = -\frac{1}{2\pi} \text{ (p.v.)} \int_{-\pi}^{\pi} S_I(\Theta,\tau) \cot\left(\frac{\omega-\Theta}{2}\right) d\Theta + k(\tau,\tau) \ . \tag{2.6.17}$$

Substituting equation (2.6.15) into equation (2.6.13) and simplifying, we obtain

$$\begin{aligned} K(\omega,\omega-\alpha) &= \sum_{\tau = -\infty}^{\infty} S_R(\omega,\tau)\cos(\alpha\tau) + S_I(\omega,\tau)\sin(\alpha\tau) \\ &\quad + i \sum_{\tau = -\infty}^{\infty} S_I(\omega,\tau)\cos(\alpha\tau) - S_R(\omega,\tau)\sin(\alpha\tau) \ . \end{aligned} \tag{2.6.18}$$

From equation (2.6.18), we may write the real and imaginary components of the transmission function as

$$K_R(\omega,\omega-\alpha) = \sum_{\tau = -\infty}^{\infty} S_R(\omega,\tau)\cos(\alpha\tau) + S_I(\omega,\tau)\sin(\alpha\tau) \tag{2.6.19}$$

and

$$K_I(\omega,\omega-\alpha) = \sum_{\tau=-\infty}^{\infty} S_I(\omega,\tau)\cos(\alpha\tau) - S_R(\omega,\tau)\sin(\alpha\tau) \ , \qquad (2.6.20)$$

respectively. Now consider that

$$\frac{1}{2\pi}(\text{p.v.})\int_{-\pi}^{\pi} K_R(\Theta,\Theta-\alpha)\cot\left(\frac{\omega-\Theta}{2}\right)d\Theta =$$

$$\sum_{\tau=-\infty}^{\infty}\frac{1}{2\pi}(\text{p.v.})\int_{-\pi}^{\pi} S_R(\Theta,\tau)\cot\left(\frac{\omega-\Theta}{2}\right)d\Theta\cos(\alpha\tau)$$

$$+\sum_{\tau=-\infty}^{\infty}\frac{1}{2\pi}(\text{p.v.})\int_{-\pi}^{\pi} S_I(\Theta,\tau)\cot\left(\frac{\omega-\Theta}{2}\right)d\Theta\sin(\alpha\tau) \ , \qquad (2.6.21)$$

or, by equations (2.6.16) and (2.6.17),

$$\frac{1}{2\pi}(\text{p.v.})\int_{-\pi}^{\pi} K_R(\Theta,\Theta-\alpha)\cot\left(\frac{\omega-\Theta}{2}\right)d\Theta =$$

$$\sum_{\tau=-\infty}^{\infty} S_I(\omega,\tau)\cos(\alpha\tau) - S_R(\omega,\tau)\sin(\alpha\tau) + \sum_{\tau=-\infty}^{\infty} k(\tau,\tau)\sin(\alpha\tau) \quad .(2.6.22)$$

From equations (2.6.22) and (2.6.20), we obtain

$$K_I(\omega,\omega-\alpha) = \frac{1}{2\pi}(\text{p.v.})\int_{-\pi}^{\pi} K_R(\Theta,\Theta-\alpha)\cot\left(\frac{\omega-\Theta}{2}\right)d\Theta - H_o(\alpha) \ , \qquad (2.6.23)$$

where

$$H_o(\alpha) = \sum_{\tau=-\infty}^{\infty} k(\tau,\tau)\sin(\alpha\tau) \ , \qquad (2.6.24)$$

an odd function of α. Proceeding in a similar fashion, we determine that

$$K_R(\omega,\omega-\alpha) = -\frac{1}{2\pi}\,(\text{p.v.})\int_{-\pi}^{\pi} K_I(\Theta,\Theta-\alpha)\cot\left(\frac{\omega-\Theta}{2}\right)d\Theta + H_e(\alpha)\,, \qquad (2.6.25)$$

where

$$H_e(\alpha) = \sum_{\tau=-\infty}^{\infty} k(\tau,\tau)\cos(\alpha\tau)\,, \qquad (2.6.26)$$

an even function of α. From equation (2.6.8), it is straightforward to show that

$$\frac{1}{2\pi}\int_{-\pi}^{\pi} K(\omega,\omega-\alpha)\,d\omega = H_e(\alpha) - iH_o(\alpha)\,. \qquad (2.6.27)$$

It should also be noted that equations (2.6.23) through (2.6.27) hold for any causal, constant-rate LTV system for which $K(\omega,\alpha)$ exists.

Consider equation (2.6.1) and note that we may express the real and imaginary components of the transmission function as

$$K_R(\omega,\omega-\alpha) = \sum_{n=-\infty}^{\infty} a_{Rn}(\omega-\alpha)\,\delta(\omega - \omega_n(\omega-\alpha)) \qquad (2.6.28)$$

and

$$K_I(\omega,\omega-\alpha) = \sum_{n=-\infty}^{\infty} a_{In}(\omega-\alpha)\,\delta(\omega - \omega_n(\omega-\alpha))\,, \qquad (2.6.29)$$

where $a_{Rn}(\alpha)$ and $a_{In}(\alpha)$ are the real and imaginary components of $a_n(\alpha)$. From equation (2.6.23), we obtain

$$\sum_{n=-\infty}^{\infty} a_{In}(\omega-\alpha)\, d(\omega - \omega_n(\omega-\alpha)) =$$

$$\sum_{n=-\infty}^{\infty} \frac{1}{2\pi} (p.v.) \int_{-\pi}^{\pi} a_{Rn}(\Theta-\alpha)\, \delta(\Theta-\omega_n(\Theta-\alpha)) \cot\left(\frac{\omega-\Theta}{2}\right) d\Theta - H_o(\alpha) \; . \quad (2.6.30)$$

Notice that the left-hand side of equation (2.6.30) is identically zero for all $\omega \neq \omega_n(\omega-\alpha)$, which implies that the summation on the right-hand side of equation (2.6.30) is identically zero for all $\omega \neq \omega_n(\omega-\alpha)$. This will occur only if $\delta(\omega-\omega_n(\omega-\alpha))$ is not a function of ω, in other words only if $\omega_n(\alpha)$ is a linear function of α. We can therefore express $\omega_n(\alpha)$ as

$$\omega_n(\alpha) = \alpha + \omega_{on} \quad , \quad (2.6.31)$$

where ω_{on} is some initial offset for the n-th response curve. From equations (2.6.1), (2.6.27), and (2.6.31), we obtain the relation

$$\frac{1}{2\pi} \int_{-\pi}^{\pi} K(\omega,\omega-\alpha)\, d\omega = \sum_{n=-\infty}^{\infty} A_n\, \delta(\alpha-\omega_{on}) \quad , \quad (2.6.32)$$

where

$$A_n = \left(\frac{1}{2\pi} \int_{-\pi}^{\pi} a_n(\beta)\, d\beta \right) \quad (2.6.33)$$

so that

$$H_e(\alpha) = \sum_{n=-\infty}^{\infty} A_{Rn}\, \delta(\alpha-\omega_{on}) \quad (2.6.34)$$

and

$$H_o(\alpha) = \sum_{n=-\infty}^{\infty} A_{In}\, \delta(\alpha-\omega_{on}) \quad , \quad (2.6.35)$$

where A_{Rn} and A_{Rn} are the real and imaginary components of A_n. To summarize, we have seen that a causal, constant-rate LTV system with an almost periodic frequency response function has a system transmission function given by

$$K(\omega,\alpha) = \sum_{n=-\infty}^{\infty} a_n(\alpha)\,\delta(\omega - \alpha - \omega_{on}) \quad . \tag{2.6.36}$$

From equation (2.6.36) above we see that the transmission function for a causal, constant-rate LPTV system is non-zero only along a set of lines with unit slope in the (ω,α) plane. The set of offset frequencies, ω_{on}, in one sense can be interpreted as the response of the LPTV system due to a constant unit input sequence and is therefore determined by $\kappa(t,0)$.

Now consider the case of a causal, integer rate-increase LPTV system, in other words a system for which $\rho = m$, an integer. From equation (2.6.8), we have the relation

$$K(\omega,m\omega-\alpha) = \sum_{t=-\infty}^{\infty} \sum_{\tau=-\infty}^{\infty} k(t,\tau)\, e^{i(m\omega-\alpha)\tau}\, e^{-i\omega t} \quad , \tag{2.6.37}$$

or by a change of variables

$$K(\omega,m\omega-\alpha) = \sum_{\tau=-\infty}^{\infty} \left(\sum_{\gamma=-\infty}^{\infty} s(\gamma,\tau)\, e^{-i\omega\gamma} \right) e^{-i\alpha\tau} \quad . \tag{2.6.38}$$

In equation (2.6.38), we have defined the one-sided sequence

$$s(\gamma,\tau) = k(\gamma+m\tau,\tau) = 0 \;,\; \gamma < 0 \quad . \tag{2.6.39}$$

The term in brackets in equation (2.6.38) is the Fourier transform of $s(\gamma,\tau)$ with respect to γ, so that the Hilbert transform relations of equations (2.6.16) and (2.6.17) still apply. Proceeding along the same lines presented for the constant-rate system, we obtain

$$K_I(\omega,m\omega-\alpha) = \frac{1}{2\pi} \text{ (p.v.)} \int_{-\pi}^{\pi} K_R(\Theta,m\Theta-\alpha) \cot\left(\frac{\omega-\Theta}{2}\right) d\Theta - H_o(\alpha) , \qquad (2.6.40)$$

where

$$H_o(\alpha) = \sum_{\tau=-\infty}^{\infty} k(m\tau,\tau) \sin(\alpha\tau) , \qquad (2.6.41)$$

and

$$K_R(\omega,m\omega-\alpha) = -\frac{1}{2\pi} \text{ (p.v.)} \int_{-\pi}^{\pi} K_I(\Theta,m\Theta-\alpha) \cot\left(\frac{\omega-\Theta}{2}\right) d\Theta + H_e(\alpha) , \qquad (2.6.42)$$

where

$$H_e(\alpha) = \sum_{\tau=-\infty}^{\infty} k(m\tau,\tau) \cos(\alpha\tau) . \qquad (2.6.43)$$

Furthermore, it is straightforward to show that

$$\frac{1}{2\pi} \int_{-\pi}^{\pi} K(\omega,m\omega-\alpha)\, d\omega = H_e(\alpha) - iH_o(\alpha) . \qquad (2.6.44)$$

It is appropriate to note that equations (2.6.40) through (2.6.44) apply for any causal, integer-rate-increase LTV system for which $K(\omega,\alpha)$ exists.

From equation (2.6.1), we may write the real and imaginary components of $K(\omega,m\omega+\alpha)$ as

$$K_R(\omega,m\omega-\alpha) = \sum_{n=-\infty}^{\infty} a_{Rn}(m\omega-\alpha)\, \delta(\omega - \omega_n(m\omega-\alpha)) \qquad (2.6.45)$$

and

$$K_I(\omega,m\omega-\alpha) = \sum_{n=-\infty}^{\infty} a_{In}(m\omega-\alpha)\,\delta(\omega - \omega_n(m\omega-\alpha)) \ , \qquad (2.6.46)$$

where $a_{Rn}(\alpha)$ and $a_{In}(\alpha)$ are the real and imaginary components of $a_n(\alpha)$. From equation (2.6.40), we obtain

$$\sum_{n=-\infty}^{\infty} a_{In}(m\omega-\alpha)\,\delta(\omega - \omega_n(m\omega-\alpha)) =$$

$$\sum_{n=-\infty}^{\infty} \frac{1}{2\pi}(\text{p.v.}) \int_{-\pi}^{\pi} a_{Rn}(m\Theta-\alpha)\delta(\Theta-\omega_n(m\Theta-\alpha))\cot\left(\frac{\omega-\Theta}{2}\right)d\Theta - H_o(\alpha) \ . \qquad (2.6.47)$$

We can again argue that the only way that both sides of equation (2.6.47) above can be zero for $\omega \neq \omega_n(m\omega-\alpha)$ is for $\delta(\omega - \omega_n(m\omega-\alpha))$ to be independent of ω. This is the case only if $\omega_n(\alpha)$ is a linear function such that

$$\omega_n(\alpha) = \frac{\alpha}{m} + \omega_{on} \ , \qquad (2.6.48)$$

where ω_{on} is some initial offset for the n-th response curve. From equations (2.6.1), (2.6.44), and (2.6.48) we obtain

$$\frac{1}{2\pi} \int_{-\pi}^{\pi} K(\omega,m\omega-\alpha)\,d\omega = \frac{1}{m} \sum_{n=-\infty}^{\infty} A_n\,\delta(\alpha-\omega_{on}) \ , \qquad (2.6.49)$$

where

$$A_n = \left(\frac{1}{2\pi} \int_{-\pi}^{\pi} a_n(\beta)\,d\beta \right) \qquad (2.6.50)$$

so that

$$H_c(\alpha) = \frac{1}{m} \sum_{n=-\infty}^{\infty} A_{Rn}\,\delta(\alpha-\omega_{on}) \qquad (2.6.51)$$

and

$$H_o(\alpha) = \frac{1}{m} \sum_{n=-\infty}^{\infty} A_{In}\, \delta(\alpha - \omega_{on}) \ , \tag{2.6.52}$$

where A_{Rn} and A_{In} are the real and imaginary components of A_n. To summarize, we have seen that a causal, integer-rate-increase LPTV system has a system transmission function given by

$$K(\omega,\alpha) = \sum_{n=-\infty}^{\infty} a_n(\alpha)\, \delta(\omega - \frac{\alpha}{m} - \omega_{on}) \ . \tag{2.6.53}$$

From equation (2.6.53) above we see that the transmission function for a causal, integer-rate-increase LPTV system is non-zero only along a set of lines with slope 1/m in the (ω,α) plane. Again, the set of offset frequencies, ω_{on}, may be determined from $\kappa(t,0)$, the response of the system to a constant unit input sequence.

Finally, assume that $k(t,\tau)$ represents a causal, stable LPTV system whose input and output sampling rates are rationally related, in other words $\rho = m/n$ for some integer m and n. For the moment, consider that we could rewrite equation (2.6.8) as

$$K(\omega,\alpha) = \sum_{j=0}^{n-1} \sum_{\gamma=-\infty}^{\infty} \sum_{t=-\infty}^{\infty} k(t,n\gamma+j)\, e^{i\alpha(n\gamma+j)}\, e^{-i\omega t} \ . \tag{2.6.54}$$

Now, for $j = 0, 1, \ldots, n-1$, define

$$t_j = \left[\frac{mj}{n} \right] \ , \tag{2.6.55}$$

so that, for $\beta = t - t_j$, equation (2.6.54) can be rewritten as

$$K(\omega,\alpha) = \sum_{j=0}^{n-1} \sum_{\gamma=-\infty}^{\infty} \sum_{\beta=-\infty}^{\infty} k(\beta+t_j,\, n\gamma+j)\, e^{i\alpha(n\gamma+j)}\, e^{-i\omega(\beta+t_j)} \ . \tag{2.6.56}$$

Rearranging terms in equation (2.6.56), we obtain

$$K(\omega,\alpha) = \sum_{j=0}^{n-1} \left(\sum_{\gamma=-\infty}^{\infty} \sum_{\beta=-\infty}^{\infty} \hat{k}_j(\beta,\gamma)\, e^{in\alpha\gamma} e^{-i\omega b} \right) e^{i\alpha j}\, e^{-i\omega t_j} \qquad (2.6.57)$$

where we have defined the function

$$\hat{k}_j(\beta,\gamma) = k(b+t_j,\, n\gamma+j) \quad . \qquad (2.6.58)$$

A great deal of insight into the behavior of the system represented by $\hat{k}_j(\beta,\gamma)$ can be obtained by a careful scrutiny of equation (2.6.58). First, consider that for each j, $\hat{k}_j(\beta,\gamma)$ is the system response function for a stable LPTV system. Stability is obtained from the fact that

$$\sum_{\gamma=-\infty}^{\infty} |\hat{k}_j(\beta,\gamma)| \qquad (2.6.59)$$

is a subseries of

$$\sum_{\tau=-\infty}^{\infty} |k(\beta,\tau)| \quad , \qquad (2.6.60)$$

which converges for each β. Similarly, it is straightforward to show that, since

$$\lim_{t_o\to\infty} \frac{1}{2t_o} \sum_{t=-t_o}^{t_o} \sum_{\tau=-\infty}^{\infty} k(t,\tau)\, e^{i\alpha\tau}\, e^{-i\omega_n(\alpha)t} \qquad (2.6.61)$$

exists for some set of $\omega_n(\alpha)$,

$$\lim_{t_o\to\infty} \frac{1}{2t_o} \sum_{\beta=-t_o}^{t_o} \sum_{\gamma=-\infty}^{\infty} \hat{k}_j(\beta,\gamma)\, e^{in\alpha\gamma}\, e^{-i\omega_n(\alpha)\beta} \qquad (2.6.62)$$

also exists for the same set of $\omega_n(\alpha)$. Finally, consider that

$$\hat{k}_j(\beta,\gamma) = 0 \text{ for all } \beta < m\gamma \; ; \qquad (2.6.63)$$

in other words, $\hat{k}_j(\beta,\gamma)$ is a causal, integer-rate-increase system.

The double summation in equation (2.6.57) above is recognized as the system transmission function corresponding to $\hat{k}_j(\beta,\gamma)$, denoted $\hat{K}_j(\omega,n\alpha)$. We therefore obtain

$$K(\omega,\alpha) = \sum_{j=0}^{n-1} \hat{K}_j(\omega,n\alpha)\, e^{i\alpha j}\, e^{-i\omega t_j} . \qquad (2.6.64)$$

From the discussion of intege.-rate-increase LPTV systems presented above, we know that $\hat{K}_j(\omega,\Theta)$ is non-zero only along a set of lines defined by

$$\omega = \frac{\Theta}{m} + \omega_{on} \quad . \qquad (2.6.65)$$

From equation (2.6.62), we know that the ω_{on} are the same for each integer-rate-increase system since $\omega_{on} = \omega_n(0)$. By inspection of equation (2.6.64), we may therefore conclude that the system transmission function for the m/n rational-rate system is non-zero only along the set of lines defined by

$$\omega = \frac{n}{m}\alpha + \omega_{on} \quad . \qquad (2.6.66)$$

Again, the set of offset frequencies may be obtained by evaluating the response of the system to a constant unit input sequence.

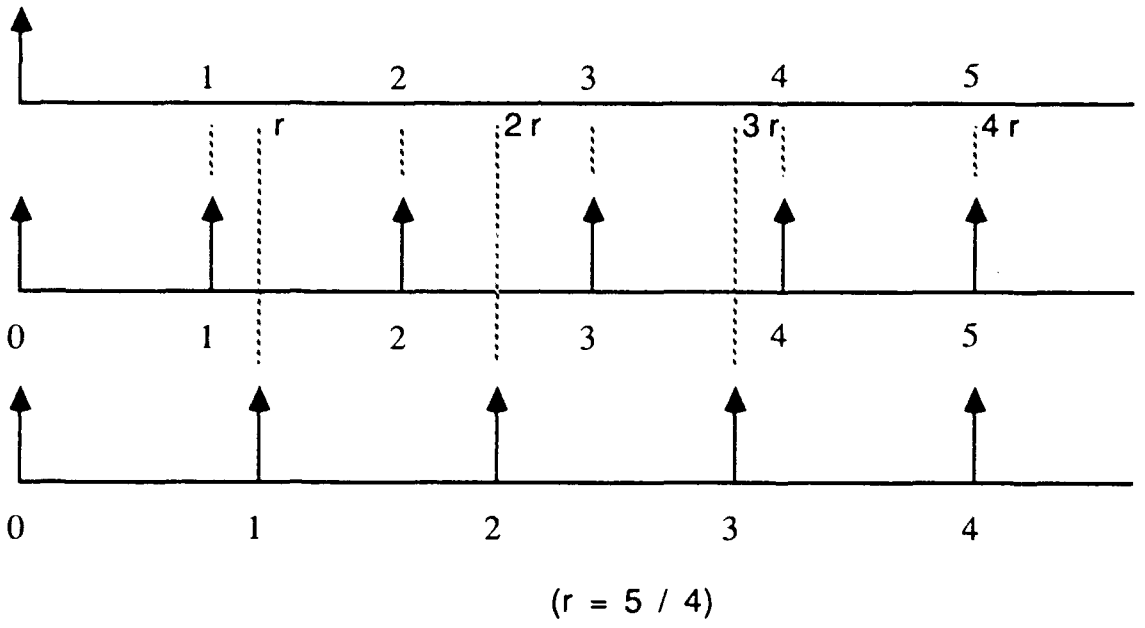

AS-91-366

FIGURE 2.6.1
INPUT AND OUTPUT SAMPLE RATE RELATIONS

2.7 CHAPTER SUMMARY

In this chapter, we have presented some of the fundamental concepts of the analysis of linear, discrete-time time-varying systems. Both time-domain and frequency-domain characterizations of discrete-time LTV systems have been presented. The implications of stability and causality for LTV systems have been discussed, along with a presentation of the analysis of LTV network structures. The discussion of classes of LTV systems will prove valuable to us when we begin to consider modeling discrete-time nonstationary random processes using LTV systems.

3. MODELING AND FREQUENCY-DOMAIN ANALYSIS OF NONSTATIONARY RANDOM PROCESSES VIA LINEAR TIME-VARYING SYSTEMS

The use of linear time-invariant system models has proven very useful in the analysis of stationary random processes. In general, one may assume an observed wide-sense stationary random process is the output of a LTI system excited by a purely random or white noise process (see Koopmans, 1974, pp. 233-238). Frequency-domain characterizations of the underlying system model yield insight into the spectral content of the observed random process (see Priestley, 1981, pp. 267-268). Time-domain characterizations for the underlying system model can be used to predict values of the observed random process or to filter the random process in some optimum sense (see Koopmans, 1974, pp. 212-217).

In a similar fashion, linear time-varying system models are useful in the analysis of nonstationary random processes. In this chapter, we will discuss modeling a nonstationary random process as the output of a LTV system excited by a white noise process. Spectral representations of the nonstationary random process which can be derived from the frequency-domain characterization of the underlying system model will then be presented. A discussion of the implications of the properties of the observed random process on the characteristics of the underlying LTV system model is presented, with particular attention paid to almost cyclostationary random processes. Finally, the characterization of certain classes of nonstationary random processes via the spectral correlation function is presented. For a more thorough treatment of these topics, see Priestly, 1981, pp. 817-866, and Gardner, 1986, pp. 301-359.

3.1 LINEAR TIME-VARYING SYSTEM MODELS FOR NONSTATIONARY RANDOM PROCESSES

In order to introduce the concept of a LTV system model for nonstationary random processes, we first review the notion of a LTI system model for stationary random processes. Let $\{y(t)\}$ be a wide-sense stationary discrete-time random process such that

$$E[y(t)] = 0 \tag{3.1.1}$$

and

$$E[\,|\,y(t)\,|^2\,] = \sigma^2 < \infty \ . \tag{3.1.2}$$

By the Wold decomposition theorem (see Koopmans, 1974, pp. 255-256), we know that $\{y(t)\}$ can be expressed as

$$y(t) = \mu(t) + v(t) \tag{3.1.3}$$

where the processes $\{\mu(t)\}$ and $\{v(t)\}$ are uncorrelated zero-mean wide-sense stationary discrete-time random processes with the following properties:

(i) $\{\mu(t)\}$ can be represented as the output of a LTI filter excited by a wide-sense stationary, zero-mean purely random (i.e., white noise) process. In other words,

$$\mu(t) = \sum_{\lambda = -\infty}^{\infty} h(t-\lambda)\, \varepsilon(\lambda) \tag{3.1.4}$$

where

$$E[\varepsilon(\lambda_1)\varepsilon^*(\lambda_2)] = \sigma^2\, \zeta(\lambda_1-\lambda_2) \ . \tag{3.1.5}$$

Furthermore, the LTI system represented by $h(\lambda)$ is causal, and has the property

$$\sum_{\lambda = -\infty}^{\infty} |\,h(\lambda)\,|^2 < \infty \ . \tag{3.1.6}$$

(ii) The process $\{v(t)\}$ is purely deterministic, in other words the present value of $\{v(t)\}$ may be completely determined by linear functions of its past values.

For the moment, we will consider the case when the deterministic component of $\{y(t)\}$ is not present, in other words assume $v(t) = 0$ for each t. We make this assumption without loss of generality since, from property (ii) above we could make a prediction for n(t) from

past observations of the process {y(t)} and remove this deterministic component from {y(t)}. We may therefore without loss of generality express {y(t)} as

$$y(t) = \sum_{\lambda = -\infty}^{\infty} h(t-\lambda)\, \varepsilon(\lambda) \ . \tag{3.1.7}$$

An extension of the Wold decomposition theory for nonstationary discrete-time random processes is given in Cramer, 1961. Again assume that {y(t)} is a discrete-time random process satisfying

$$E[y(t)] = 0 \tag{3.1.8}$$

and

$$E[\ |\ y(t)\ |^2\ ] < \infty \tag{3.1.9}$$

for each t, but now assume {y(t)} is nonstationary. We can then express y(t) as

$$y(t) = \mu(t) + \nu(t) \tag{3.1.10}$$

where the processes {μ(t)} and {ν(t)} are uncorrelated zero-mean discrete-time random processes with the following properties:

(i) {μ(t)} can be represented as the output of a LTV filter excited by a wide-sense stationary, zero-mean purely random process. In other words,

$$\mu(t) = \sum_{\tau = -\infty}^{\infty} k(t,\tau)\, \varepsilon(\tau) \tag{3.1.11}$$

where

$$E[\varepsilon(\tau_1)\varepsilon^*(\tau_2)] = \sigma^2\, \zeta(\tau_1-\tau_2) \ . \tag{3.1.12}$$

Furthermore, the LTV system represented by $k(t,\tau)$ is causal, and has the property

$$\sum_{\tau=-\infty}^{\infty} | k(t,\tau) |^2 < \infty \quad . \tag{3.1.13}$$

(ii) The process $\{v(t)\}$ is purely deterministic; in other words, the present value of $\{v(t)\}$ may be completely determined by linear functions of its past values.

Consider that, since $v(t)$ is purely deterministic, we can predict its current value from past observations of $y(t)$ and so remove its contribution from the observed random process. We may therefore without loss of generality restrict our attention to nonstationary random processes of the form

$$y(t) = \sum_{\tau=-\infty}^{\infty} k(t,\tau)\, \varepsilon(\tau) \quad . \tag{3.1.14}$$

Note that equation (3.1.13) does not ensure BIBO stability for the LTV system for each t. However, from the theory of Fourier series (see Koopmans, 1974, pp. 19-21) we know that equation (3.1.13) holds if there exists some function $\kappa(t,\alpha)$, periodic in α with period 2π, which is continuous for almost all α such that

$$\kappa(t,\alpha) = \sum_{\tau=-\infty}^{\infty} k(t,\tau)\, e^{i\alpha\tau} \quad . \tag{3.1.15}$$

Furthermore, we have the relationship

$$\frac{1}{2\pi} \int_{-\pi}^{\pi} | \kappa(t,\alpha) |^2 \, d\alpha = \sum_{\tau=-\infty}^{\infty} | k(t,\tau) |^2 \tag{3.1.16}$$

for each t (see Koopmans, 1974, p. 20). We will make use of the fact that the frequency response function for the LTV system model exists when we consider frequency-domain representations of nonstationary random processes.

Notice that equation (3.1.13) ensures that the LTV system model will exhibit limited memory, as discussed in Section 2.2. In other words, the contribution to some present value of $\{y(t)\}$ due to an input in the remote past is negligible. Causality of the LTV system model guarantees that $\{y(t)\}$ does not depend on future values of the input. We may therefore argue that input values contributing significantly to $\{y(t)\}$ at some present time are distinct from those input values contributing significantly to $\{y(t)\}$ in the remote past. If we further assume that the $\{\varepsilon(\tau)\}$ are independent and identically distributed, then we may make a mixing assumption for $\{y(t)\}$, i.e., present values of $\{y(t)\}$ are virtually independent of values of $\{y(t)\}$ in the remote past. This mixing assumption for $\{y(t)\}$ will ensure that appropriate statistical averages involving $\{y(t)\}$ are asymptotically convergent (see Billingsley, 1968, pp. 166-167).

3.2 SPECTRAL REPRESENTATIONS FOR NONSTATIONARY RANDOM PROCESSES

Assume $\{y(t)\}$ is a nonstationary, discrete-time random process satisfying

$$E[y(t)] = 0 \tag{3.2.1}$$

and

$$E[\,|y(t)|^2\,] < \infty \ . \tag{3.2.2}$$

By the discussion presented in the previous section, we know that $y(t)$ can be represented as

$$y(t) = \sum_{\tau=-\infty}^{\infty} k(t,\tau)\,\varepsilon(\tau) \tag{3.2.3}$$

where $\varepsilon(\tau)$ is a zero-mean, wide-sense stationary, purely random discrete-time process with variance σ^2. From the theory of spectral representations for wide-sense stationary random processes, we know that $\{\varepsilon(\tau)\}$ can be represented as

$$\varepsilon(\tau) = \frac{1}{2\pi} \int_{-\pi}^{\pi} e^{i\alpha\tau}\, dZ(\alpha) \ , \tag{3.2.4}$$

where $\{Z(\alpha)\}$ is a zero-mean complex-valued random process over $(-\pi,\pi)$ with orthogonal increments; in other words,

$$E[dZ(\alpha_1)dZ^*(\alpha_2)] = 2\pi\sigma^2\,\delta(\alpha_1-\alpha_2)\,d\alpha_1\,d\alpha_2 \tag{3.2.5}$$

(see Priestley, 1981, pp. 250-251).

Now consider substituting the spectral representation for $\varepsilon(\tau)$ given by equation (3.2.4) into the LTV system model for y(t) given by equation (3.2.3). Our expression for y(t) then becomes

$$y(t) = \sum_{\tau=-\infty}^{\infty} k(t,\tau)\left(\frac{1}{2\pi}\int_{-\pi}^{\pi} e^{i\alpha\tau}\,dZ(\alpha)\right) . \tag{3.2.6}$$

Interchanging the order of summation and integration in equation (3.2.6) above, we obtain

$$y(t) = \frac{1}{2\pi}\int_{-\pi}^{\pi}\left(\sum_{\tau=-\infty}^{\infty} k(t,\tau)\,e^{i\alpha\tau}\right)dZ(\alpha) . \tag{3.2.7}$$

Note that the summation in brackets in (3.2.7) above is the frequency response function for the LTV system, $\kappa(t,\alpha)$. We know that the frequency response function exists from equation (3.1.15). Substituting the frequency response function into equation (3.2.7) above, we obtain

$$y(t) = \frac{1}{2\pi}\int_{-\pi}^{\pi} \kappa(t,\alpha)\,dZ(\alpha) . \tag{3.2.8}$$

Equation (3.2.8) defines the evolutionary spectral representation of the nonstationary (or evolutionary) random process $\{y(t)\}$ (see Priestley, 1965, and Priestley, 1981, pp. 825-826). As such, it is analogous to the spectral representation for wide-sense stationary random processes. We will see that this representation of a nonstationary random process is useful in the characterization of nonstationary signals. We will also present the implications of various properties of the process $\{y(t)\}$ on the behavior of the underlying system model, $k(t,\tau)$.

3.3 CLASSES OF NONSTATIONARY RANDOM PROCESSES AND IMPLICATIONS OF LINEAR TIME-VARYING SYSTEM MODELS

We have seen in the previous section that a zero-mean, finite variance nonstationary random process $\{y(t)\}$ may be modeled as the output of a LTV system excited by a wide-sense stationary random process; in other words,

$$y(t) = \sum_{\tau=-\infty}^{\infty} k(t,\tau)\, \varepsilon(\tau) \quad . \tag{3.3.1}$$

The evolutionary spectral representation of the process, given by

$$y(t) = \frac{1}{2\pi} \int_{-\pi}^{\pi} \kappa(t,\alpha)\, dZ(\alpha) \quad , \tag{3.3.2}$$

was also presented. Consider from equation (3.3.2) that the statistical properties of the random function, $\{y(t)\}$, are intimately related to the properties of the frequency response function of the underlying LTV system model, $\kappa(t,\alpha)$. In this section we will consider the implications of the system response function, $\kappa(t,\alpha)$, on the statistical properties of $\{y(t)\}$ for the class of almost cyclostationary random processes.

Define the (symmetric) autocorrelation function for the random process $\{y(t)\}$ as

$$R_{yy}(t,\lambda) = E\left[\, y(t+\lambda)y^*(t-\lambda) \,\right] \quad . \tag{3.3.3}$$

The random process $\{y(t)\}$ is said to be almost cyclostationary if $R_{yy}(t,\lambda)$ is an almost periodic function of t for each λ (see Gardner, 1986, p. 302). In other words,

$$R_{yy}(t,\lambda) = \sum_{n=-\infty}^{\infty} r_n(\lambda)\, e^{i\phi_n t} \tag{3.3.4}$$

where

$$r_n(\lambda) = \lim_{T\to\infty} \frac{1}{2T} \sum_{t=-T}^{T} R_{yy}(t,\lambda)\, e^{-i\phi_n t} \tag{3.3.5}$$

and $\{\phi_n\}$ is a sequence of increasing frequencies independent of λ.

The random process $\{y(t)\}$ is almost cyclostationary if the underlying LTV model for $\{y(t)\}$ has a frequency response function which is almost periodic in t for all a, in other words if $k(t,\tau)$ represents a LPTV system. In order to understand this, first assume that the frequency response function for the underlying LTV system model is almost periodic in t. From the discussion of almost periodic frequency response functions presented in Chapter 2, we know that

$$\kappa(t,\alpha) = \sum_{n=-\infty}^{\infty} a_n(\alpha)\, e^{i\omega_n(\alpha)t} \tag{3.3.6}$$

where

$$a_n(\alpha) = \lim_{t_o\to\infty} \frac{1}{2t_o} \sum_{t=-t_o}^{t_o} \kappa(t,\alpha)\, e^{-i\omega_n(\alpha)t} \quad . \tag{3.3.7}$$

From the LTV system model for $\{y(t)\}$ given by (3.3.1), we obtain

$$y(t) = \sum_{n=-\infty}^{\infty} \frac{1}{2\pi} \int_{-\pi}^{\pi} a_n(\alpha)\, e^{i\omega_n(\alpha)t}\, dZ(\alpha) \quad . \tag{3.3.8}$$

Substituting equation (3.3.8) into the expression for $R_{yy}(t,\lambda)$ given by equation (3.3.3) and simplifying, we obtain

$$R_{yy}(t,\lambda) = \sigma^2 \sum_{\tau=-\infty}^{\infty} k(t+\lambda,\tau)k^*(t-\lambda,\tau) \quad . \tag{3.3.9}$$

It is straightforward to show that

$$R_{yy}(t,\lambda) = \frac{\sigma^2}{2\pi} \int_{-\pi}^{\pi} \kappa(t+\lambda,\alpha)\kappa^*(t-\lambda,\alpha)\, d\alpha \quad . \tag{3.3.10}$$

Substituting for $\kappa(t,\alpha)$ from equation (3.3.6) into (3.3.10), we obtain

$$R_{yy}(t,\lambda) = \frac{\sigma^2}{2\pi} \int_{-\pi}^{\pi} \sum_{n=-\infty}^{\infty} \sum_{m=-\infty}^{\infty} a_n(\alpha)a^*_m(\alpha)\, e^{i\omega_n(\alpha)(t+\lambda)} e^{-i\omega_m(\alpha)(t-\lambda)}\, d\alpha \,. \tag{3.3.11}$$

Recall that the LTV system represented by $k(t,\tau)$ is causal, and so from the discussion of causal LPTV systems presented in Chapter 2, we know that

$$\omega_n(\alpha) = \rho\alpha + \omega_{on} \quad . \tag{3.3.12}$$

Our expression for $R_{yy}(t,\lambda)$ can therefore be rewritten as

$$R_{yy}(t,\lambda) = \frac{\sigma^2}{2\pi} \sum_{n=-\infty}^{\infty} \sum_{m=-\infty}^{\infty} \int_{-\pi}^{\pi} a_n(\alpha)a^*_m(\alpha) e^{i(2\rho\alpha+\omega_{on}+\omega_{om})\lambda} d\alpha\, e^{i(\omega_{on}-\omega_{om})t} \,. \tag{3.3.13}$$

Notice that the sequence

$$\{\omega_{on}-\omega_{om}:\ n = \ldots, -1, 0, 1, \ldots ;\ m = \ldots, -1, 0, 1, \ldots\} \tag{3.3.14}$$

can be thought of as a sequence

$$\{\phi_j:\ j = \ldots, -1, 0, 1, \ldots\} \tag{3.3.15}$$

of distinct, increasing frequencies. Now define

$$r_j(\lambda) = \frac{\sigma^2}{2\pi} \sum_{NM_j} \int_{-\pi}^{\pi} a_n(\alpha)a^*_m(\alpha)\, e^{i(2\rho\alpha+\omega_{on}+\omega_{om})\lambda} d\alpha \tag{3.3.16}$$

where the set

$$NM_j = \{\ n,m:\ \omega_{on}-\omega_{om} = \phi_j\ \}\ . \tag{3.3.17}$$

Our expression for $R_{yy}(t,\lambda)$ may therefore be rewritten as

$$R_{yy}(t,\lambda) = \sum_{j=-\infty}^{\infty} r_j(\lambda)\, e^{i\phi_j t}\ ; \tag{3.3.18}$$

in other words, $R_{yy}(t,\lambda)$ is an almost periodic function in t. So, if the underlying LTV system frequency response function is an almost periodic function of t, then $\{y(t)\}$ will be an almost cyclostationary process.

Next, assume that $\{y(t)\}$ is almost cyclostationary, but the frequency response function for the underlying LTV system model is not almost periodic. In other words, assume that

$$\lim_{t_o\to\infty} \frac{1}{2t_o} \sum_{t=-t_o}^{t_o} \kappa(t,\alpha)\, e^{-i\omega t} = 0 \tag{3.3.19}$$

for any choice of ω or α. Consider that equation (3.3.19) implies that

$$\sum_{t=-\infty}^{\infty} \kappa(t,\alpha)\, e^{-i\omega t} \tag{3.3.20}$$

exists for all ω and α. Since the product of convergent series is convergent, equation (3.3.20) implies that

$$\sum_{t_1\,=\,-\infty}^{\infty} \sum_{t_2\,=\,-\infty}^{\infty} \kappa(t_1,\alpha)\kappa^*(t_2,\alpha)\, e^{-i\omega_1 t_1}\, e^{-i\omega_2 t_2} \tag{3.3.21}$$

exists, or by a change of variables,

$$\sum_{\lambda\,=\,-\infty}^{\infty} \sum_{t\,=\,-\infty}^{\infty} \kappa(t+\lambda,\alpha)\kappa^*(t-\lambda,\alpha)\, e^{-i\phi t}\, e^{-i\psi\lambda} \tag{3.3.22}$$

exists for all ϕ and ψ.

Since $\{y(t)\}$ is almost cyclostationary,

$$\lim_{T\to\infty} \frac{1}{2T} \sum_{t=-T}^{T} R_{yy}(t,\lambda)\, e^{-i\phi_n t} \tag{3.3.23}$$

exists and is nonzero for some sequence of $\{\phi_n\}$ and some λ. From equation (3.3.10), we obtain

$$\int_{-\pi}^{\pi} \lim_{T\to\infty} \frac{1}{2T} \sum_{t=-T}^{T} \kappa(t+\lambda,\alpha)\kappa^*(t-\lambda,\alpha)\, e^{-i\phi_n t}\, d\alpha \tag{3.3.24}$$

exists and is nonzero. Notice that equation (3.3.24) implies that

$$\lim_{T\to\infty} \frac{1}{2T} \sum_{t=-T}^{T} \kappa(t+\lambda,\alpha)\kappa^*(t-\lambda,\alpha)\, e^{-i\phi_n t} \tag{3.3.25}$$

exists and is nonzero over some interval in α. Moreover, equation (3.3.25) implies that

$$\sum_{t=-\infty}^{\infty} \kappa(t+\lambda,\alpha)\kappa^*(t-\lambda,\alpha)\, e^{-i\phi_n t} \tag{3.3.26}$$

diverges. Notice that if the sum in equation (3.3.26) diverges, then the sum in equation (3.3.22) also diverges, which is a contradiction.

From the discussion presented above, we see that the characterization of almost cyclostationary random processes is intimately related to the characterization of LTV systems with almost periodic frequency response functions. We will make use of this fact when we consider the empirical analysis of LTV systems in Chapter 4.

3.4 SPECTRAL CORRELATION FUNCTIONS FOR NONSTATIONARY RANDOM PROCESSES

The conventional power spectrum has proven to be a useful means of characterizing wide-sense stationary random processes in the frequency domain. Various extensions of the concept of the power spectrum for nonstationary random processes have been proposed over the years (see Lyones, 1968, and Cohen, 1989, for a review of the subject). In this section, we will discuss a technique which has proven useful in the study of finite-energy and almost cyclostationary random processes. This technique is based on the fact that, for a nonstationary random process, correlation exists between distinct frequency components of the spectral representation. Estimates of the spectral correlation function therefore provide a means of characterizing the random process in the frequency domain. For a more thorough treatment of the subject of spectral correlation functions, see Gardner, 1986, pp. 301-359, and Bendat and Piersol, 1986, pp. 447-468.

Assume that $\{x(\tau)\}$ and $\{y(t)\}$ are discrete-time random processes such that

$$E[\, x(\tau) \,] = 0 \ , \tag{3.4.1}$$

$$E[\, |\, x(\tau) \,|^2 \,] < \infty \ , \tag{3.4.2}$$

and

$$|\, x(\tau) \,| < \infty \tag{3.4.3}$$

for each τ and for every realization of $\{x(\tau)\}$, and such that

$$E[\, y(t) \,] = 0 \ , \tag{3.4.4}$$

$$E[\, |\, y(t) \,|^2 \,] < \infty \ , \tag{3.4.5}$$

and

$$|\, y(t) \,| < \infty \tag{3.4.6}$$

for each t and for every realization of $\{y(t)\}$. Define the finite-duration Fourier transforms of $\{x(\tau)\}$ and $\{y(t)\}$ as

$$X_0(\alpha) = \sum_{\tau=-\tau_0}^{\tau_0} x(\tau)\, e^{-i\alpha\tau} \tag{3.4.7}$$

and

$$Y_0(\omega) = \sum_{t=-t_0}^{t_0} y(t)\, e^{-i\omega t} . \tag{3.4.8}$$

Note that both $X_0(\alpha)$ and $Y_0(\omega)$ exist since, from equations (3.4.3) and (3.4.6), they are finite sums of finite-amplitude sequences. Formally define the cross-spectral correlation function as

$$S_{YX}(\omega,\alpha) = \lim_{t_0\to\infty} \lim_{\tau_0\to\infty} E\left[Y_0(\omega)X_0^*(\alpha)\right] \tag{3.4.9}$$

(see Bendat and Piersol, 1986, pp. 448-450). Notice that, in some sense, the cross-spectral correlation function indicates the amount of correlation between distinct spectral components of the two random processes, $\{x(\tau)\}$ and $\{y(t)\}$. Substituting the definitions for the finite-duration Fourier transforms given by equations (3.4.7) and (3.4.8) into (3.4.9), we obtain

$$S_{YX}(\omega,\alpha) = \lim_{t_0\to\infty} \lim_{\tau_0\to\infty} \sum_{t=-t_0}^{t_0} \sum_{\tau=-\tau_0}^{\tau_0} R_{YX}(t,\tau)\, e^{i\alpha\tau}\, e^{-i\omega t} \tag{3.4.10}$$

where we have defined the (asymmetric) autocorrelation function

$$R_{YX}(t,\tau) = E[y(t)\, x^*(\tau)] \quad . \tag{3.4.11}$$

Assuming that the limit in equation (3.4.10) exists, we obtain

$$S_{YX}(\omega,\alpha) = \sum_{t=-\infty}^{\infty} \sum_{\tau=-\infty}^{\infty} R_{YX}(t,\tau)\, e^{i\alpha\tau}\, e^{-i\omega t} \quad . \tag{3.4.12}$$

For the moment, assume that $\{x(\tau)\}$ and $\{y(t)\}$ are wide-sense stationary random processes so that

$$R_{YX}(t,\tau) = \mathcal{R}_{YX}(t-\tau) \quad . \tag{3.4.13}$$

From equation (3.4.12), we obtain

$$S_{YX}(\omega,\alpha) = \sum_{t=-\infty}^{\infty} \sum_{\tau=-\infty}^{\infty} \mathcal{R}_{YX}(t-\tau)\, e^{i\alpha\tau}\, e^{-i\omega t} \quad , \tag{3.4.14}$$

or by the change of variables $\lambda = t-\tau$,

$$S_{YX}(\omega,\alpha) = \sum_{\tau=-\infty}^{\infty} \left(\sum_{\lambda=-\infty}^{\infty} \mathcal{R}_{YX}(\lambda)\, e^{-i\omega\lambda} \right) e^{-i(\omega-\alpha)\tau} \quad . \tag{3.4.15}$$

Notice that the summation in brackets in equation (3.4.15) above is the conventional cross-power spectrum, $S_{YX}(\omega)$ (see Bendat and Piersol, 1986, p. 121). Equation (3.4.15) therefore becomes

$$S_{YX}(\omega,\alpha) = S_{YX}(\omega)\, \delta(\omega-\alpha) \quad . \tag{3.4.16}$$

In other words, wide-sense stationary random processes exhibit spectral correlation only on the line $\omega = \alpha$ in the (ω,α) bifrequency plane.

Consider the system indicated schematically in Figure 3.4.1. The purely random process $\{\varepsilon(\tau)\}$ excites an LTV system represented by $k(t,\tau)$ to produce the nonstationary random process $\{y(t)\}$. This same purely random process also excites the LTI system represented by $h(\tau)$ to produce the wide-sense stationary random process $\{x(\tau)\}$. From the discussion of Chapter 2, we know that $x(\tau)$ is given by

$$x(\tau) = \sum_{\lambda=-\infty}^{\infty} h(\tau-\lambda)\, \varepsilon(\lambda) \quad . \tag{3.4.17}$$

From the spectral representation of $\{\varepsilon(\tau)\}$ given by equation (3.2.4), we obtain

$$x(\tau) = \frac{1}{2\pi} \int_{-\pi}^{\pi} \sum_{\lambda=-\infty}^{\infty} h(\tau-\lambda)\, e^{i\gamma\lambda}\, dZ(\gamma) \quad , \tag{3.4.18}$$

or simply

$$x(\tau) = \frac{1}{2\pi} \int_{-\pi}^{\pi} H(\gamma)\, e^{i\gamma\tau}\, dZ(\gamma) \quad , \tag{3.4.19}$$

where $H(\gamma)$ is the frequency response function of the LTI system given by equation (2.3.6). Substituting equation (3.4.19) into the definition of $X_0(\alpha)$ given by equation (3.4.7), we obtain

$$X_0(\alpha) = \frac{1}{2\pi} \int_{-\pi}^{\pi} H(\gamma) \left(\sum_{\tau=-\tau_0}^{\tau_0} e^{i(\gamma-\alpha)\tau} \right) dZ(\gamma) \, . \tag{3.4.20}$$

Recall from equation (3.2.8) that $\{y(t)\}$ admits the evolutionary spectral representation

$$y(t) = \frac{1}{2\pi} \int_{-\pi}^{\pi} \kappa(t,\alpha)\, dZ(\alpha) \quad . \tag{3.4.21}$$

Substituting equation (3.4.21) into the definition for $Y_0(\omega)$ given by equation (3.4.8), we obtain

$$Y_0(\omega) = \frac{1}{2\pi} \int_{-\pi}^{\pi} \left(\sum_{t=-t_0}^{t_0} \kappa(t,\alpha)\, e^{-i\omega t} \right) dZ(\alpha) \quad . \tag{3.4.22}$$

From the definition of the cross-spectral correlation function given by equation (3.4.9), we obtain

$$S_{YX}(\omega,\alpha) = \lim_{t_0\to\infty} \lim_{\tau_0\to\infty} E\left[Y_0(\omega)X_0^*(\alpha)\right]$$

$$= \frac{\sigma^2}{2\pi} \int_{-\pi}^{\pi} K(\omega,\beta)\, H^*(\beta)\, \delta(\beta-\alpha)\, d\beta \quad , \tag{3.4.23}$$

or, simply,

$$S_{YX}(\omega,\alpha) = \frac{\sigma^2}{2\pi} K(\omega,\alpha)\, H^*(\alpha) \quad . \tag{3.4.24}$$

Notice that equation (3.4.24) gives a very straightforward relationship between the cross-spectral correlation function for $\{y(t)\}$ and $\{x(\tau)\}$ and the linear systems which produced these random processes. We will make use of this fact when we consider the empirical analysis of linear time-varying systems in Chapter 4.

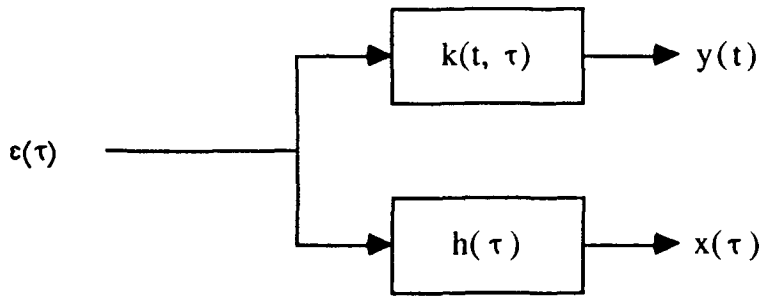

AS-91-367

FIGURE 3.4.1
LTV AND LTI SYSTEMS EXCITED BY A PURELY RANDOM PROCESS

3.5 CHAPTER SUMMARY

In this chapter we have introduced some of the fundamental concepts regarding the modeling of nonstationary random processes using linear time-varying filters. The use of a frequency-domain characterization of the LTV system model to obtain an evolutionary spectral representation for a nonstationary random process was also presented. Finally, the relationship between the LTV system models for nonstationary random processes and the spectral correlation function for these random processes was presented. In the following chapters, these concepts will be applied to the characterization of LTV systems excited by random signals.

4. CHARACTERIZATION OF LINEAR PERIODICALLY TIME-VARYING SYSTEMS

In previous chapters, we reviewed the principal methods for analytically describing a discrete time linear time-varying system and noted the properties of such system descriptions. Techniques for the frequency-domain analysis of the nonstationary signals arising as the outputs of time-varying systems were also presented. We now turn our attention to the problem of empirically characterizing LPTV systems. To be more specific, we require techniques for obtaining a reliable estimate of the system transmission function, $K(\omega,\alpha)$, for a given LPTV system. The development and assessment of these techniques will rely heavily on the concepts and definitions presented earlier.

4.1 CHARACTERIZATION OF LINEAR PERIODICALLY TIME-VARYING SYSTEMS via DETERMINISTIC SIGNALS

Recall the definition of the time-varying system transmission function, $K(\omega,\alpha)$, given by equation (2.3.25)

$$K(\omega,\alpha) = \sum_{t=-\infty}^{\infty} \kappa(t,\alpha)\, e^{-i\omega t} , \tag{4.1.1}$$

where $\kappa(t,\alpha)$ is the time-varying frequency response function. Since $\kappa(t,\alpha)$ is defined as the response of the LPTV system to a complex sinusoid of frequency α, the system transmission function can be viewed as the Fourier transform of the output signal produced by an applied complex sinusoid of frequency α. This observation suggests that one straightforward method of estimating the system transmission function for a given LPTV system would be to apply a complex sinusoid of a known frequency, observe the resulting output signal, and compute an estimate of its Fourier transform. This would yield an estimate of the system transmission function, $K(\omega,\alpha)$, for some specific input frequency, α. Estimates of the system transmission function for other input frequencies could be obtained by repeating this process for each desired input frequency.

Consider applying a complex sinusoid of frequency α to a causal, stable LPTV system. Assume that the input signal, $x(\tau)$, as given by

$$x(\tau) = \cos(\alpha\tau) + i \sin(\alpha\tau) = e^{i\alpha\tau} , \tag{4.1.2}$$

has been applied to the system of interest for a sufficient time for the system to have reached a steady-state condition. If we obtain N samples of the resulting output sequence, y(t), we may compute the Fourier transform of the output sequence, $Y(\omega)$, as

$$Y(\omega) = \sum_{t=0}^{N-1} \kappa(t,\alpha)\, e^{-i\omega t} \quad . \tag{4.1.3}$$

From the properties of the Fourier transform, we obtain

$$Y(\omega) = \frac{1}{2\pi} \int_{-\pi}^{\pi} K(\gamma,\alpha)\, F_N(\gamma-\omega)\, d\gamma \quad , \tag{4.1.4}$$

where $F_N(\gamma)$ is the Fejer kernel, defined as

$$F_N(\gamma) = \sum_{t=0}^{N-1} e^{-i\gamma t} \tag{4.1.5}$$

(see Papoulis, 1962, pp. 42-47). For N sufficiently large, the Fejer kernel may be approximated by a Dirac delta function, and so

$$Y(\omega) \approx K(\omega,\alpha) \quad . \tag{4.1.6}$$

Several points can be made concerning the method of estimating $K(\omega,\alpha)$ presented above. First, the accuracy of the approximation of $K(\omega,\alpha)$ by $Y(\omega)$ is intimately related to the available length of observed data, N. This issue of distortion of the estimate of $K(\omega,\alpha)$ due to finite data lengths closely parallels the issue of distortion of spectral estimates due to finite data lengths. The familiar method of applying a windowing function to the observed data to reduce the effects of finite data lengths could also be applied to improve our estimate of $K(\omega,\alpha)$ (see Harris, 1978). Secondly, this method provides an estimate for $K(\omega,\alpha)$ for some specific input frequency, α. Estimation of $K(\omega,\alpha)$ for other values of α requires that the frequency of the applied signal be changed and that a new record of the output sequence be obtained after sufficient time has passed for a steady-state condition to be reached.

The final point to be made regarding this method relates to the generation of the applied input signal. For a digital implementation of the LPTV system, obtaining a complex sinusoidal input is a relatively straightforward matter, involving no more than the generation of a sequence of sines and cosines. However, in a LPTV system in which analog signals are digitized and then processed to obtain digital sequences, it is impossible to generate a complex input signal. One may overcome this problem by applying two separate input signals, $\cos(\alpha\tau)$ and $\sin(\alpha\tau)$, and computing the Fourier transforms for each resulting output sequence separately. An estimate for $K(\omega,\alpha)$ could then be obtained from these two Fourier transforms. To illustrate, let $y_R(t)$ and $y_I(t)$ designate the outputs obtained from the LPTV system due to application of the input signals $\cos(\alpha\tau)$ and $\sin(\alpha\tau)$, respectively. By linearity of the system of interest and of the Fourier transform, we have

$$Y_R(\omega) + iY_I(\omega) = Y(\omega) \approx K(\omega,\alpha) \ , \tag{4.1.7}$$

where $Y_R(\omega)$ and $Y_I(\omega)$ are the N-length Fourier transforms of $y_R(t)$ and $y_I(t)$, respectively.

Note that the accuracy of our estimate for the system transmission function is now dependent on both the length of the observation interval and on the relative phase of the two input signals. Assume that there is a phase error of ϕ between the two input signals; in other words, assume that we apply $\cos(\alpha\tau)$ and $\sin(\alpha\tau + \phi)$ at the input of the LPTV system. For small values of phase error,

$$\sin(\alpha\tau+\phi) \approx \sin(\alpha\tau) + \phi\cos(\alpha\tau) \ , \tag{4.1.8}$$

so that

$$x_\phi(\tau) = \cos(\alpha\tau) + i\,\sin(\alpha\tau+\phi) \approx e^{i\alpha\tau} + \frac{\phi}{2} e^{-i\alpha\tau} \ . \tag{4.1.9}$$

Forming our estimate for the system transmission function as before, we obtain

$$Y_\phi(\omega) \approx K(\omega,\alpha) + \frac{\phi}{2} K(\omega,-\alpha) \ . \tag{4.1.10}$$

The significance of this distortion in our estimate of the system transmission function depends on the magnitude of the phase error and on the nature of $K(\omega,\alpha)$.

4.2 CHARACTERIZATION OF LINEAR TIME-VARYING SYSTEMS via NONDETERMINISTIC SIGNALS

We now consider a technique for estimating the system transmission function of a LPTV system by observing the response of the system to a nondeterministic input signal. This technique is based on the observation made in Section 3.4 that the cross-spectral correlation function between the output of a LPTV system and the random input to the system is directly proportional to the LPTV system transmission function. In this section, we will derive the approximate statistical properties of the estimated cross-spectral correlation function and of the estimated system transmission function.

Let $\{\varepsilon(\tau)\}$ by a wide-sense stationary, complex Gaussian purely random process satisfying

$$E[\,\varepsilon(\tau)\,] = 0\ , \tag{4.2.1}$$

and

$$E[\,\varepsilon(\tau_1)\,\varepsilon^*(\tau_2)\,] = \begin{cases} \sigma^2 & ; \quad \tau_1 = \tau_2 \\ 0 & ; \quad \text{else} \end{cases}\ . \tag{4.2.2}$$

Next, assume that $\{\varepsilon(\tau)\}$ is applied to the input of a causal, stable LPTV system with the simple system transmission function

$$K(\omega,\alpha) = H_o(\alpha)\,\delta\left(\omega-\omega_o - \frac{\alpha}{\rho}\right)\ , \tag{4.2.3}$$

where ρ is the rate of the system. Note that for this LPTV system, $K(\omega,\alpha)$ is non-zero only along the line

$$\omega = \omega_o + \frac{\alpha}{\rho}\ . \tag{4.2.4}$$

More sophisticated LPTV systems may be considered to be linear combinations of systems of this particular form.

Recall from equation (3.2.4) that the spectral representation for $\{\varepsilon(\tau)\}$ is given by

$$\varepsilon(\tau) = \frac{1}{2\pi} \int_{-\pi}^{\pi} e^{i\beta\tau} \, dZ(\beta) \quad . \tag{4.2.5}$$

The K-length discrete Fourier transform of $\{\varepsilon(\tau)\}$ is given by

$$\mathcal{E}_K(\alpha_k) = \sum_{\tau = 0}^{K-1} \varepsilon(\tau) \, e^{-i\alpha_k \tau} \quad , \tag{4.2.6}$$

where

$$\alpha_k = \frac{2\pi k}{K}, \; k = 0, 1, \ldots , K-1 \; . \tag{4.2.7}$$

Substituting for the spectral representation for $\{\varepsilon(\tau)\}$ into equation (4.2.6), we obtain

$$\mathcal{E}_K(\alpha_k) = \frac{1}{2\pi} \int_{-\pi}^{\pi} F_K(\beta-\alpha_k) \, dZ(\beta) \quad , \tag{4.2.8}$$

where $F_K(\beta)$ is the Fejer kernel of equation (4.1.5). From equation (4.2.8) we see that the $\{\mathcal{E}_K(\alpha_k)\}$ are a set of zero-mean, complex Gaussian random variables. Furthermore, note that

$$E\left[\mathcal{E}_K(\alpha_k) \, \mathcal{E}^*_K(\alpha_j)\right] = \frac{\sigma^2}{2\pi} \int_{-\pi}^{\pi} F_K(\beta-\alpha_k) \, F^*_K(\beta-\alpha_j) \, d\beta \; , \tag{4.2.9}$$

or simplifying,

$$E\left[\mathcal{E}_K(\alpha_k) \, \mathcal{E}^*_K(\alpha_j)\right] = \begin{cases} K\sigma^2 & ; \; k = j \\ 0 & ; \; else \end{cases} \quad , \tag{4.2.10}$$

so that $\{\mathcal{E}_K(\alpha_k)\}$ are a set of i.i.d. complex Gaussian random variables with zero mean and variance $K\sigma^2$.

Now define the N-length discrete Fourier transform of the system output, y(t), as

$$Y_N(\omega_n) = \sum_{t=0}^{N-1} y(t)\, e^{-i\omega_n t} \quad . \tag{4.2.11}$$

Recall from equation (3.2.8) that we may express y(t) as

$$y(t) = \frac{1}{2\pi} \int_{-\pi}^{\pi} \kappa(t,\alpha)\, dZ(\alpha) \quad , \tag{4.2.12}$$

where $\kappa(t,\alpha)$ is the system response function. For the LPTV system under discussion,

$$\kappa(t,\gamma) = \frac{1}{2\pi} \int_{-\pi}^{\pi} K(\omega,\gamma)\, e^{i\omega t}\, dt \quad , \tag{4.2.13}$$

or

$$\kappa(t,\gamma) = H_o(\gamma)\, \exp\{\, i(\omega_o + \frac{\gamma}{\rho})t \,\} \quad . \tag{4.2.14}$$

Substituting for the system response function in equation (4.2.12), we obtain

$$y(t) = \frac{1}{2\pi} \int_{-\pi}^{\pi} H_o(\gamma)\ \exp\{\, i(\omega_o + \frac{\gamma}{\rho})t \,\}\, dZ(\gamma) \quad , \tag{4.2.15}$$

so that

$$Y_N(\omega_n) = \frac{1}{2\pi} \int_{-\pi}^{\pi} H_o(\gamma)\ F_N\,(\omega_n - \omega_o - \frac{\gamma}{\rho})\, dZ(\gamma) \quad . \tag{4.2.16}$$

Notice that the $\{Y_N(\omega_n)\}$ are a set of complex, zero-mean Gaussian random variables. Furthermore, consider that

$$E\{Y_N(\omega_n)\, Y^*_N(\omega_j)\} = \frac{\sigma^2}{2\pi} \int_{-\pi}^{\pi} |H_o(\gamma)|^2 F_N(\omega_n - \omega_o - \frac{\gamma}{\rho})\, F^*_N(\omega_j - \omega_o - \frac{\gamma}{\rho})\, d\gamma \quad (4.2.17)$$

so that for N sufficiently large,

$$E\{Y_N(\omega_n)\, Y^*_N(\omega_j)\} \approx \begin{cases} N\sigma^2 |H_o(\rho(\omega_n - \omega_o))|^2; & n = j \\ 0 \quad ; & else \end{cases} . \quad (4.2.18)$$

Now consider choosing N, the length of the output DFT, and K, the length of the input DFT, so that

$$\frac{N}{K} = \rho . \quad (4.2.19)$$

For any $\omega_n = \frac{2\pi n}{N}$ and any $\alpha_k = \frac{2\pi k}{K}$, we may write

$$\omega_n = \frac{2\pi(n-k)}{N} + \frac{2\pi k}{\rho K} = \omega_{n-k} + \frac{\alpha_k}{\rho} . \quad (4.2.20)$$

From equation (4.2.20) we note that the set of points

$$\{ (\omega_{n+m}, \alpha_{k+m}):\ m = 0, \pm 1, \ldots, \pm M/2 \} \quad (4.2.21)$$

lie along a line of slope $\frac{1}{\rho}$ passing through the point (ω_n, α_k).

Now consider the two-dimensional complex random variable

$$I(\omega_n, \alpha_k) = \frac{1}{N} Y_N(\omega_n)\, \mathcal{E}^*_K(\alpha_k) . \quad (4.2.22)$$

Note that

$$E\{I(\omega_n,\alpha_k)\} = \frac{1}{N}\frac{\sigma^2}{2\pi}\int_{-\pi}^{\pi} H_o(\gamma)\, F_N(\omega_n-\omega_o-\frac{\gamma}{\rho})\, F^*_K(\gamma-\alpha_k)\, d\gamma \ , \qquad (4.2.23)$$

or, for N and K sufficiently large,

$$E\{I(\omega_n,\alpha_k)\} \approx \begin{cases} \sigma^2 H_o(\rho(\omega_n-\omega_o)) & ; \ \omega_n = \omega_o + \dfrac{\alpha_k}{\rho} \\ 0 & ; \ \text{else} \end{cases} \ . \qquad (4.2.24)$$

Furthermore, note that

$$E\{\,|I(\omega_n,\alpha_k)|^2\} = |E\{I(\omega_n,\alpha_k)\}|^2 + \frac{\sigma^4}{\rho}|H_o(\rho(\omega_n-\omega_o))|^2 \ , \qquad (4.2.25)$$

so that

$$\mathrm{Var}\{\,I(\omega_n,\alpha_k)\,\} = \frac{\sigma^4}{\rho}|H_o(\rho(\omega_n-\omega_o))|^2 \ . \qquad (4.2.26)$$

From equations (4.2.24) and (4.2.26) we see that $I(\omega_n,\alpha_k)$ is an inconsistent estimator for the system transmission function.

Recall that our choice of N and K led to a set of discrete frequency points such that $\{(\omega_{n+m},\alpha_{k+m})$: $m = 0, \pm 1, \ldots, \pm M/2\}$ lies along a line of slope $1/\rho$ in the (ω,α) bifrequency plane. If we assume that $K(\omega,\alpha)$ is essentially constant over this set of points, we could consider estimating $K(\omega,\alpha)$ by smoothing $I(\omega_n,\alpha_k)$. Define the random variable

$$S_M(w_n,\alpha_k) = \frac{1}{M+1}\sum_{m=-M/2}^{M/2} I(\omega_{n+m},\alpha_{k+m}) \ , \qquad (4.2.27)$$

and note that

$$E\{\,S_M(\omega_n,\alpha_k)\,\} = \frac{1}{M+1}\sum_{m=-M/2}^{M/2} E\{\,I(\omega_{n+m},\alpha_{k+m})\,\} \ . \qquad (4.2.28)$$

For N and K sufficiently large, and assuming that $K(\omega,\alpha)$ is constant over the set of points $\{ (\omega_{n+m},\alpha_{k+m}):\ m = 0, \pm 1, \ldots, \pm M/2 \}$, we obtain

$$E\{ S_M(\omega_n,\alpha_k) \} \approx \begin{cases} \sigma^2 H_o(\alpha_k) \ ; \ \omega_n = \omega_o + \dfrac{\alpha_k}{\rho} \\ 0 \ ; \ else \end{cases} . \qquad (4.2.29)$$

Further, note that

$$E\{ | S_M(\omega_n,\alpha_k) |^2 \} = | E\{ S_M(\omega_n,\alpha_k) \} |^2 + \frac{\sigma^4}{\rho(M+1)} | H_o(\rho(\omega_n-\omega_o)) |^2 , \qquad (4.2.30)$$

so that

$$Var\{ S_M(\omega_n,\alpha_k) \} = \frac{\sigma^4}{\rho(M+1)} | H_o(\rho(\omega_n-\omega_o)) |^2 . \qquad (4.2.31)$$

If we pick M so that as M, N, and K increase without bounds $M/N \to 0$ and $M/K \to 0$, then $S_M(\omega_n,\alpha_k)$ is a consistent estimator of the system transmission function.

We now consider the statistical properties of $S_M(\omega_n,\alpha_k)$. First, notice from equation (4.2.27) that

$$S_M(\omega_n,\alpha_k) = \frac{1}{M+1} \sum_{m=-M/2}^{M/2} \frac{1}{N} Y_N(\omega_{n+m}) \mathcal{E}^*_K(\alpha_{k+m}) . \qquad (4.2.32)$$

For M sufficiently large, and for $\omega_n \neq \omega_o + \dfrac{\alpha_k}{\rho}$,

$$\{ Y_N(\omega_{n+m}) \mathcal{E}^*_K(\alpha_{k+m}):\ m = 0, \pm 1, \ldots, \pm M/2 \} \qquad (4.2.33)$$

are a set of uncorrelated, identically distributed complex random variables. We can therefore argue that $S_M(\omega_n,\alpha_k)$ is approximately Gaussian distributed with zero mean and variance $\dfrac{\sigma^4}{\rho(M+1)} | H_o(\rho(\omega_n-\omega_o)) |^2$. For $\omega_n = \omega_o + \dfrac{\alpha_k}{\rho}$, $S_M(\omega_n,\alpha_k)$ is approximately Gaussian distributed with mean $\sigma^2 H_o(\rho(\omega_n-\omega_o))$ and variance $\dfrac{\sigma^4}{\rho(M+1)} | H_o(\rho(\omega_n-\omega_o)) |^2$.

Finally, assume that we estimate the noise variance, σ^2, from the given observations of $\{\varepsilon(\tau)\}$ as

$$\hat{\sigma}^2 = \frac{1}{K} \sum_{\tau=0}^{K-1} | \varepsilon(\tau) |^2 = \frac{\sigma^2}{K} \chi^2_{2K} \ , \tag{4.2.34}$$

where χ^2_{2K} is a chi-square distributed random variable with 2K degrees of freedom. Our estimate for the system transmission function is therefore given by

$$\hat{K}(\omega_n,\alpha_k) = \frac{1}{\hat{\sigma}^2} S_M(\omega_n,\alpha_k) \ . \tag{4.2.35}$$

For K large, $\hat{\sigma}^2$ is approximated by

$$\hat{\sigma}^2 \approx \sigma^2 \eta \tag{4.2.36}$$

where η is a Gaussian random variable with unit mean and variance 1/K. Our estimated system transmission function is therefore approximated by

$$\hat{K}(\omega_n,\alpha_k) \approx \begin{cases} K(\omega_n,\alpha_k) + \dfrac{H_o(\rho(\omega_n-\omega_o))}{\sqrt{\rho(M+1)}} \mu & ; \ \omega_n = \omega_o + \dfrac{\alpha_k}{\rho} \\ \dfrac{H_o(\rho(\omega_n-\omega_o))}{\sqrt{\rho(M+1)}} \mu & ; \ \text{else} \end{cases} \ , \tag{4.2.37}$$

where μ is a complex, zero-mean, unit variance Gaussian random variable.

Now consider a more sophisticated LPTV system composed of linear combinations of systems of the form assumed above. In other words, assume that

$$K(\omega,\alpha) = \sum_o H_o(\alpha) \, \delta(\omega-\omega_o-\frac{\alpha}{\rho}) \tag{4.2.38}$$

for some set of distinct $\{\omega_o\}$. Notice that $\mathcal{E}_K(\alpha_k)$ is still described by equation (4.2.8), but that now

$$Y_N(\omega_n) = \sum_o \frac{1}{2\pi} \int_{-\pi}^{\pi} H_o(\gamma)\, F_N(\omega_n - \omega_o - \frac{\gamma}{\rho})\, dZ(\gamma) \quad . \tag{4.2.39}$$

Since the $\{\omega_c\}$ are distinct, for N sufficiently large we obtain

$$E\{ Y_N(\omega_n)\, Y^*_N(\omega_j) \} \approx \begin{cases} N\sigma^2 \sum_o |H_o(\rho(\omega_n - \omega_o))|^2 \; ; & n = j \\ 0 \; ; & \text{else} \end{cases} \quad . \tag{4.2.40}$$

If we again define $I(\omega_n,\alpha_k)$ by equation (4.2.23), we obtain

$$E\{ I(\omega_n,\alpha_k) \} \approx \begin{cases} \sigma^2 H_o(a_k) \; ; & \omega_n = \omega_o + \frac{\alpha_k}{\rho} \\ 0 \; ; & \text{else} \end{cases} \tag{4.2.41}$$

and

$$\text{Var}\{ I(\omega_n,\alpha_k) \} = \frac{\sigma^4}{\rho} \left| \sum_o H_o(\rho(\omega_n - \omega_o)) \right|^2 \quad . \tag{4.2.42}$$

Using equation (4.2.28) as our definition for $S_M(\omega_n,\alpha_k)$, we obtain

$$E\{ S_M(\omega_n,\alpha_k) \} \approx \begin{cases} \sigma^2 H_o(\alpha_k) \; ; & \omega_n = \omega_o + \frac{\alpha_k}{\rho} \\ 0 \; ; & \text{else} \end{cases} \tag{4.2.43}$$

and

$$\text{Var}\{ S_M(\omega_n,\alpha_k) \} = \frac{\sigma^4}{\rho(M+1)} \left| \sum_o H_o(\rho(\omega_n - \omega_o)) \right|^2 \quad . \tag{4.2.44}$$

Defining our estimate for the system transmission function by equation (4.2.35) yields a complex random variable which is approximated by

$$\hat{K}(\omega_n,\alpha_k) \approx \begin{cases} K(\omega_n,\alpha_k) + \dfrac{\sum_o H_o(\rho(\omega_n-\omega_o))}{\sqrt{\rho(M+1)}}\mu \; ; \; \omega_n = \omega_o + \dfrac{\alpha_k}{\rho} \\ \dfrac{\sum_o H_o(\rho(\omega_n-\omega_o))}{\sqrt{\rho(M+1)}}\mu \; ; \; \text{else} \end{cases} , \quad (4.2.45)$$

where μ is a complex Gaussian random variable with zero mean and unit variance.

Finally, consider the case of applying this technique for estimating $K(\omega,\alpha)$ when both $\{\varepsilon(\tau)\}$ and $\{y(t)\}$ are observed in the presence of additive, stationary independent white noise, as indicated schematically in Figure 4.2.1. Assume that the input observation noise, $\{\phi(\tau)\}$, and the output observation noise, $\{\zeta(t)\}$, are wide sense stationary complex Gaussian random variables such that

$$E\{\zeta(t_1)\zeta^*(t_2)\} = \begin{cases} \sigma_\zeta^2 \; ; \; t_1 = t_2 \\ 0 \; ; \; \text{else} \end{cases} \quad (4.2.46)$$

and

$$E\{\phi(\tau_1)\phi^*(\tau_2)\} = \begin{cases} \sigma_\phi^2 \; ; \; \tau_1 = \tau_2 \\ 0 \; ; \; \text{else} \end{cases} . \quad (4.2.47)$$

Further, assume that $\{\phi(\tau)\}$ and $\{\zeta(t)\}$ are mutually independent, and independent of $\{\varepsilon(\tau)\}$.

The discrete Fourier transforms of the observed input, $\{r(\tau)\}$, and the observed output, $\{x(t)\}$, are given by

$$R_K(\alpha_k) = \sum_{\tau=0}^{K-1} r(\tau)\, e^{-i\alpha_k\tau} = \mathcal{E}_K(\alpha_k) + \zeta_K(\alpha_k), \quad (4.2.48)$$

and

$$X_N(\omega_n) = \sum_{t=0}^{N-1} x(t)\, e^{-i\omega_n t} = Y_N(\omega_n) + \Phi_N(\omega_n) \qquad (4.2.49)$$

where

$$\zeta_K(\alpha_k) = \sum_{\tau=0}^{K-1} \zeta(\tau)\, e^{-i\alpha_k \tau} = \frac{1}{2\pi} \int_{-\pi}^{\pi} F_K(\gamma-\alpha_k)\, dZ_\zeta(\gamma) \quad , \qquad (4.2.50)$$

and

$$\Phi_N(\omega_n) = \sum_{t=0}^{N-1} \phi(t)\, e^{-i\omega_n t} = \frac{1}{2\pi} \int_{-\pi}^{\pi} F_K(\gamma-\alpha_k)\, dZ_\phi(\gamma) \quad . \qquad (4.2.51)$$

Now define the random variable $I'(\omega_n,\alpha_k)$ as

$$I'(\omega_n,\alpha_k) = \frac{1}{N} X_N(\omega_n)\, R^*_K(\alpha_k) \quad , \qquad (4.2.52)$$

and let

$$S'_M(\omega_n,\alpha_k) = \frac{1}{M+1} \sum_{m=-M/2}^{M/2} I'(\omega_{n+m},\alpha_{k+m}) \quad , \qquad (4.2.53)$$

so that

$$\begin{aligned} S'_M(\omega_n,\alpha_k) \quad & + \frac{1}{M+1} \sum_{m=-M/2}^{M/2} \frac{1}{N} Y_N(\omega_{n+m})\, \mathcal{E}^*_K(\alpha_{k+m}) \\ & + \frac{1}{M+1} \sum_{m=-M/2}^{M/2} \frac{1}{N} Y_N(\omega_{n+m})\, \Phi^*_K(\alpha_{k+m}) \\ & + \frac{1}{M+1} \sum_{m=-M/2}^{M/2} \frac{1}{N} \zeta_N(\omega_{n+m})\, \mathcal{E}^*_K(\alpha_{k+m}) \\ & + \frac{1}{M+1} \sum_{m=-M/2}^{M/2} \frac{1}{N} \zeta_N(\omega_{n+m})\, \Phi^*_K(\alpha_{k+m}) \quad . \end{aligned} \qquad (4.2.54)$$

Consider the term

$$\frac{1}{M+1} \sum_{m=-M/2}^{M/2} \frac{1}{N} \zeta_N(\omega_{n+m}) \mathcal{E}^*_K(\alpha_{k+m}) \tag{4.2.55}$$

in equation (4.2.55) above. Since $\{\zeta(t)\}$ and $\{\varepsilon(\tau)\}$ are independent Gaussian random variables,

$$E\left\{ \frac{1}{N} \zeta_N(\omega_n) \mathcal{E}^*_K(\alpha_k) \right\} = 0 \tag{4.2.56}$$

and

$$E\left\{ \left(\frac{1}{N} \zeta_N(\omega_n) \mathcal{E}^*_K(\alpha_k) \right) \left(\frac{1}{N} \zeta_N(\omega_{n+j}) \mathcal{E}^*_K(\alpha_{k+j}) \right)^* \right\}$$

$$= \begin{cases} \dfrac{\sigma^2 \sigma_\zeta^2}{\rho} & ; \quad j = 0 \\ 0 & ; \quad \text{else} \end{cases} . \tag{4.2.57}$$

For large M, the summation of equation (4.2.55) is approximated by a complex Gaussian random variable with zero mean and variance $\frac{\sigma^2 \sigma_\zeta^2}{\rho(M+1)}$. Similarly, the term

$$\frac{1}{M+1} \sum_{m\,=\,-M/2}^{M/2} \frac{1}{N} \zeta_N(\omega_{n+m}) \Phi^*_K(\alpha_{k+m}) \tag{4.2.58}$$

is approximated by a complex Gaussian random variable with zero mean and variance $\frac{\sigma_\phi^2 \sigma_\zeta^2}{\rho(M+1)}$.

Now consider the term

$$\frac{1}{M+1} \sum_{m=-M/2}^{M/2} \frac{1}{N} Y_N(\omega_{n+m}) \Phi^*_K(\alpha_{k+m}) , \tag{4.2.59}$$

and note that, since $\{\varepsilon(\tau)\}$ and $\{\phi(\tau)\}$ are independent,

$$E\left\{ \frac{1}{N} Y_N(\omega_n) \Phi^*_K(\alpha_k) \right\} = 0 \ . \qquad (4.2.60)$$

Furthermore,

$$E\left\{ \left(\frac{1}{N} Y_N(\omega_n) \Phi^*_K(\alpha_k) \right) \left(\frac{1}{N} Y_N(\omega_{n+j}) \Phi^*_K(\alpha_{k+j}) \right)^* \right\}$$

$$= b\left(\frac{1}{N}\right)^2 \sigma^2\sigma_\phi^2 \sum_o \sum_p \left(\frac{1}{2\pi}\right)^2 \int_{-\pi}^{\pi} \int_{-\pi}^{\pi} H_o(\gamma)\, H^*_p(\gamma)$$

$$F_N(\omega_n - \omega_o - \frac{\gamma}{\rho})\, F^*_N(\omega_{n+j} - \omega_p - \frac{\gamma}{\rho})\, F_K(\beta - \alpha_k)\, F_K(\beta - \alpha_{k+j})\, d\gamma\, d\beta \ . \qquad (4.2.61)$$

For N and K sufficiently large,

$$E\left\{ \left(\frac{1}{N} Y_N(\omega_n) \Phi^*_K(\alpha_k) \right) \left(\frac{1}{N} Y_N(\omega_{n+j}) \Phi^*_K(\alpha_{k+j}) \right)^* \right\}$$

$$\approx \begin{cases} \dfrac{\sigma^2\sigma_\phi^2}{\rho} \displaystyle\sum_o \left| H_o(\rho(\omega_n - \omega_o)) \right|^2 \ ; & j = 0 \\ 0 \ ; & \text{else} \end{cases} \ . \qquad (4.2.62)$$

Therefore, the term given in equation (4.2.59) is approximated by a zero mean complex Gaussian random variable with variance $\dfrac{\sigma^2\sigma_\phi^2}{\rho(M+1)} \displaystyle\sum_o \left| H_o(\rho(\omega_n - \omega_o)) \right|^2$.

Our estimate for the variance of the input noise process is given by

$$\hat{\sigma}^2 = \frac{1}{K} \sum_{\tau=0}^{K-1} \left| r(\tau) \right|^2 \ . \qquad (4.2.63)$$

For K large, we may approximate $\hat{\sigma}^2$ by

$$\hat{\sigma}^2 = \sigma^2 + \sigma_o^2 \ . \qquad (4.2.64)$$

Our estimate for the system transmission function is now given by

$$\hat{K}(\omega_n,\alpha_k) = \frac{1}{\hat{\sigma}^2} S'_M(\omega_n,\alpha_k) \quad , \tag{4.2.65}$$

or, from the discussion presented above,

$$\hat{K}(\omega_n,\alpha_k) \approx \begin{cases} \dfrac{\sigma^2}{\sigma^2+\sigma_\phi^2} H_o(\rho(\omega_n-\omega_o))+\mu_0+\mu_1+\mu_2+\mu_3 \; ; \; \omega_n = \omega_o + \dfrac{\alpha_k}{\rho} \\ \mu_0+\mu_1+\mu_2+\mu_3 \quad ; \quad \text{else} \end{cases} \tag{4.2.66}$$

where μ_0, μ_1, μ_2, and μ_3 are complex zero-mean Gaussian random variables with variances

$$\sigma_0^2 = \frac{\sigma^2}{\rho(M+1)(\sigma^2+\sigma_\phi^2)} \sum_o | H_o(\rho(\omega_n-\omega_o)) |^2, \tag{4.2.67}$$

$$\sigma_1^2 = \frac{\sigma^2\sigma_\zeta^2}{\rho(M+1)(\sigma^2+\sigma_\phi^2)} \quad , \tag{4.2.68}$$

$$\sigma_2^2 = \frac{\sigma^2\sigma_\phi^2}{\rho(M+1)(\sigma^2+\sigma_\phi^2)} \quad , \tag{4.2.69}$$

and

$$\sigma_3^2 = \frac{\sigma^2\sigma_\phi^2}{\rho(M+1)(\sigma^2+\sigma_\phi^2)} \sum_o | H_o(\rho(\omega_n-\omega_o)) |^2, \tag{4.2.70}$$

respectively.

The results obtained above for frequency-smoothed estimates of $K(\omega,\alpha)$ may be extended to time-averaged estimates for the system transmission function. To be specific, assume that we obtain L observations of the input and output signals of length K and N, respectively. If the L observations of the output process are obtained in such a manner that the input samples producing one set of output samples are unrelated to the input samples producing any other set of output samples then we may invoke the mixing assumption of Section 3.1 to claim that the L output observations are statistically independent. For each observation, form the discrete Fourier transform of the input and output signal in

accordance with equations (4.2.6) and (4.2.11). The estimate for the system transmission function is obtained from

$$\hat{K}(\omega_n,\alpha_k) = \frac{1}{\hat{\sigma}^2} S_L(\omega_n,\alpha_k) \ , \tag{4.2.71}$$

where $\hat{\sigma}^2$ is the estimate for the input noise variance based on the LK available samples of the input process, and

$$S_L(\omega_n,\alpha_k) = \frac{1}{L} \sum_{l=1}^{L} \frac{1}{N} Y_{N,l}(\omega_n) \mathcal{E}^*_{K,l}(\alpha_k) \ . \tag{4.2.72}$$

In equation (4.2.72), $Y_{N,l}(\omega_n)$ and $\mathcal{E}_{K,l}(\alpha_k)$ are the l-th discrete Fourier transform of the input and output signals. Following a line of argument identical to that presented for frequency-smoothed estimates, we obtain

$$\hat{K}(\omega_n,\alpha_k) \approx \begin{cases} \frac{\sigma^2}{\sigma^2+\sigma_\phi^2} H_o(\rho(\omega_n-\omega_o))+v_0+v_1+v_2+v_3 \ ; \ \omega_n = \omega_o + \frac{\alpha_k}{\rho} \\ v_0+v_1+v_2+v_3 \quad ; \ \text{else} \end{cases} \tag{4.2.73}$$

where v_0, v_1, v_2, and v_3 are complex zero-mean Gaussian random variables with variances

$$\sigma_1^2 = \frac{\sigma^2}{\rho L(\sigma^2+\sigma_\phi^2)} \sum_o | H_o(\rho(\omega_n-\omega_o)) |^2, \tag{4.2.74}$$

$$\sigma_2^2 = \frac{\sigma^2\sigma_\zeta^2}{\rho L(\sigma^2+\sigma_\phi^2)} \ , \tag{4.2.75}$$

$$\sigma_3^2 = \frac{\sigma^2\sigma_\phi^2}{\rho L(\sigma^2+\sigma_\phi^2)} \ , \tag{4.2.76}$$

and

$$\sigma_4^2 = \frac{\sigma^2\sigma_\phi^2}{\rho L(\sigma^2+\sigma_\phi^2)} \sum_o | H_o(\rho(\omega_n-\omega_o)) |^2 \ . \tag{4.2.77}$$

respectively.

Several comments can be made regarding the method for estimating $K(\omega,\alpha)$ presented above. First, we again assumed that a complex input signal was applied to the system under consideration. For systems in which only real signals may be applied to the system, we could apply the real and imaginary components of the input signal to the system independently and linearly combine the observed outputs to estimate the system transmission function, as was described in Section 4.1. However, for a complex white noise process, it is required that the real and imaginary components be independent and identically distributed (see Koopmans, p. 263). The real and imaginary components for the input signal could therefore be obtained from two K-length observations of data obtained from a single white noise generator.

Secondly, we assumed that the input noise process had a flat spectrum, i.e., we assumed that its power spectrum was constant for all frequencies. In practice, we cannot guarantee that the input noise process has a flat spectrum. However, we could estimate the spectrum of the input noise process, $S_\varepsilon(\alpha)$, from the given observations, and estimate our system transmission function by

$$\hat{K}(\omega_n,\alpha_k) = \frac{S_M(\omega_n,\alpha_k)}{S_\varepsilon(\alpha_k)} \quad . \tag{4.2.78}$$

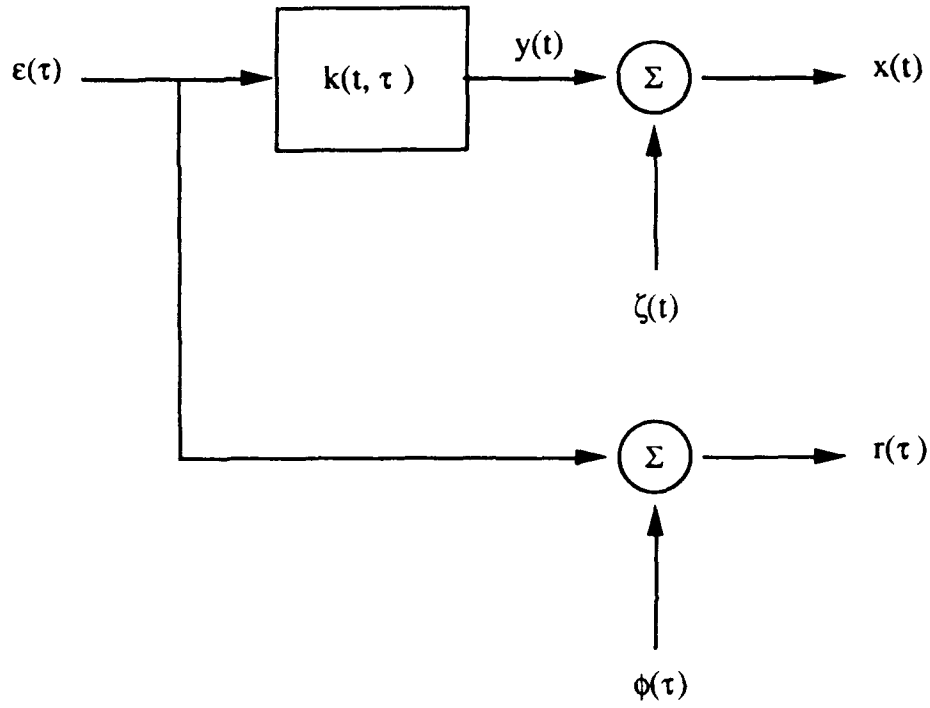

FIGURE 4.2.1
ESTIMATION OF K(ω,α) IN THE PRESENCE OF OBSERVATION NOISE

4.3 CHAPTER SUMMARY

In this chapter we presented two techniques for empirically characterizing linear periodically time varying systems. The properties and limitations of both techniques were discussed. We now turn our attention to the results of implementing these two techniques to the characterization of several LPTV systems of interest.

5. RESULTS OF IMPLEMENTATION OF METHODS FOR THE CHARACTERIZATION OF LINEAR TIME-VARYING SYSTEMS

We now briefly present the results of implementation of the methods for characterizing linear periodically time-varying systems presented in Chapter 4. Characterizations of a set of LPTV systems were conducted using both deterministic and nondeterministic input signals. We begin by considering the theoretical system transmission functions for the LPTV systems of interest.

5.1 THEORETICAL SYSTEM TRANSMISSION FUNCTIONS FOR THE LPTV SYSTEMS OF INTEREST

A set of five LPTV systems were used to evaluate the methods for characterizing LPTV systems described earlier. The first two of these five systems were selected because they represented basic elements that are commonly found in more complicated LPTV systems. Characterization of these basic system elements is therefore a necessary first step towards characterizing more complicated LPTV systems. The final three LPTV systems evaluated here are complicated systems based on the interconnection of simpler system elements.

Figure 5.1.1 presents the block diagram of the first LPTV system of interest, a simple rate 1/2 decimator. In this system, the input signal, $x(\tau)$, is sampled at output sample times, t, such that $\tau = 2t$ to produce the output signal $y(t)$. The system response function $k_1(t,\tau)$, is therefore given by

$$k_1(t,\tau) = \begin{cases} 1 & ; \quad \tau = 2t \\ 0 & ; \quad \text{else} \end{cases} . \tag{5.1.1}$$

Using equation (2.6.8), the system transmission function is given by

$$K_1(\omega,\alpha) = \sum_{t=-\infty}^{\infty} e^{-i(\omega-2\alpha)t} = \sum_{n=-\infty}^{\infty} \delta(\omega-2\pi n-2\alpha) . \tag{5.1.2}$$

This function is indicated schematically in Figure 5.1.2. For this figure, the squared magnitude of $K_1(\omega,\alpha)$ was evaluated at the set of discrete points in the (ω,α) bifrequency plane defined by

$$\omega_n = \frac{2\pi n}{N} \quad , \tag{5.1.3}$$

and

$$\alpha_k = \frac{2\pi k}{K} \tag{5.1.4}$$

where $N = 128$ and $K = 64$. Note that input and output frequencies have been normalized by π in Figure 5.1.2.

Figure 5.1.3 presents the block diagram for the second LPTV system of interest, a simple quadrature demodulator. In this system, the input signal, $x(\tau)$, is demodulated by a complex sinusoid of frequency ω_o to obtain the output signal $y(\tau)$. The system response function, $k_2(t,\tau)$, is therefore given by

$$k_2(t,\tau) = \begin{cases} e^{-i(\omega-\omega_o)t} & ; \quad \tau = t \\ 0 & ; \quad else \end{cases} \quad . \tag{5.1.5}$$

The system transmission function for this system is given by

$$K_2(\omega,\alpha) = \sum_{t=-\infty}^{\infty} e^{-i(\omega+\omega_o-\alpha)t} \quad , \tag{5.1.6}$$

or

$$K_2(\omega,\alpha) = \sum_{n=-\infty}^{\infty} \delta(\omega-2\pi n+\omega_o-\alpha) \quad . \tag{5.1.7}$$

This system transmission function is indicated schematically in Figure 5.1.4. The squared magnitude of $K_2(\omega,\alpha)$ was again evaluated at a discrete set of points in the (ω,α)

bifrequency plane according to equations (5.1.3) and (5.1.4) with N = K = 64. Input and output frequencies have been normalized by π in Figure 5.1.4.

Figure 5.1.5 presents the block diagram for the third LPTV system of interest, a rate 3/2 interpolation system. In this system, the input signal is up-sampled (i.e., zero-padded) by a factor of three, passed through a LTI low pass filter, and decimated by a factor of two. The system response function for the rate 3 up-sampling is given by

$$k(t,\tau) = \begin{cases} 1 & ; \quad 3\tau = t \\ 0 & ; \quad \text{else} \end{cases} \quad . \tag{5.1.8}$$

The system transmission function for the rate 3 up-sampling is therefore given by

$$K(\beta,\alpha) = \sum_{n=-\infty}^{\infty} \delta(\beta\ 2\pi n - \alpha/3) \quad . \tag{5.1.9}$$

The overall system transmission function for the rate 3/2 interpolation system, $K_o(\omega,\alpha)$, is given by

$$K_o(\omega,\alpha) = \frac{1}{2\pi} \int_{-\pi}^{\pi} K_1(\omega,\beta)\ H(\beta)\ K(\beta,\alpha)\ d\beta \quad , \tag{5.1.10}$$

or simply

$$K_o(\omega,\alpha) = \sum_{m=-\infty}^{\infty} \sum_{n=-\infty}^{\infty} 2\ H(\alpha/3+2\pi n)\ \delta(\omega - 2\pi(m-2n) - 2\alpha/3) \quad . \tag{5.1.11}$$

Figure 5.1.6 schematically indicates this system transmission function. Figure 5.1.7 presents a three-dimensional view of $K_o(\omega,\alpha)$. For these plots, the squared magnitude of the system transmission function was evaluated at a set of discrete points in the (ω,α) bifrequency plane according to equations (5.1.3) and (5.1.4) with N=96 and K=64.

Figure 5.1.8 presents a block diagram for the fourth LPTV system of interest, a rate 1/2 quadrature sampling system. In this system, the input signal, $x(\tau)$, is demodulated

by $\cos(\frac{\pi}{2}\tau)$ and $-i\sin(\frac{\pi}{2}\tau)$, and sampled in quadrature to obtain the in-phase and quadrature components of a digital quadrature representation for $x(\tau)$ (see Baugh, 1988). The system response function for this system is given by

$$k(t,\tau) = \begin{cases} \cos(\frac{\pi}{2}\tau) & ; \quad \tau = 2t \\ -i\sin(\frac{\pi}{2}\tau) & ; \quad \tau = 2t+1 \\ 0 & ; \quad else \end{cases} . \tag{5.1.12}$$

The system transmission function for the rate 1/2 quadrature sampling system is therefore given by

$$K(\omega,\alpha) = (1-i\,e^{i\alpha}) \sum_{n=-\infty}^{\infty} \delta(\omega-2\pi n-2\alpha-\pi) + \delta(\omega-2\pi n-2\alpha+\pi) . \tag{5.1.13}$$

This system transmission function is indicated schematically in Figure 5.1.9, with the input and output frequencies again normalized by π. Figure 5.1.10 presents a three-dimensional view of this system transmission function. Again, the squared magnitude of the system transmission function was evaluated at a set of discrete points in the (ω,α) bifrequency plane according to equations (5.1.3) and (5.1.4) with N=128 and K=64. Figure 5.1.11 presents the result of plotting the largest value of $K(\omega,\alpha)$ over all ω for each α. In a sense, this plot gives an indication of the response of the LPTV system to each input frequency. All frequencies have been normalized by π. Consider that on the lines

$$\omega = 2\alpha+\pi \tag{5.1.14}$$

and

$$\omega = 2\alpha-\pi \tag{5.1.15}$$

the square-magnitude of $K(\omega,\alpha)$ is given by

$$|K(\omega,\alpha)|^2 = 2(1+\sin\alpha) . \tag{5.1.16}$$

This function is clearly indicated in Figure 5.1.11.

Figure 5.1.12 presents the block diagram for the fifth LPTV system of interest, a rate 1/2 quadrature demodulator. Note that this system is a series connection of the simple quadrature demodulator of Figure 5.1.3 with a gain of 2, a linear time-invariant low pass filter, and the rate 1/2 decimator of Figure 5.1.1. Using the results of Section 2.4 for the analysis of LPTV network structures, we may express the system transmission function for this LPTV system, $K_3(\omega,\alpha)$, as

$$K_3(\omega,\alpha) = \frac{1}{2\pi} \int_{-\pi}^{\pi} 2K_1(\omega,\beta)\, H(\beta)\, K_2(\beta,\alpha)\, d\beta \quad , \tag{5.1.17}$$

where $H(\beta)$ is the frequency response of the LTI system. Substituting equations (5.1.2) and (5.1.7) into (5.1.17), we obtain

$$K_3(\omega,\alpha) = \sum_{m=-\infty}^{\infty} \sum_{n=-\infty}^{\infty} 2\, H(\alpha-\omega_o+2\pi n)\, \delta(\omega-2\pi(m-2n)+2\omega_o-2\alpha) \quad . \tag{5.1.18}$$

This system transmission function is indicated schematically in Figure 5.1.13, with the input and output frequencies again normalized by π. Figure 5.1.14 presents a three-dimensional view of this system transmission function, indicating the modulation of the impulse sheet by $H(\beta)$, the LTI frequency response function. For these plots, the squared magnitude of the system transmission function was evaluated at a set of discrete points in the (ω,α) bifrequency plane according to equations (5.1.3) and (5.1.4) with N=128 and K=64. Figure 5.1.15 presents the result of plotting the largest value of $K_3(\omega,\alpha)$ over all ω for each α.

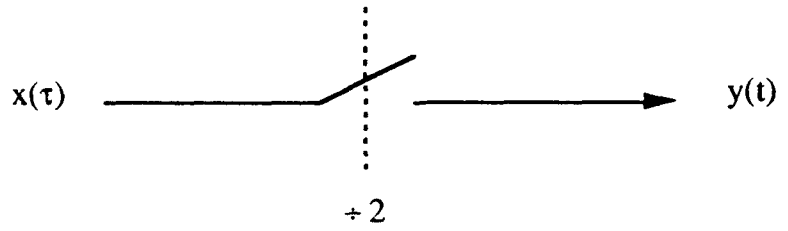

AS-91-369

FIGURE 5.1.1
BLOCK DIAGRAM FOR THE SIMPLE RATE 1/2 DECIMATOR

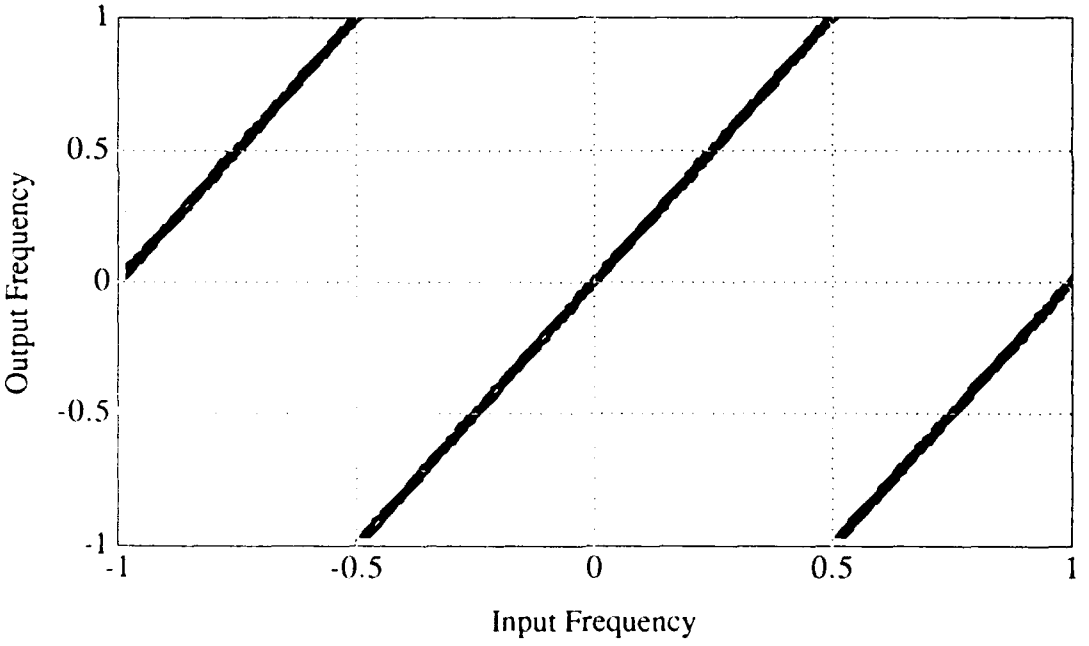

AS-91-370

FIGURE 5.1.2
THEORETICAL SYSTEM TRANSMISSION FUNCTION FOR A SIMPLE RATE 1/2 DECIMATOR

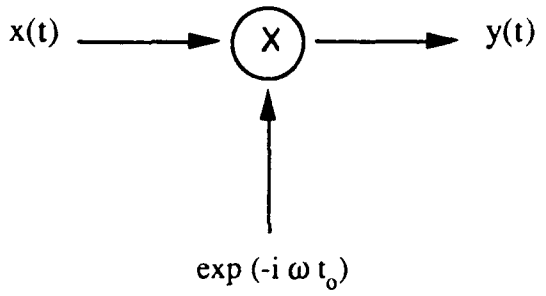

AS-91-371

FIGURE 5.1.3
BLOCK DIAGRAM FOR THE SIMPLE QUADRATURE DEMODULATOR

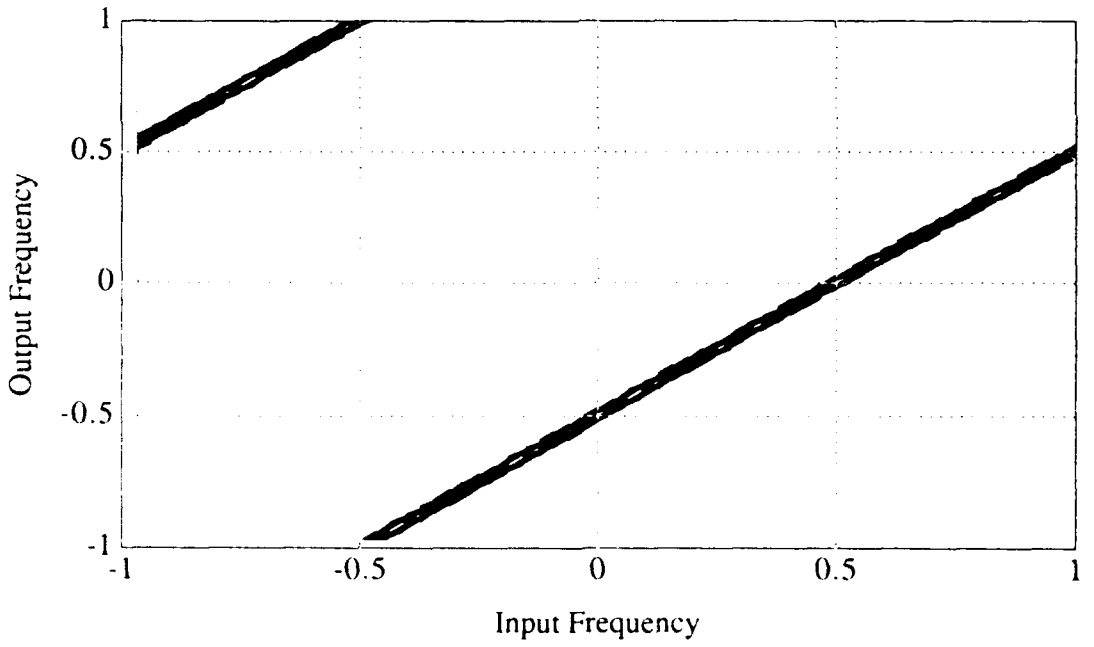

AS-91-372

FIGURE 5.1.4
THEORETICAL SYSTEM TRANSMISSION FUNCTION FOR A SIMPLE QUADRATURE DEMODULATOR

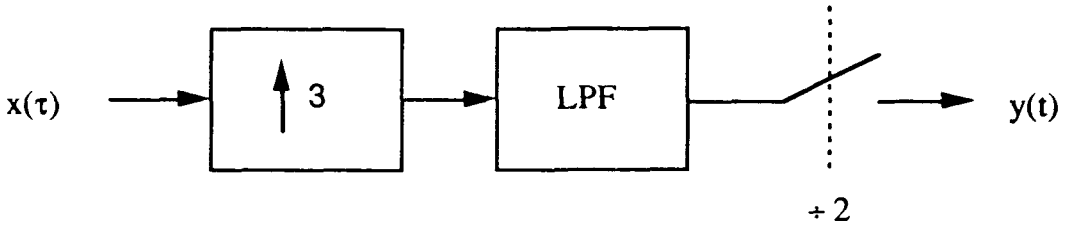

AS-91-373

FIGURE 5.1.5
BLOCK DIAGRAM FOR THE RATE 3/2 INTERPOLATOR

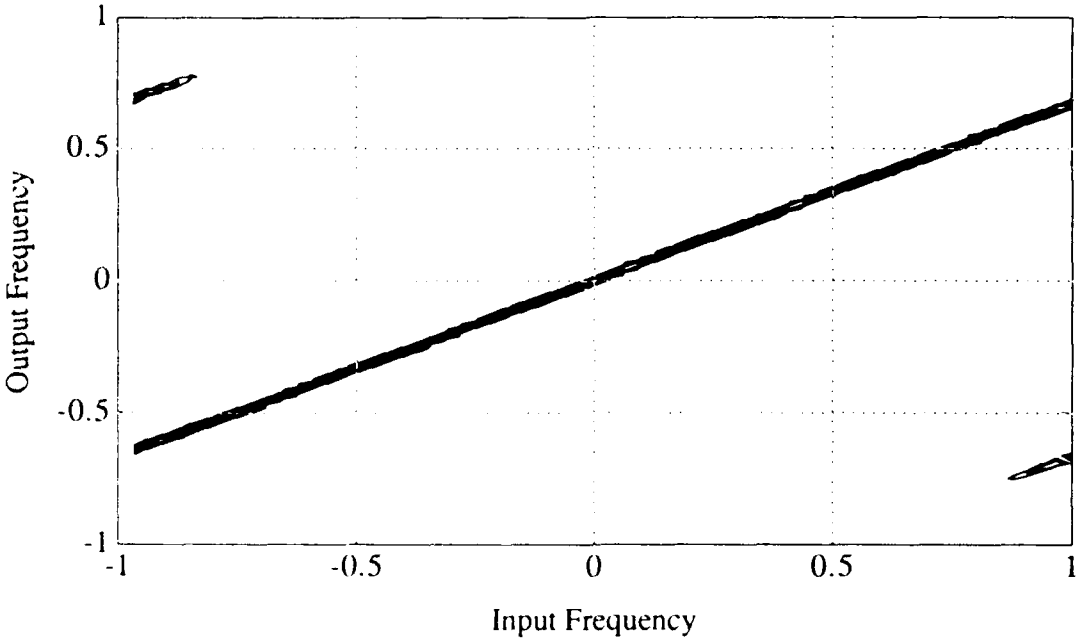

AS-91-374

FIGURE 5.1.6
THEORETICAL SYSTEM TRANSMISSION FUNCTION FOR THE RATE 3/2 INTERPOLATION SYSTEM

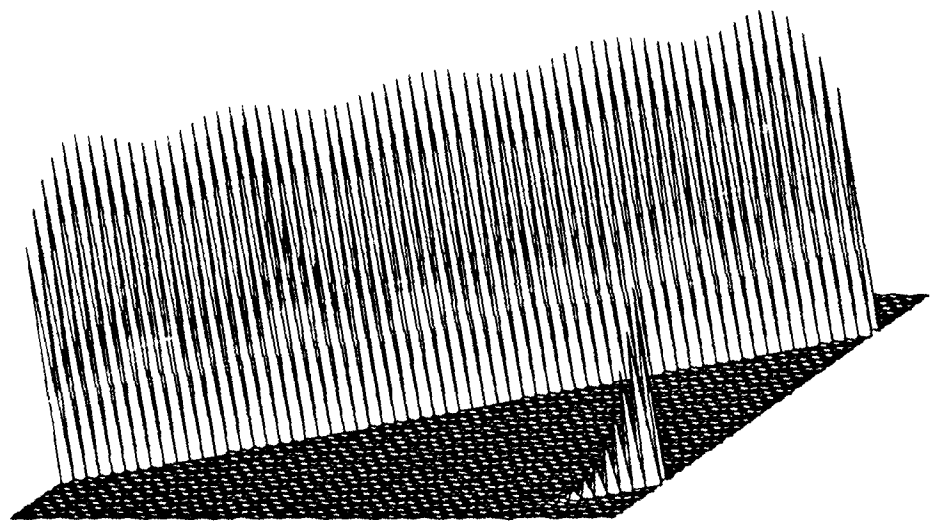

AS-91-375

FIGURE 5.1.7
THEORETICAL SYSTEM TRANSMISSION FUNCTION FOR THE RATE 3/2 INTERPOLATION SYSTEM

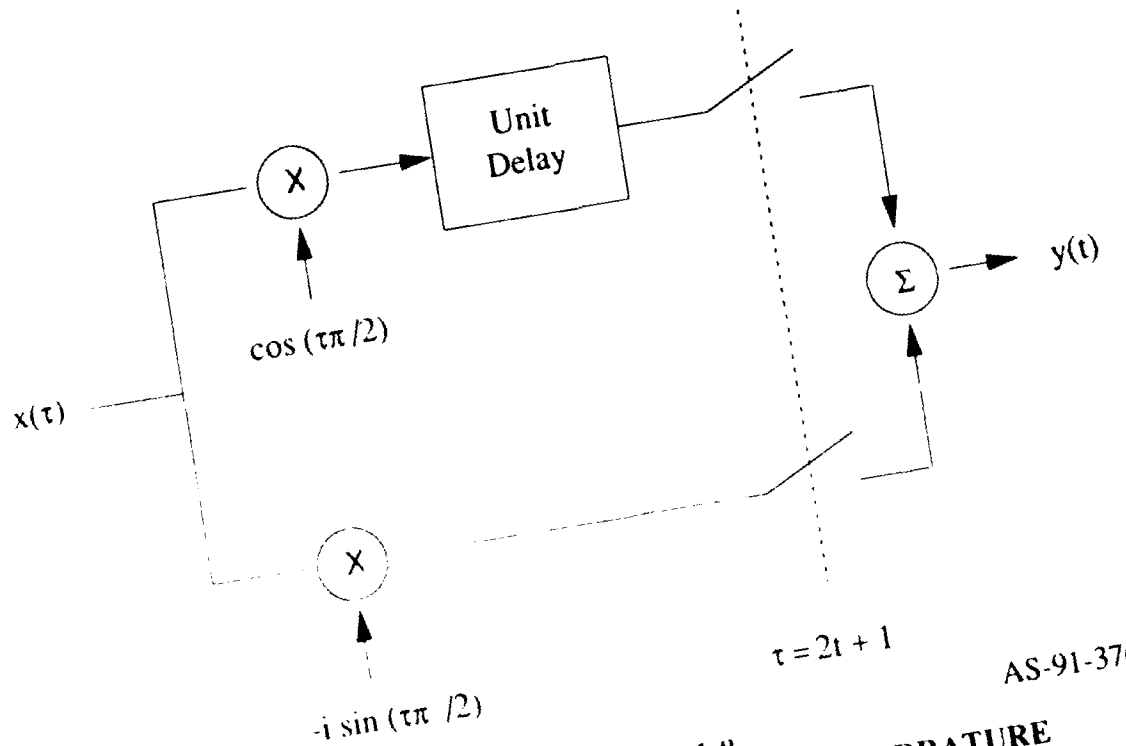

AS-91-376

FIGURE 5.1.8
BLOCK DIAGRAM FOR THE RATE 1/2 QUADRATURE SAMPLING SYSTEM

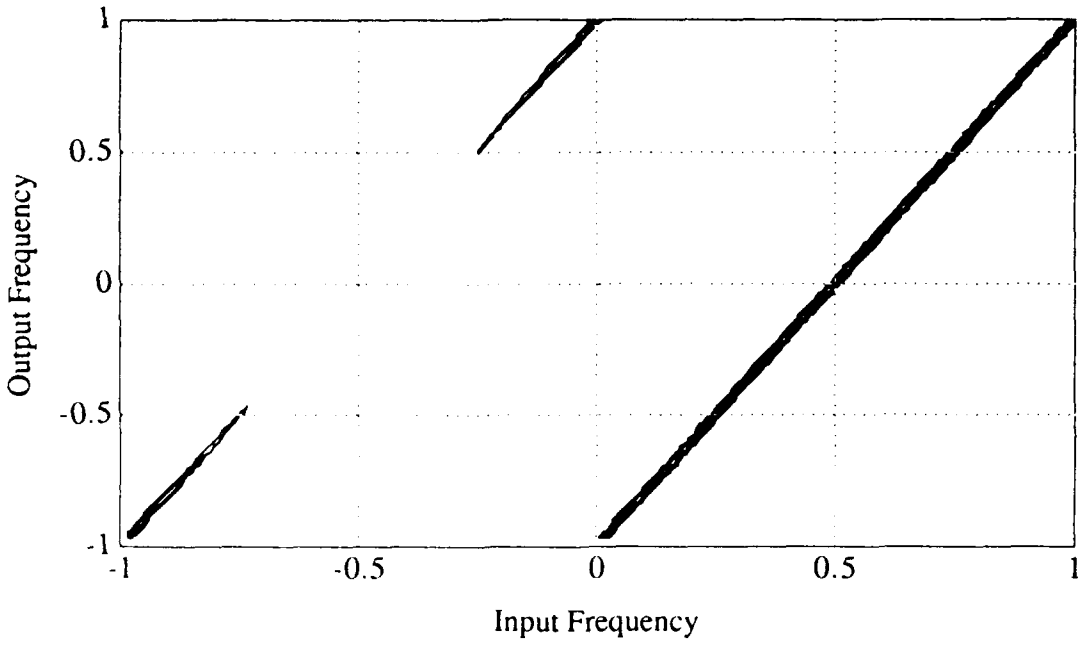

AS-91-377

FIGURE 5.1.9
THEORETICAL SYSTEM TRANSMISSION FUNCTION FOR THE RATE 1/2 QUADRATURE SAMPLING SYSTEM

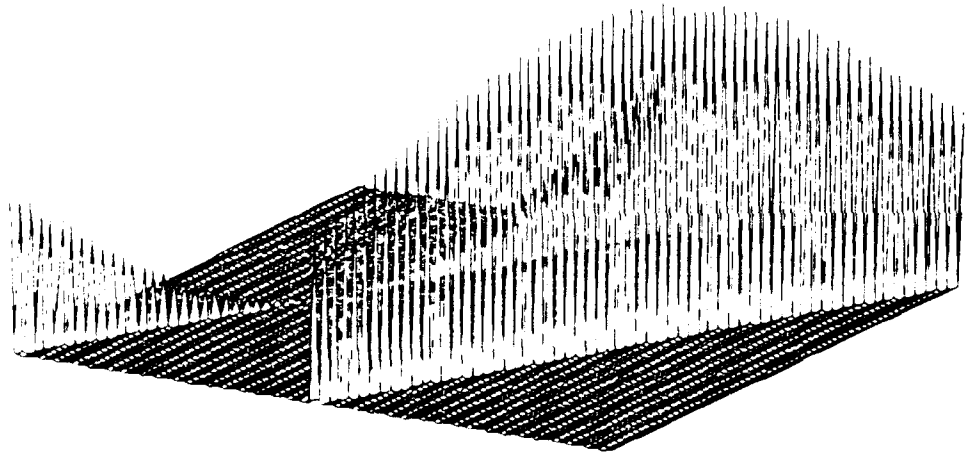

AS-91-378

FIGURE 5.1.10
THEORETICAL SYSTEM TRANSMISSION FUNCTION FOR THE RATE 1/2 QUADRATURE SAMPLING SYSTEM

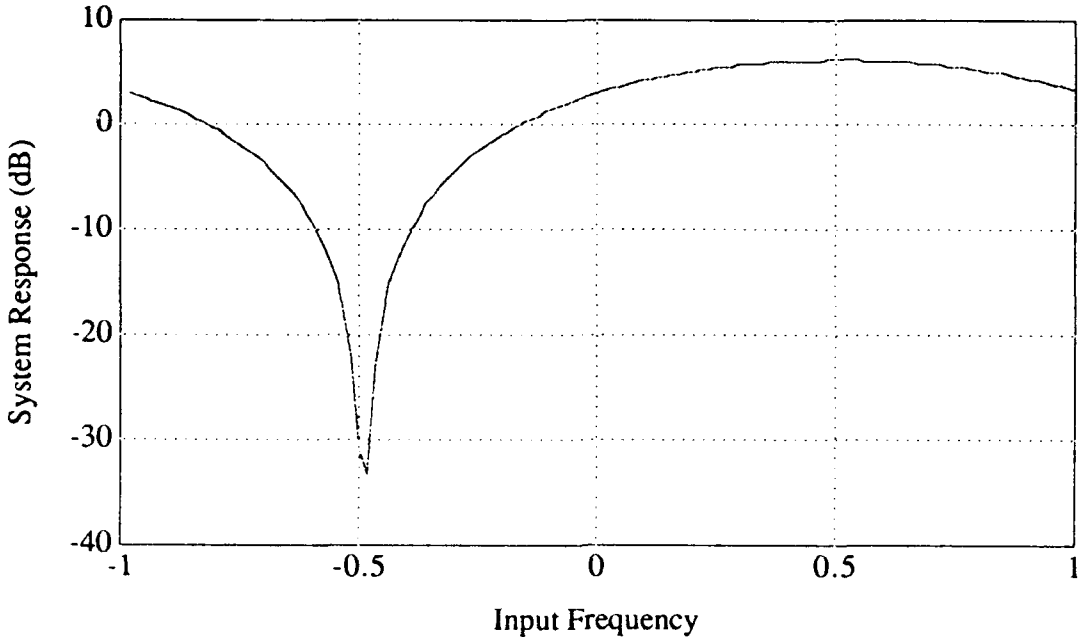

AS-91-379

FIGURE 5.1.11
THEORETICAL SYSTEM RESPONSE FOR THE RATE 1/2 QUADRATURE SAMPLING SYSTEM

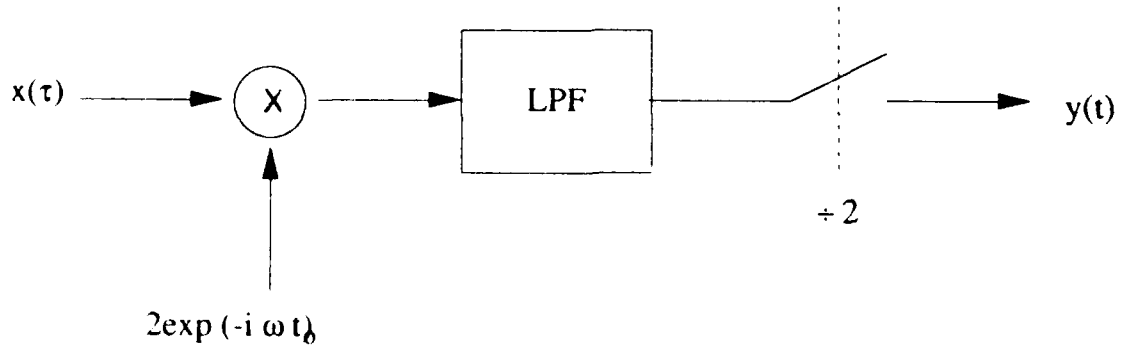

AS-91-380

FIGURE 5.1.12
BLOCK DIAGRAM FOR THE RATE 1/2 QUADRATURE DEMODULATOR

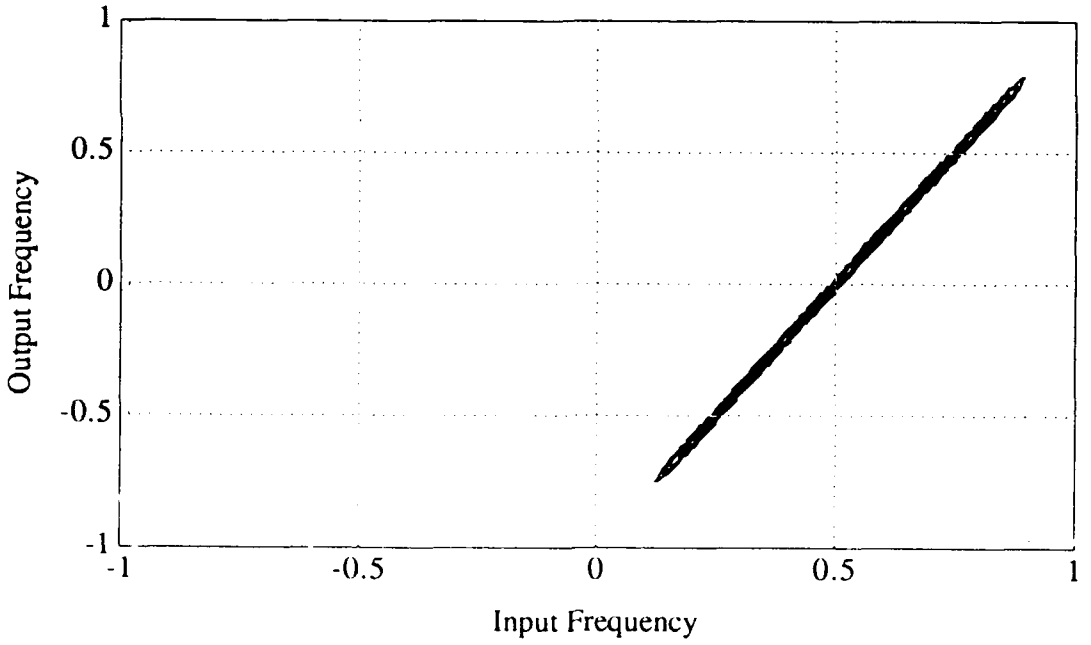

AS-91-381

FIGURE 5.1.13
THEORETICAL SYSTEM TRANSMISSION FUNCTION FOR THE RATE 1/2 QUADRATURE DEMODULATION SYSTEM

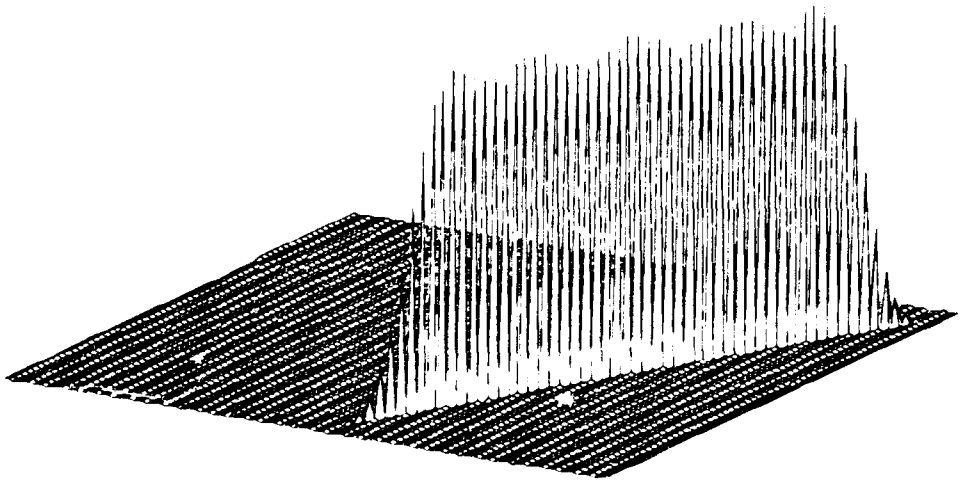

AS-91-382

FIGURE 5.1.14
THEORETICAL SYSTEM TRANSMISSION FUNCTION FOR THE RATE 1/2 QUADRATURE DEMODULATION SYSTEM

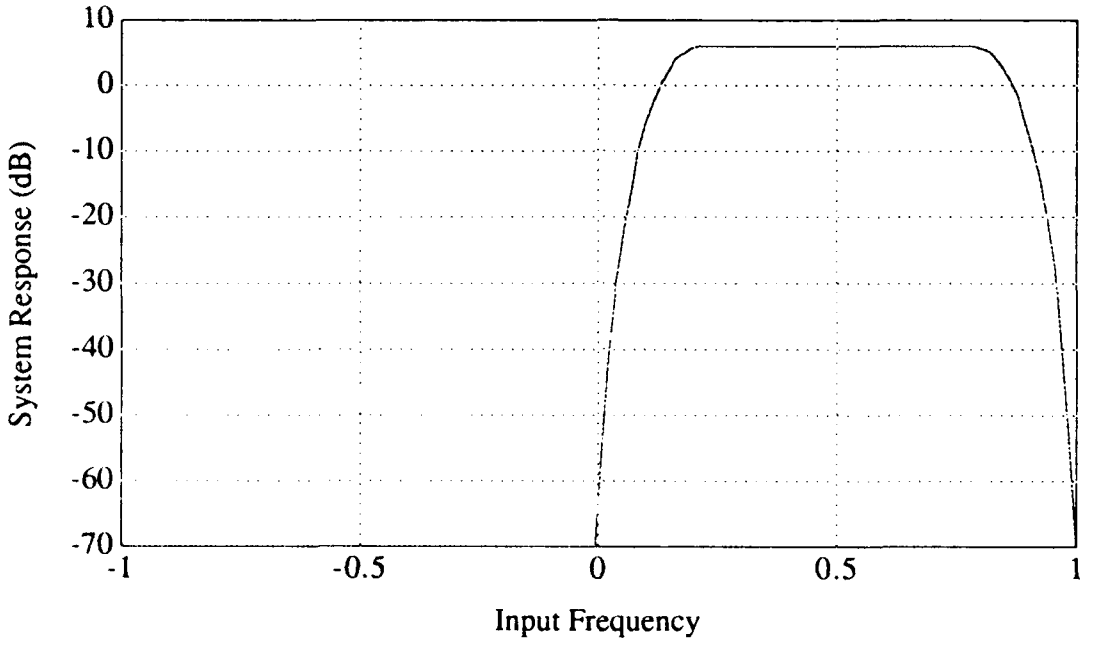

AS-91-383

FIGURE 5.1.15
THEORETICAL SYSTEM RESPONSE FOR THE RATE 1/2
QUADRATURE DEMODULATION SYSTEM

5.2 CHARACTERIZATION via DETERMINISTIC SIGNALS

The method of characterizing LPTV systems using deterministic signals described in Section 4.1 was applied to the five systems of interest. A complex sinusoid of a specific frequency was generated and applied to the LPTV system of interest. A 512-sample record of the system output was obtained, and a minimum 3-term Blackman-Harris windowing function was then applied to this output record (see Harris, 1978). The 512-point discrete Fourier transform of this windowed output data record was computed. The resulting DFT was smoothed using M = 8 in order to reduce the number of points in the resulting estimate for $K(\omega,\alpha)$, and so simplify the plotting of the data. This 64-point smoothed DFT was used as the estimate for the system transmission function for the specific input frequency. The procedure was then repeated for each of K discrete input frequencies, $\alpha_k = \frac{2\pi}{K}$, where K was chosen so that N/K = ρ, the rate of the LPTV system under evaluation.

Figures 5.2.1 and 5.2.2 present the estimated system transmission functions for the simple rate 1/2 decimator and the simple quadrature demodulator obtained using this method. Note the close agreement between these estimates and the theoretical system transmission functions of Figures 5.1.2 and 5.1.4. Figure 5.2.3 presents the estimated system transmission function for the rate 3/2 interpolator as a logarithmic contour plot. Figure 5.2.4 presents a three-dimensional view of this estimated system transmission function. Figure 5.2.5 presents the estimated system transmission function for the rate 1/2 quadrature sampling system. Figure 5.2.6 presents a three-dimensional view of the estimated transmission function. Figure 5.2.7 presents the result of plotting the largest value of the estimate for $K(\omega,\alpha)$ over all ω for each α. Note the close agreement between the estimated system transmission function and the theoretical value plotted in Figures 5.1.9, 5.1.10 and 5.1.11. Figure 5.2.8 presents the estimated system transmission function for the rate 1/2 quadrature demodulator. In this contour plot, the magnitudes are presented in logarithmic form. Figure 5.2.9 presents a three-dimensional view of the estimated system transmission function for the rate 1/2 quadrature demodulator. Figure 5.2.10 presents the result of plotting the largest value of $K(\omega,\alpha)$ over all ω for each α. Again there is close agreement between the estimated system transmission function and the theoretical values presented in Figures 5.1.13, 5.1.14, and 5.1.15.

A simulation of the effects of quadrature phase error between the real and imaginary components of the input reference sinusoid was also conducted. Specifically, the real and

imaginary parts of the input reference sinusoid were generated and applied separately to the input of the rate 1/2 quadrature demodulator. A quadrature phase error of 1° was introduced between the real and imaginary components of the input reference sinusoid. From the discussion of Section 4.1, we would expect to see the term $\frac{\phi}{2} K(\omega,-\alpha)$ appear in our estimate, where $\frac{\phi}{2}$ is roughly -41 dB. Figure 5.2.11 presents a contour plot of the logarithm of the estimated system transmission function obtained using the given reference sinusoids. Figure 5.2.12 presents the result of plotting the largest value of $K(\omega,\alpha)$ over all ω for each α. From these two figures we note that quadrature phase error in the input reference sinusoids does indeed lead to the term $\frac{\phi}{2} K(\omega,-\alpha)$ in our estimated system transmission function.

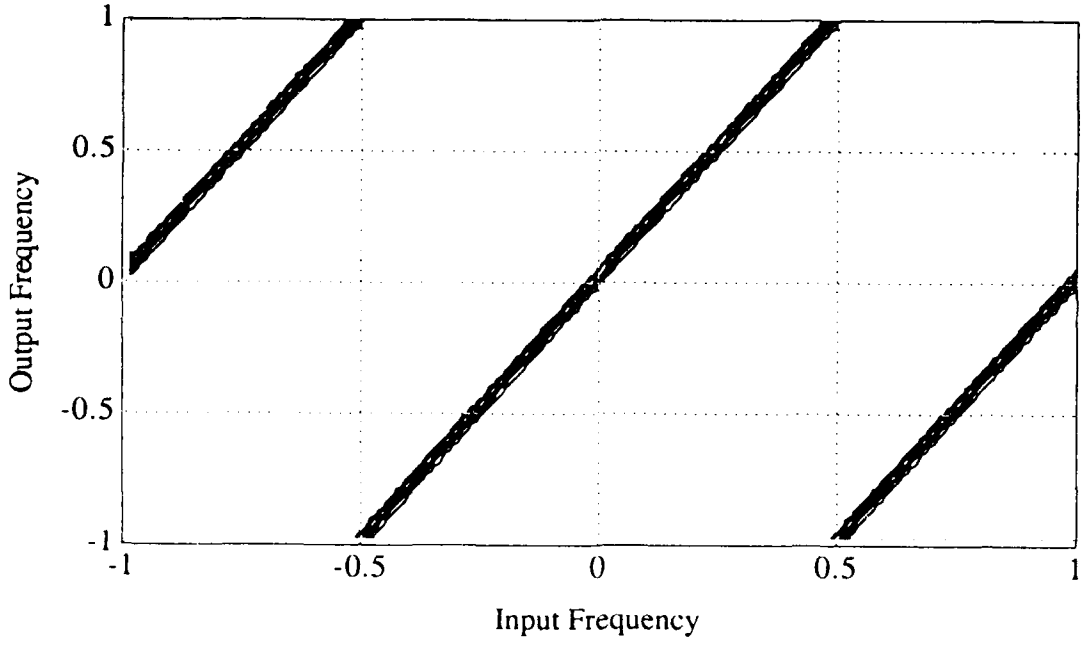

AS-91-384

FIGURE 5.2.1
ESTIMATED SYSTEM TRANSMISSION FUNCTION FOR THE SIMPLE RATE 1/2 DECIMATOR

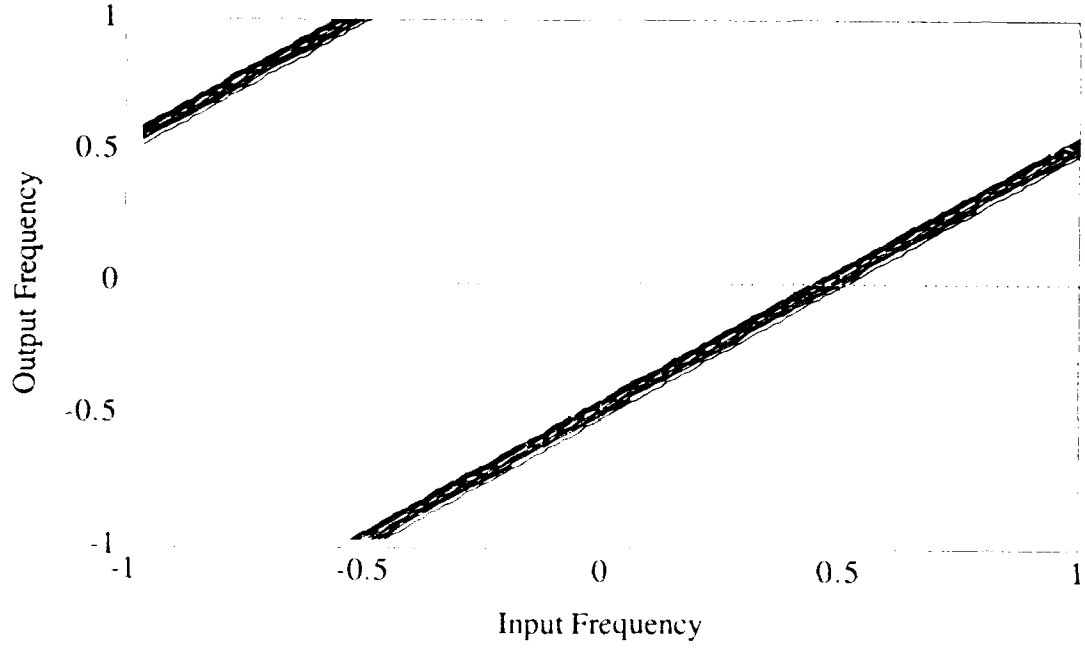

AS-91-385

FIGURE 5.2.2
ESTIMATED SYSTEM TRANSMISSION FUNCTION FOR THE SIMPLE QUADRATURE DEMODULATOR

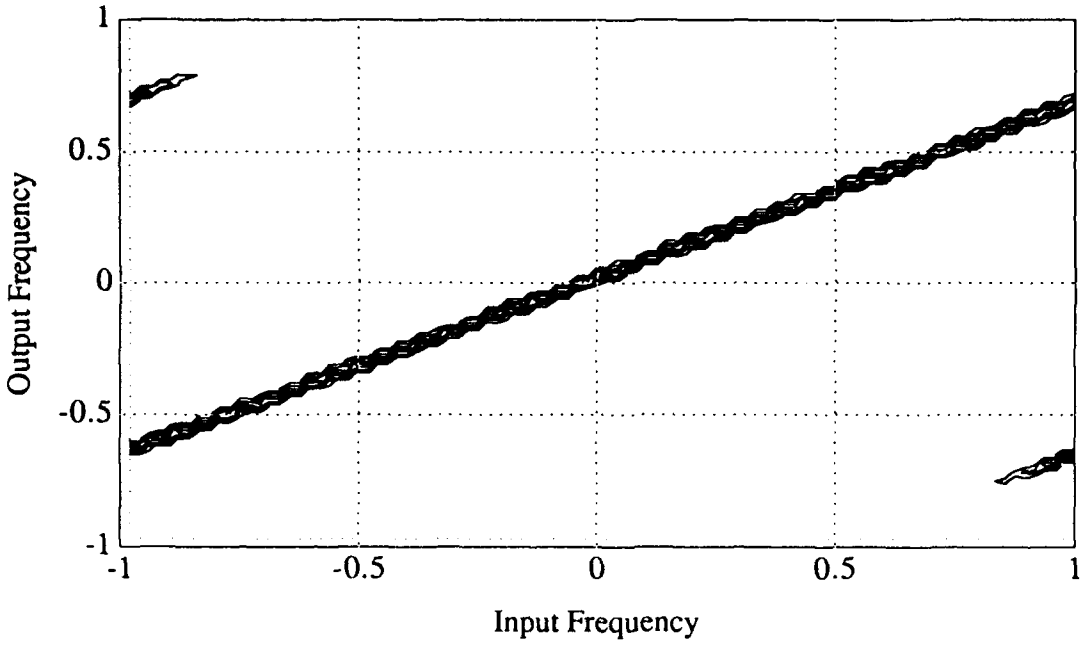

AS-91-386

FIGURE 5.2.3
ESTIMATED SYSTEM TRANSMISSION FUNCTION FOR THE RATE 3/2 INTERPOLATOR

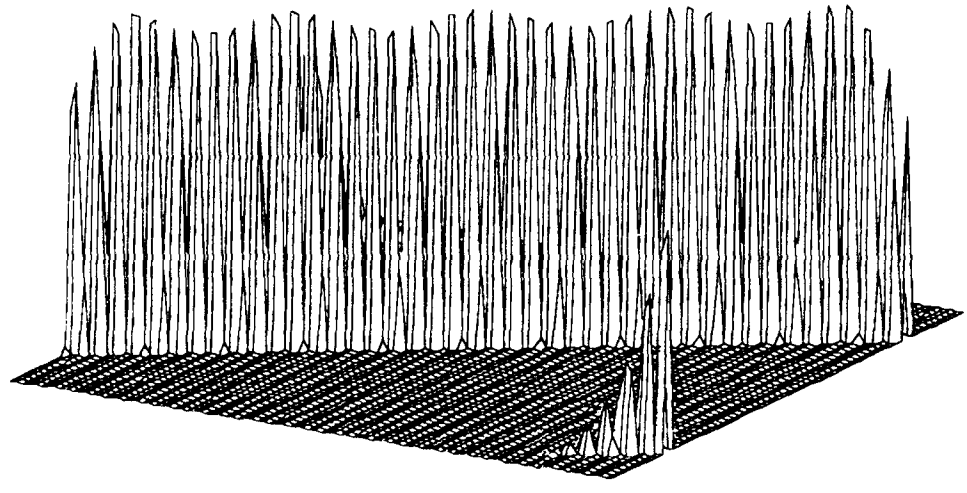

AS-91-387

FIGURE 5.2.4
ESTIMATED SYSTEM TRANSMISSION FUNCTION FOR THE RATE 3/2 INTERPOLATOR

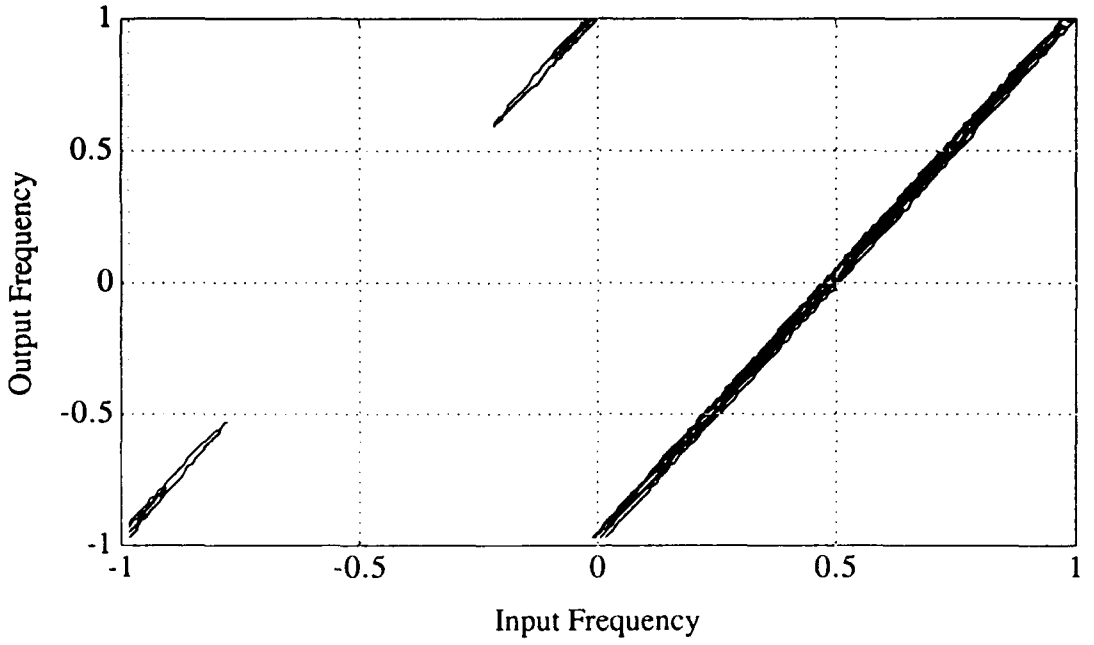

AS-91-388

FIGURE 5.2.5
ESTIMATED SYSTEM TRANSMISSION FUNCTION FOR THE RATE 1/2 QUADRATURE SAMPLING SYSTEM

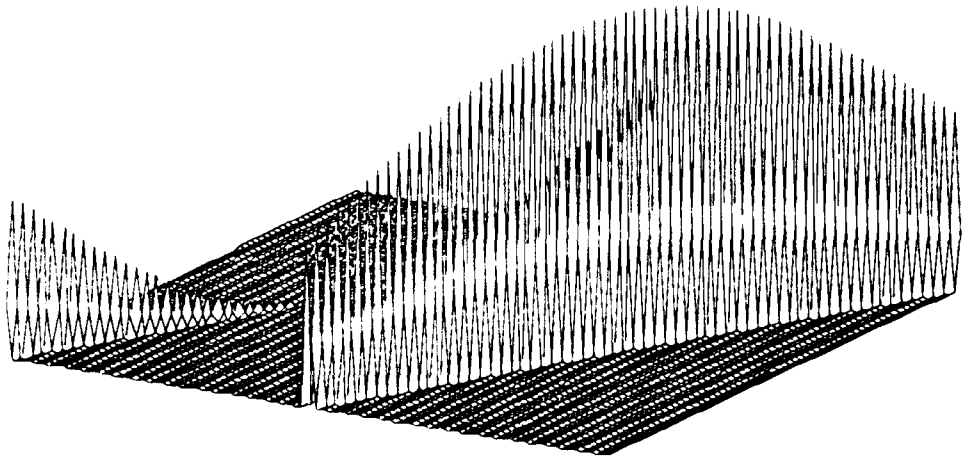

AS-91-389

FIGURE 5.2.6
ESTIMATED SYSTEM TRANSMISSION FUNCTION FOR THE RATE 1/2 QUADRATURE SAMPLING SYSTEM

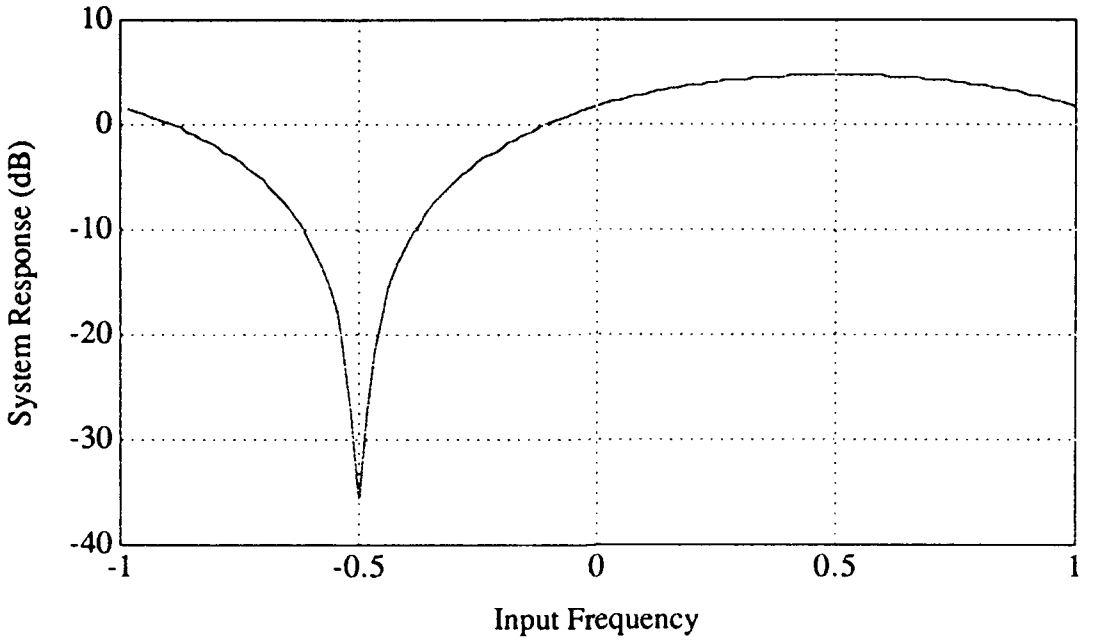

AS-91-390

FIGURE 5.2.7
ESTIMATED SYSTEM RESPONSE FOR THE RATE 1/2 QUADRATURE SAMPLING SYSTEM

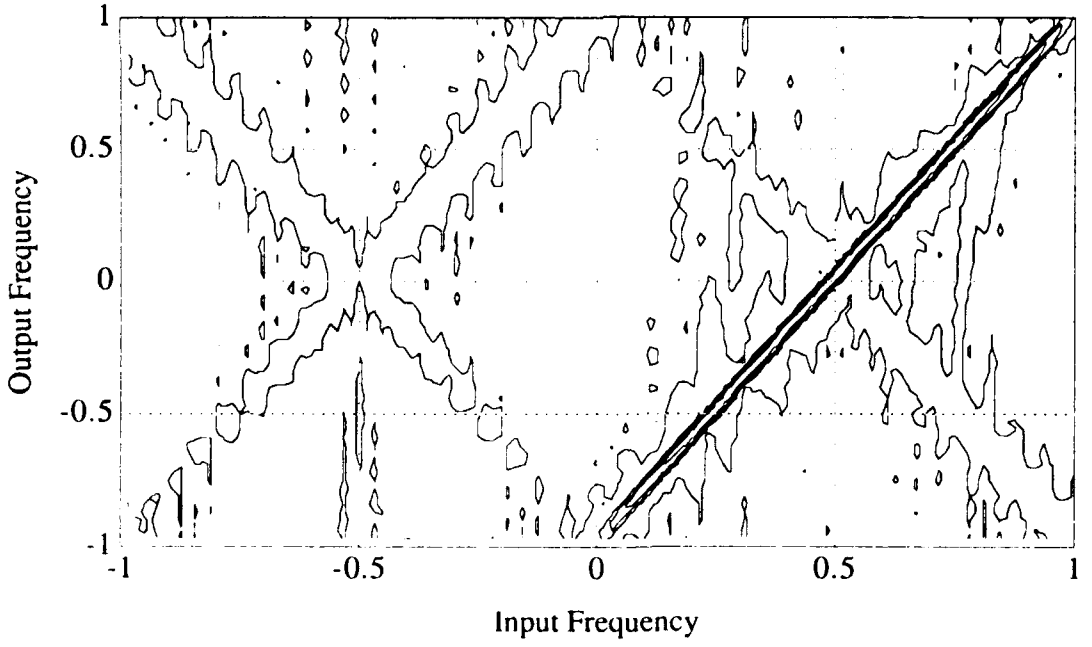

AS-91-391

FIGURE 5.2.8
ESTIMATED SYSTEM TRANSMISSION FUNCTION FOR THE RATE 1/2 QUADRATURE DEMODULATOR

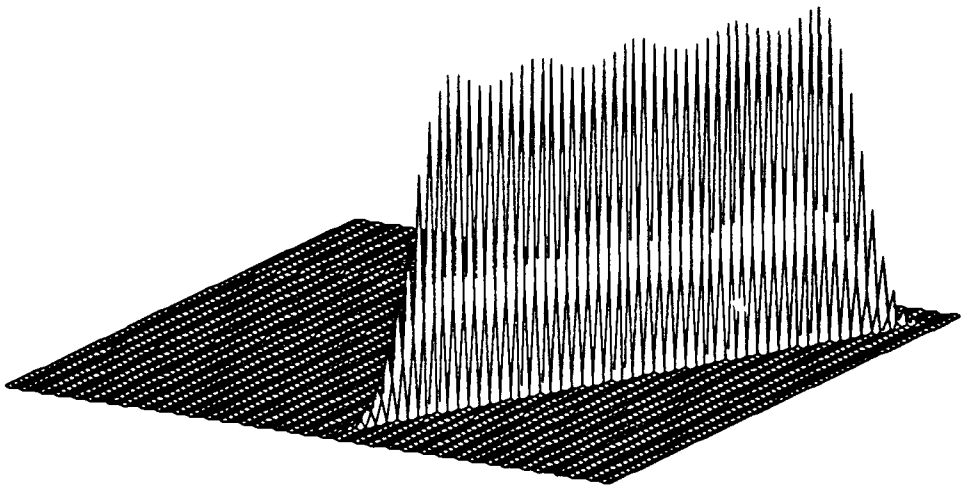

AS-91-392

FIGURE 5.2.9
ESTIMATED SYSTEM TRANSMISSION FUNCTION FOR THE RATE 1/2 QUADRATURE DEMODULATOR

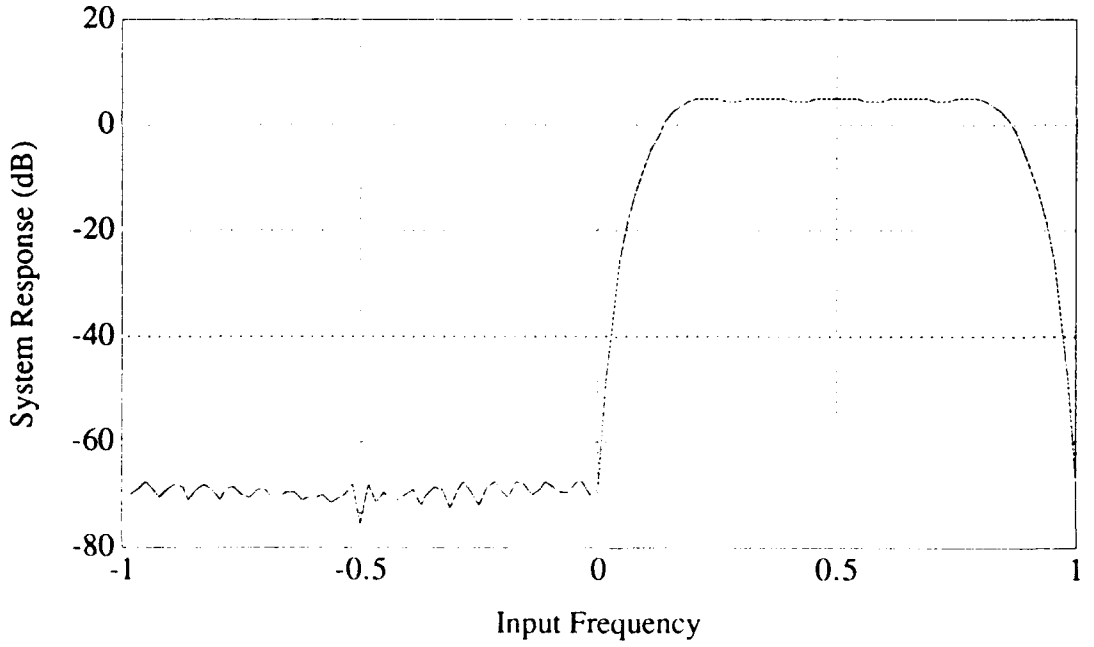

AS-91-393

FIGURE 5.2.10
ESTIMATED SYSTEM RESPONSE FOR THE RATE 1/2 QUADRATURE DEMODULATION SYSTEM

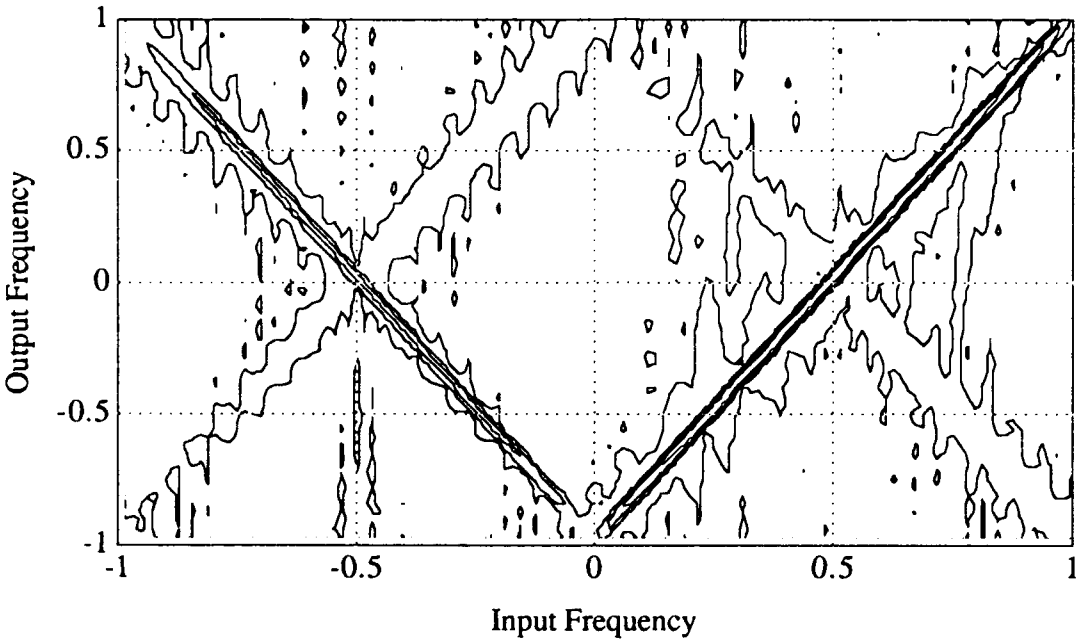

AS-91-394

FIGURE 5.2.11
ESTIMATED SYSTEM TRANSMISSION FUNCTION FOR THE RATE 1/2 QUADRATURE DEMODULATION SYSTEM WITH 1 DEGREE OF QUADRATURE PHASE ERROR

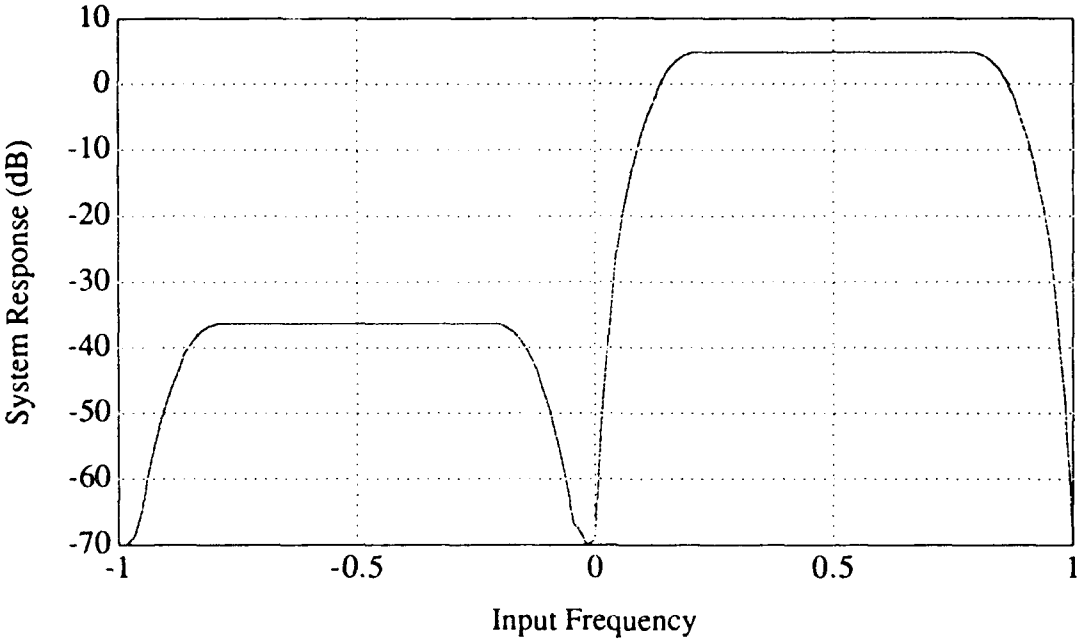

AS-91-395

FIGURE 5.2.12
ESTIMATED SYSTEM RESPONSE FOR THE RATE 1/2 QUADRATURE DEMODULATION SYSTEM WITH 1 DEGREE OF QUADRATURE PHASE ERROR

5.3 CHARACTERIZATION via NONDETERMINISTIC SIGNALS

The method of characterizing LPTV systems using nondeterministic input signals was used to estimate the system transmission functions for the five LPTV systems of interest. In each case, a Gaussian input sequence was applied to the system of interest, and an estimate of the system transmission function was obtained by the appropriate time and frequency smoothing of the discrete spectral components. Normalization of the estimated system transmission function by the estimated input noise power spectrum was used, as described in Section 4.2.

Figure 5.3.1 presents a contour plot of the logarithm of the estimated system transmission function for the simple rate 1/2 decimator. For this simulation, the input DFT length, K, was 512, the output DFT length, N, was 1024, the frequency smoothing length, M, was 8, and the number of averages, L, was 512. Figure 5.3.2 presents the contour plot of the logarithm of the estimated system transmission function for the simple quadrature demodulator. For this simulation, K=N=512, M=8, and L=512.

Figure 5.3.3 presents a contour plot of the logarithm of the estimated system transmission function for the rate 3/2 interpolator. Figure 5.3.4 presents a three-dimensional view of this estimate. For this simulation, K=512, N=768, M=8, and L=512.

Figure 5.3.5 presents a contour plot of the logarithm of the estimated system transmission function for the rate 1/2 quadrature sampling system. Figure 5.3.6 presents a three-dimensional view of this estimate. Figure 5.3.7 presents the result of plotting the largest value of $K(\omega,\alpha)$ over all ω for each α. For this simulation, K=512, N=1024, M=8, and L=512.

Figure 5.3.8 presents a contour plot of the logarithm of the estimated system transmission function for the rate 1/2 quadrature demodulator. Figure 5.3.9 presents a three-dimensional view of this estimate. Figure 5.3.10 presents the result of plotting the largest value of $K(\omega,\alpha)$ over all ω for each α. For this simulation, K=512, N=1024, M=8, and L=512. Note that we obtain reasonably good agreement with the theoretical response presented in Section 5.1.

A simulation of the effects of using separate real and imaginary input signal components was also conducted. For this simulation, a single Gaussian noise sequence

was generated and applied to the input of the rate 1/2 quadrature demodulation system. Alternating records of the observed input and output sequences were used to produce the real and imaginary parts of the estimated system transmission function. As in the previous simulation for the rate 1/2 quadrature demodulation system, K=512, N=1024, M=8, and L=512. Figure 5.3.11 presents the contour plot of the logarithm of the estimated system transmission function obtained from this simulation. Figure 5.3.12 presents a three-dimensional view of the estimate.

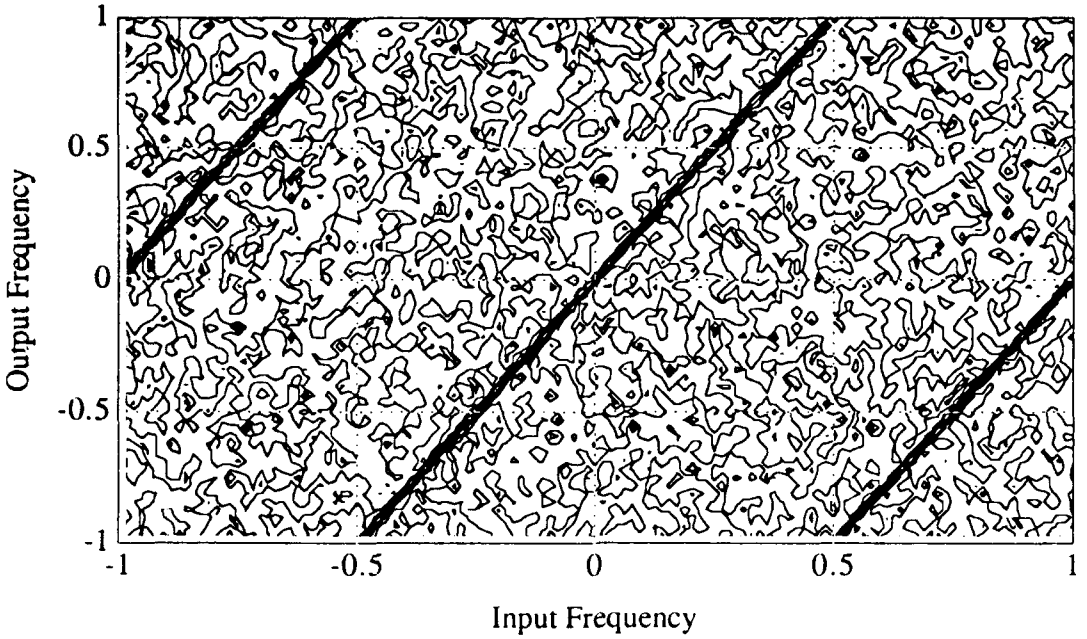

AS-91-396

FIGURE 5.3.1
ESTIMATED SYSTEM TRANSMISSION FUNCTION FOR THE SIMPLE RATE 1/2 DECIMATOR

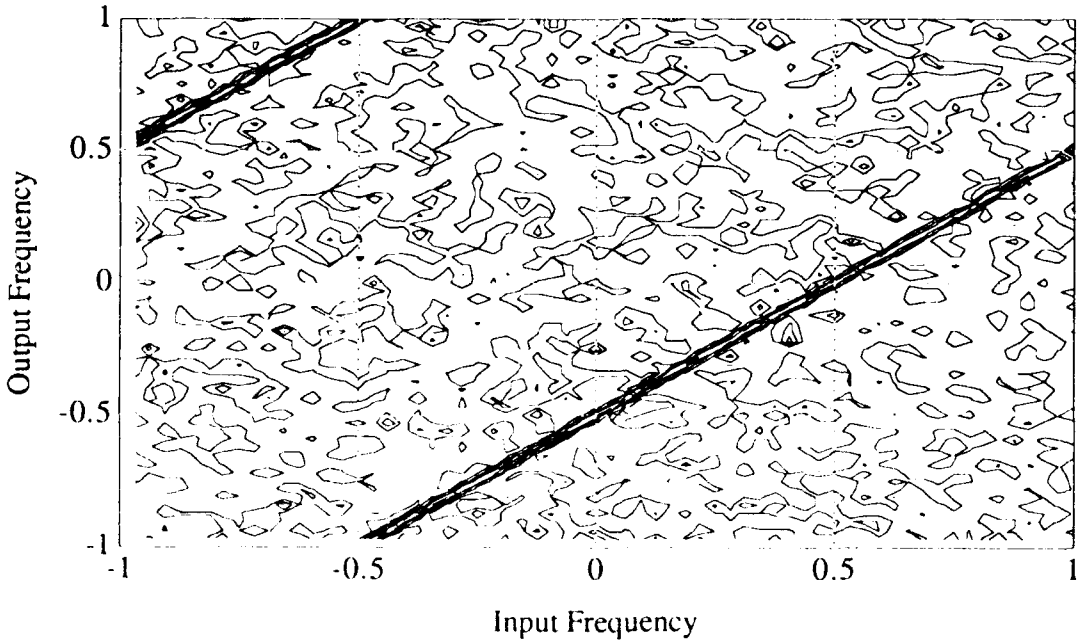

AS-91-397

FIGURE 5.3.2
ESTIMATED SYSTEM TRANSMISSION FUNCTION FOR THE SIMPLE QUADRATURE DEMODULATOR

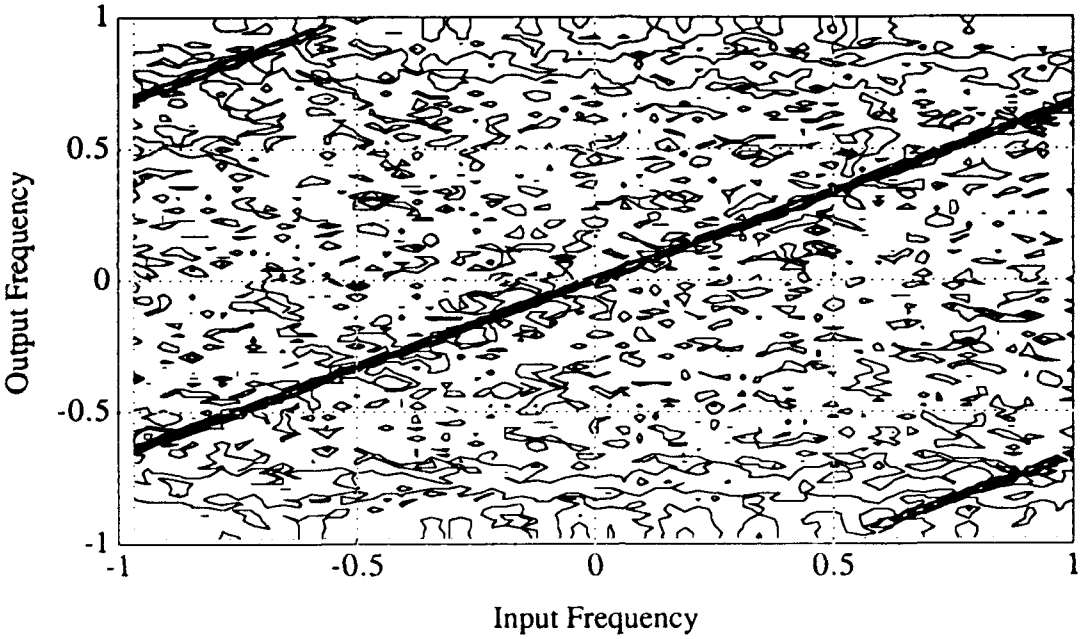

AS-91-398

FIGURE 5.3.3
ESTIMATED SYSTEM TRANSMISSION FUNCTION FOR THE RATE 3/2 INTERPOLATOR

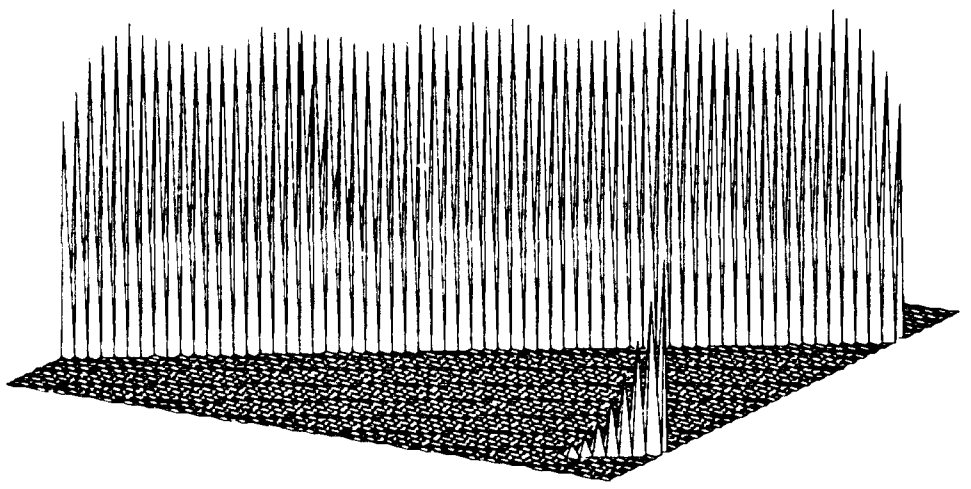

AS-91-399

FIGURE 5.3.4
ESTIMATED SYSTEM TRANSMISSION FUNCTION FOR THE RATE 3/2 INTERPOLATOR

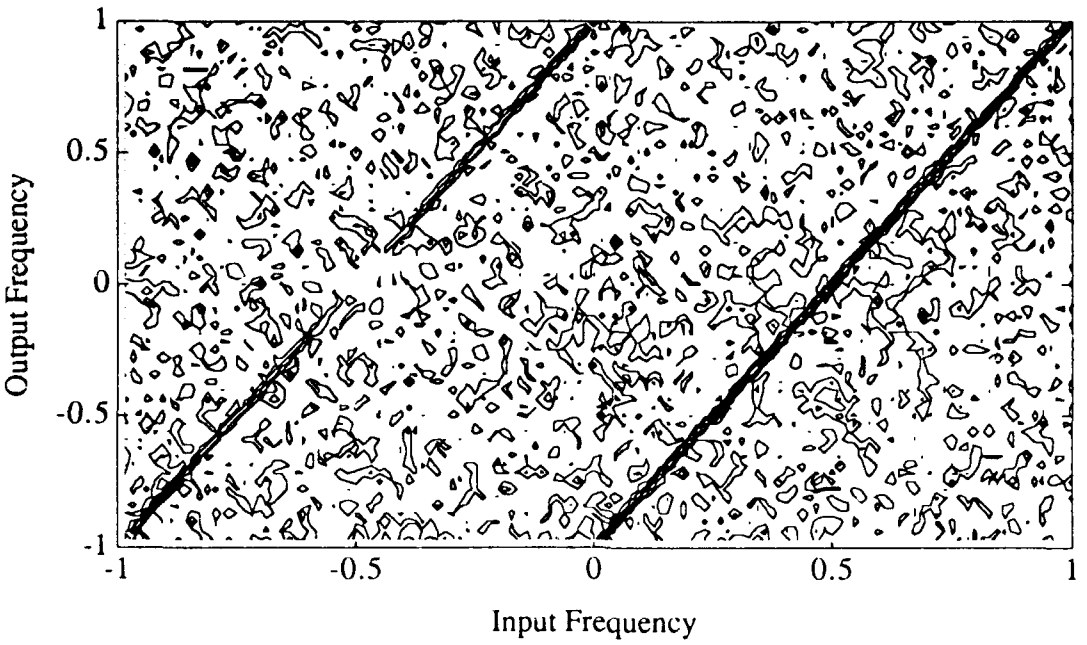

AS-91-400

FIGURE 5.3.5
ESTIMATED SYSTEM TRANSMISSION FUNCTION FOR THE RATE 1/2 QUADRATURE SAMPLING SYSTEM

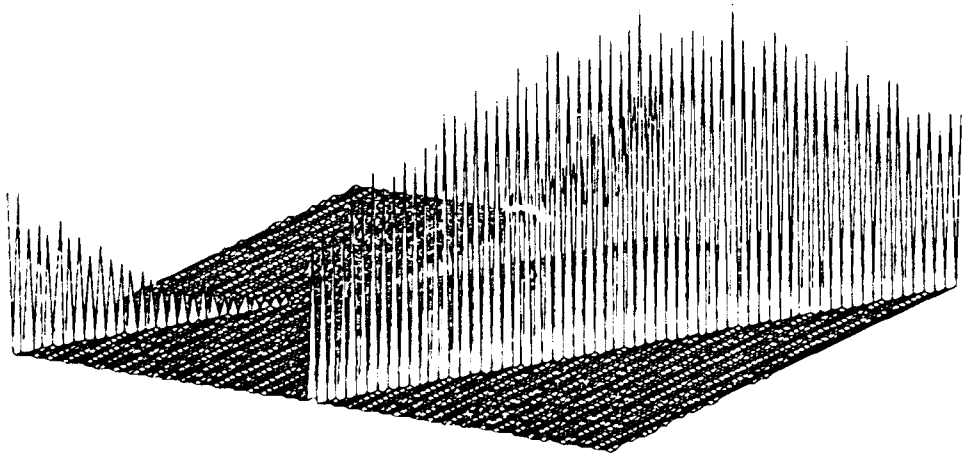

AS-91-401

FIGURE 5.3.6
ESTIMATED SYSTEM TRANSMISSION FUNCTION FOR THE RATE 1/2 QUADRATURE SAMPLING SYSTEM

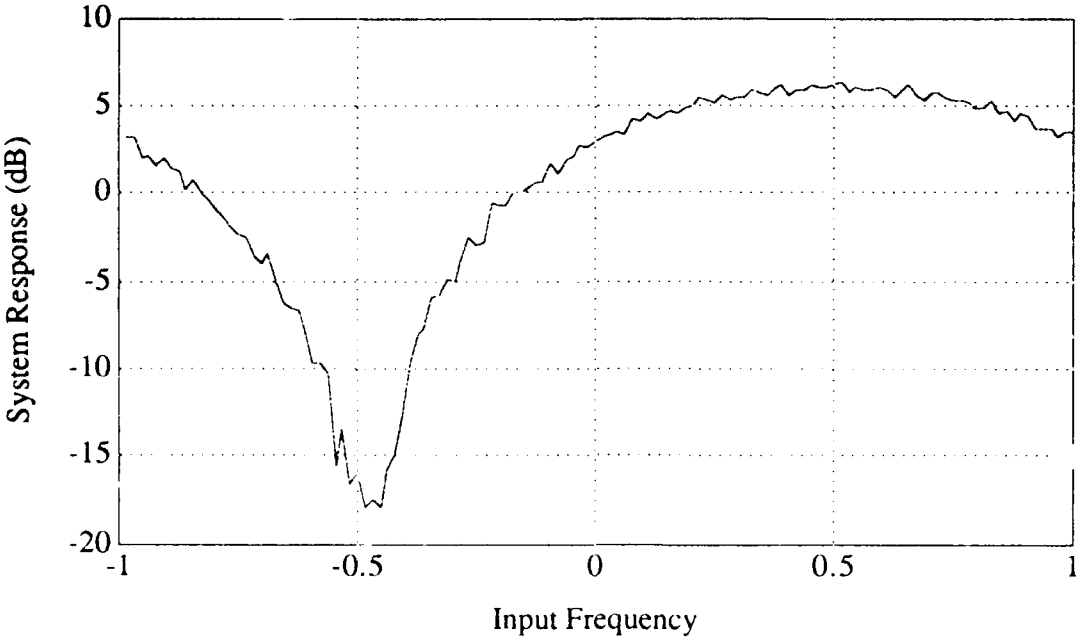

AS-91-402

FIGURE 5.3.7
ESTIMATED SYSTEM RESPONSE FOR THE RATE 1/2 QUADRATURE SAMPLING SYSTEM

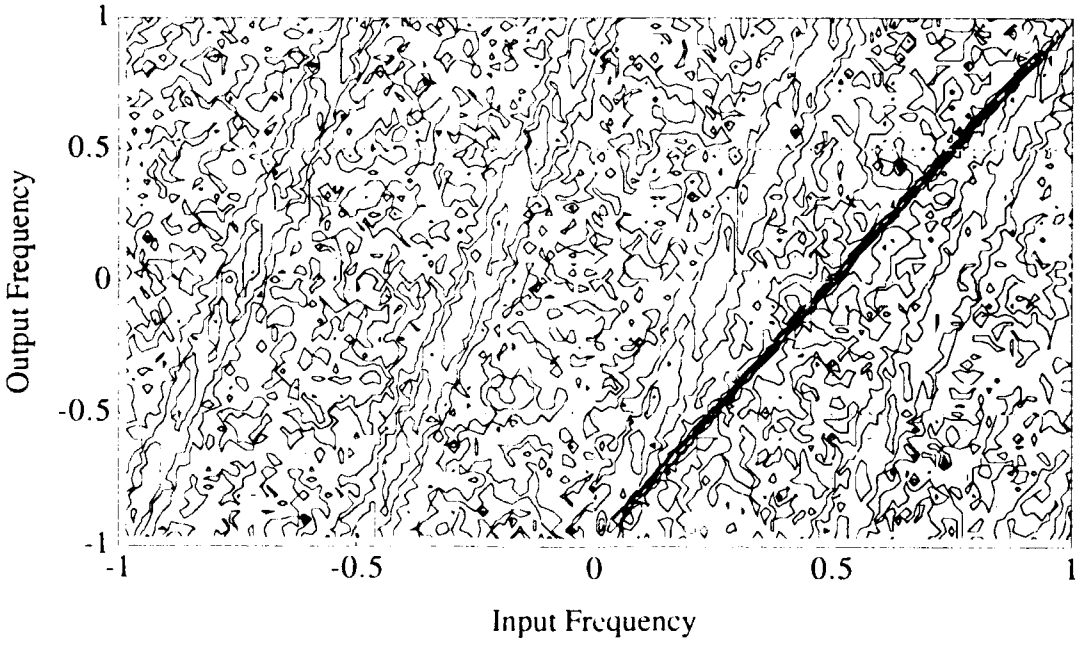

AS-91-403

FIGURE 5.3.8
ESTIMATED SYSTEM TRANSMISSION FUNCTION FOR THE RATE 1/2 QUADRATURE DEMODULATOR

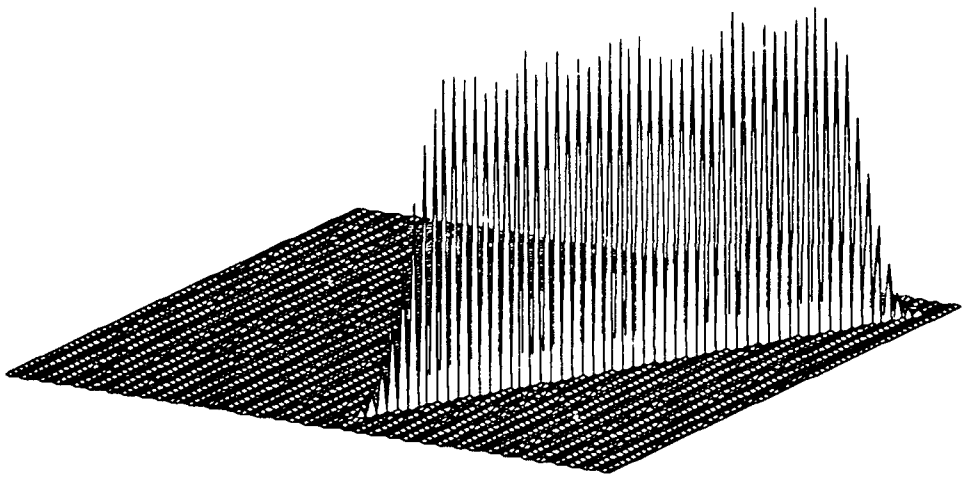

AS-91-404

FIGURE 5.3.9
ESTIMATED SYSTEM TRANSMISSION FUNCTION FOR THE RATE 1/2 QUADRATURE DEMODULATOR

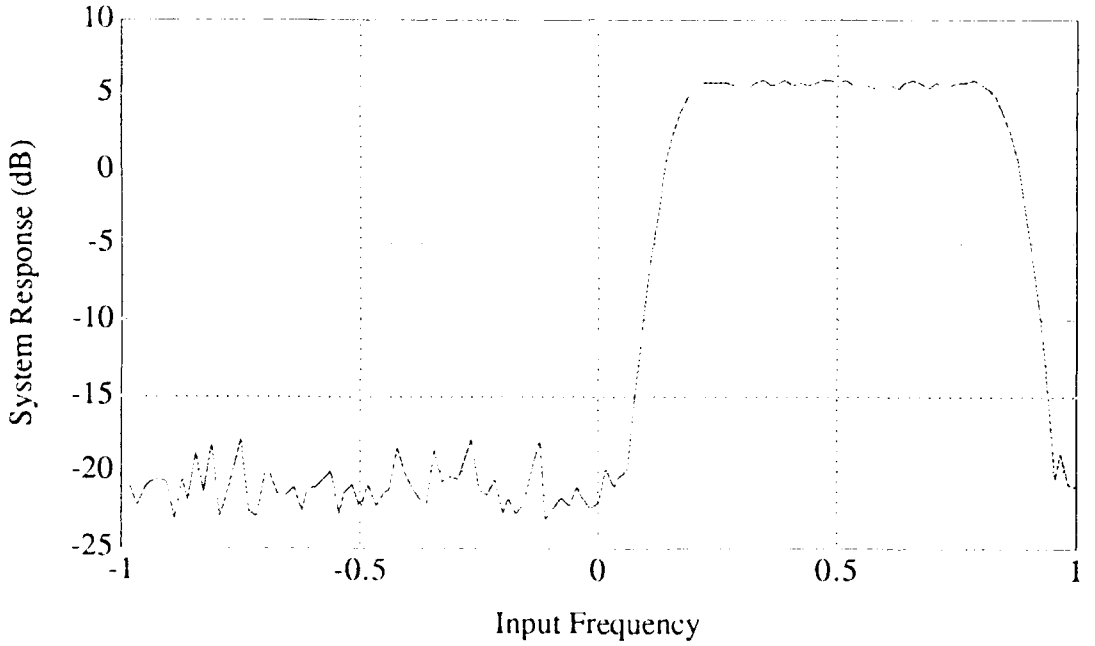

AS-91-405

FIGURE 5.3.10
ESTIMATED SYSTEM RESPONSE FOR THE RATE 1/2 QUADRATURE DEMODULATOR

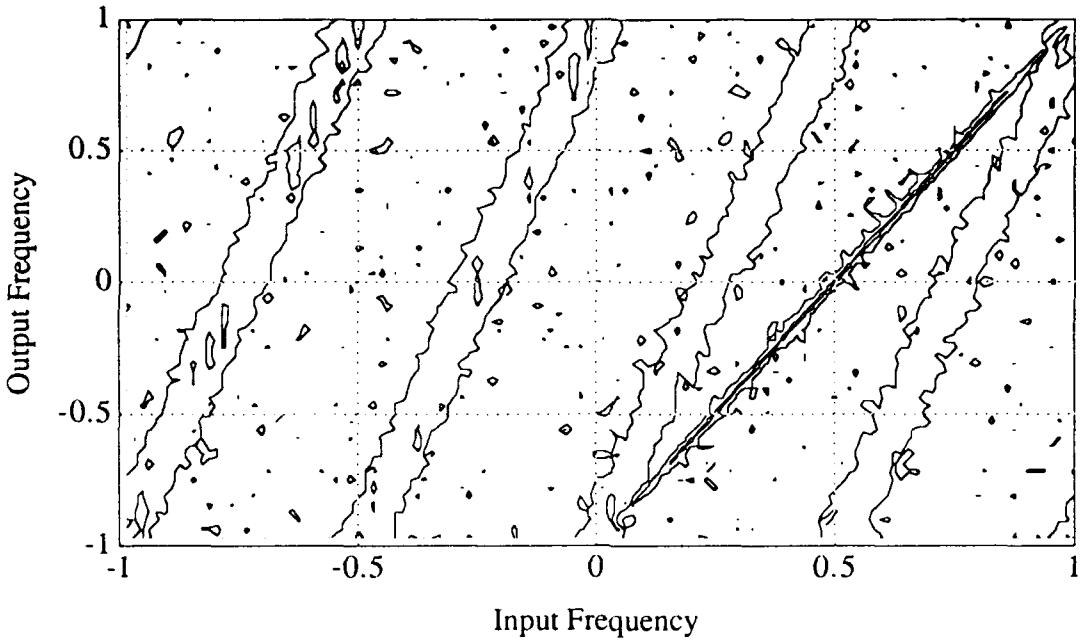

AS-91-406

FIGURE 5.3.11
ESTIMATED SYSTEM TRANSMISSION FUNCTION FOR THE RATE 1/2 QUADRATURE DEMODULATION SYSTEM USING REAL INPUT SIGNALS

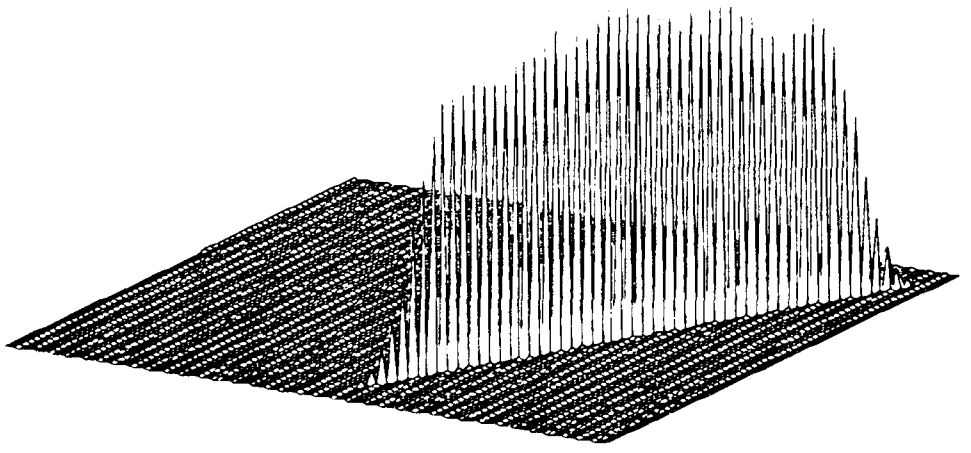

AS-91-407

FIGURE 5.3.12
ESTIMATED SYSTEM TRANSMISSION FUNCTION FOR THE RATE 1/2 QUADRATURE DEMODULATION SYSTEM USING REAL INPUT SIGNALS

5.4 CHAPTER SUMMARY

In this chapter, the techniques for characterizing LPTV systems described in Chapter 4 were applied to several systems of interest. The consequences of quadrature phase error and independent application of the real and imaginary components of the input signal were also demonstrated.

6. CONCLUSIONS

In this paper we have presented two techniques for the empirical characterization of discrete-time linear periodically time-varying systems. These techniques were developed amid a framework of concepts related to the analysis of discrete-time LPTV systems and to the signals produced by such systems. The results of applying these techniques to several LPTV systems of interest were also presented.

From the tests presented in Chapter 5, we see that characterization of LPTV systems using deterministic sinusoidal reference inputs provides an accurate estimate of the system transmission function only when the quadrature phase error between the real and imaginary components of the reference input is maintained within some tight limit over the analysis bandwidth of interest. In those situations where we may apply only real input signals, so that the real and imaginary components must be applied separately, this requirement may place a severe limitation on the design of the reference signal generator. In contrast, the use of non-deterministic input signals for characterization of LPTV systems may proceed by applying independent real and imaginary input signal components to the system of interest. The design of the reference signal generator is therefore greatly simplified.

In conclusion, the characterization of discrete-time LPTV systems using deterministic signals is appropriate in those situations where a fine estimate of the system transmission function is required at a particular frequency, or across some relatively narrow band of frequencies. The use of non-deterministic signals for LPTV system characterization is appropriate in those situations where an estimate of the system transmission function is required over a broad range of frequencies, or where the direct application of a reference sinusoid would be impractical.

REFERENCES

Aseltine, J. A., 1954. "A Transform Method for Linear Time-Varying Systems," Journal of Applied Physics 25(6), 761-764 (1954).

Baugh, K. W., 1988. "Review and Comparative Performance of Techniques for Obtaining Digital Quadrature Representations of Analog Bandpass Signals," Applied Research Laboratories Technical Report No. 88-13 (ARL-TR-88-13), Applied Research Laboratories, The University of Texas at Austin.

Bendat, J. S., and Piersol, A. G., 1986. Random Data: Analysis and Measurement Procedures (John Wiley and Sons, New York).

Billingsley, P., 1968. Convergence of Probability Measures (John Wiley and Sons, New York).

Brikker, I. N., 1966. "The Frequency Analysis of Linear Variable-Parameter Systems," Automation and Remote Control 27(8), 1375-1388 (1966).

Claasen, T. A., and Mecklenbrauker, W. F. G., 1982. "On Stationary Linear Time-Varying Systems," IEEE Trans. Circuits and Systems CAS-29(3), 169-184 (1982).

Cohen, L., 1989. "Time-Frequency Distributions: A Review," Proc. IEEE 77(7), 941-981 (1989).

Cramer, H., 1961. "On Some Classes of Nonstationary Stochastic Processes," Proceedings of the Fourth Berkeley Symposium on Mathematical Statistics and Probability (University of California Press, Berkeley, California), 57-78.

Crochiere, R. E., and Rabiner, L. R., 1983. Multirate Digital Signal Processing (Prentice-Hall, Englewood Cliffs, New Jersey).

D'Angelo, H., 1970. Linear Time-Varying Systems: Analysis and Synthesis (Allyn and Bacon, Boston, Massachusetts).

Gardner, W. A., 1986. Introduction to Random Processes (Macmillan, New York).

Gersho, A., 1963. "Characterization of Time-Varying Linear Systems," Proc. IEEE 51(1), 238 (1963).

Harris, F. J., 1978. "On the Use of Windows for Harmonic Analysis with the Discrete Fourier Transform," Proceedings of the IEEE 66(1), 57-83.

Johnson, G. W., and Kilmer, F. G., 1962. "Integral Transforms for Algebraic Analysis and Design of a Class of Linear-Variable and Adaptive Control Systems," IRE Trans. Automatic Control AC-7(2), 97-106 (1962).

Kaplan, W., 1962. Operational Methods for Linear Systems (Addison-Wesley, Reading, Massachusetts).

Koopmans, L. H., 1974. The Spectral Analysis of Time Series (Academic Press, San Diego, California).

Lyones, R. M., 1968. "On the Concept of the Spectrum for Non-Stationary Processes (with Discussion)," J. Roy. Stat. Soc., Series B, 30(1), 1-30 (1968).

Oppenhein, A. V., and Schafer, R. W., 1975. Digital Signal Processing (Prentice-Hall, Englewood Cliffs, New Jersey).

Papoulis, A., 1962. The Fourier Integral and its Applications (McGraw-Hill, New York, New York).

Priestley, M. B., 1981. Spectral Analysis and Time Series (Academic Press, San Diego, California).

Priestley, M. B., 1965. "Evolutionary Spectra and Non-Stationary Processes (with Discussion)," J. Roy. Stat. Soc., Series B, 27(2), 204-237 (1965).

Wiener, N., 1933. The Fourier Integral and Certain of its Applications (Dover Publications, New York, New York).

Zadeh, L. A., 1950. "Frequency Analysis of Variable Networks," Proc. IRE 38, 291-299 (1950).

Zadeh, L. A., 1961. "Time-Varying Networks, I," Proc. IRE 49, 1488-1503, (1961).

Zadeh, L. A., and Desoer, C. A., 1963. Linear System Theory: The State Space Approach (McGraw-Hill, New York, New York).

26 July 1991

DISTRIBUTION LIST FOR ARL-TR-91-20 UNDER ARL:UT INDEPENDENT RESEARCH AND DEVELOPMENT PROGRAM

Copy No.

Commander
Naval Sea Systems Command
Department of the Navy
Washington, D.C. 20362-5101

1 Attn: E. Plummer (Code 06UR)
2 R. Dosti (PMS409)
3 Y. Yam (Code 06UR)

Officer in Charge
Naval Underwater Systems Center
New London Laboratory
New London, CT 06320

4 Attn: R. Tompkins (Code 3111)
5 R. Radlinski (Code 333)
6 K. Scarbrough (Code 304)
7 R. Tozier (Code 2121)
8 Library

Director
David Taylor Research Center
Bethesda, MD 20084

9 Attn: J. Niemiec (Code 1945)
10 L. Becker (Code 0114)
11 Library

Department of Electrical Engineering
The University of Texas at Austin
Austin, TX 78712

12 Attn: H. W. Smith
13 F. X. Bostick

Office of the Chief of Naval Research
Department of the Navy
Arlington, VA 22217-5000

14 Attn: J. Smith (Code 1211)
15 R. Hansen (Code 121)
16 T. Goldsberry (Code 23)
17 N. Gerr (Code 1111)
18 Library

Distribution List for ARL-TR-91-20 under ARL:UT IR&D Program
(cont'd)

Copy No.

Office of Naval Intelligence
Department of the Navy
Washington, D.C. 20350-2000
19 Attn: L. Long (NIC-054)

Commanding Officer
David Taylor Research Center Detachment
Puget Sound Naval Shipyard
Bremerton, WA 98314-5212
20 Attn: D. Groutage (Code 1910.2)
21 B. Kipple (Code 1911)

Commanding Officer
Naval Ocean Systems Center
San Diego, CA 92145
22 Attn: C. Persons (Code 732)
23 E. McDaid (Code 733)
24 J. Lockwood (Code 733)
25 Library

Commander
Naval Space and Warfare Systems Command
Department of the Navy
Washington, D.C. 20363-5101
26 Attn: Library

Commanding Officer
Naval Oceanographic and Atmospheric Research Laboratory
Stennis Space Center, MS 39529-5001
27 Attn: Library

Commanding Officer
Naval Oceanographic Office
Stennis Space Center, MS 39522-5001
28 Attn: Library

Director
Naval Research Laboratory
Washington, D.C. 20375-5000
29 Attn: Library

Officer in Charge
Naval Surface Warfare Center
Dahlgren Laboratory
Dahlgren, VA 22448
30 Attn: Library

Distribution List for ARL-TR-91-20 under ARL:UT IR&D Program
(cont'd)

Copy No.	
	Commanding Officer Naval Coastal Systems Center Panama City, FL 32401
31	Attn: Library
	Officer in Charge Naval Ocean Systems Center Hawaii Laboratory Kailua, HI 96734-0977
32	Attn: Library
	Office of the Chief of Naval Research Office of Naval Technology Department of the Navy Arlington, VA 22217-5000
33	Attn: Library
	Defense Advanced Research Projects Agency 1400 Wilson Boulevard Arlington, VA 22209-2309
34	Attn: Library
	National Aeronautics and Space Administration Langley Research Center Hampton, VA 23665
35	Attn: Library
	Defense Mapping Agency Hydrographic/Topographic Center Washington, D.C. 20315-0030
36	Attn: Library
37-39	Commanding Officer and Director Defense Technical Information Center Cameron Station, Building 5 5010 Duke Street Alexandria, VA 22314
	Tracor Applied Sciences, Inc. AARD/Sea Operations 35 Thomas Griffin Rd. New London, CT 06320
40	Attn: D. Turbes
	Planning Systems, Inc. 792 S. Westpark Dr. McLean, VA 22102
41	Attn: H. Warner

Distribution List for ARL-TR-91-20 under ARL:UT IR&D Program
(cont'd)

Copy No.

Lockheed Missile and Space Corporation
0/6580, B/582N
1111 Lockheed Way
Sunnyvale, CA 94088-3504
42 Attn: W. Eugene Brown

National Academy of Sciences
National Research Council
2101 Constitution Avenue
Washington, D.C. 20418
43 Attn: Library

Applied Research Laboratory
The Pennsylvania State University
P.O. Box 30
State College, PA 16801
44 Attn: Library

Applied Physics Laboratory
The Johns Hopkins University
Johns Hopkins Road
Laurel, MD 20810
45 Attn: Library

Applied Physics Laboratory
The University of Washington
1013 Northeast 40th Street
Seattle, WA 98015
46 Attn: Library

Marine Physical Laboratory
The Scripps Institution of Oceanography
The University of California at San Diego
San Diego, CA 92152
47 Attn: Library

Woods Hole Oceanographic Institution
86-95 Water Street
Woods Hole, MA 02543
48 Attn: Library

49 Signal Physics Group, ARL:UT

50 Martin L. Barlett, ARL:UT

51 Garland R. Barnard, ARL:UT

52 Kevin W. Baugh, ARL:UT

53 M. Gette Beauvais, ARL:UT

Distribution List for ARL-TR-91-20 under ARL:UT IR&D Program
(cont'd)

Copy No.	
54	Glen E. Ellis, ARL:UT
55	Joseph F. England, ARL:UT
56	Douglas J. Fox, ARL:UT
57	Marshall E. Frazer, ARL:UT
58	Keith R. Hardwicke, ARL:UT
59	Melvin J. Hinich, ARL:UT
60	James L. Lamb, ARL:UT
61	Fredrick W. Machell, ARL:UT
62	Chetna S. Mathur, ARL:UT
63	Sara S. Matzner, ARL:UT
64	Thomas G. Muir, ARL:UT
65	Clark S. Penrod, ARL:UT
66	F. Michael Pestorius, ARL:UT
67	Edward J. Powers, ARL:UT
68	Jack H. Sheehan, ARL:UT
69	Ronald O. Stearman, ARL:UT
70	Robert T. Trochta, ARL:UT
71	J. Kenneth Vaughan, ARL:UT
72	Joseph F. Willman, ARL:UT
73	Gary R. Wilson, ARL:UT
74	Library, ARL:UT
75 - 85	Reserve, ARL:UT